NSF/ENG-85055

PB86-163672

STRUCTURES & MECHANICS

UNIVERSITY OF WASHINGTON

COLLEGE OF ENGINEERING

DEPARTMENT OF CIVIL ENGINEERING

USE OF THERMAL STRESS FOR SEISMIC DAMAGE REPAIR

CHARLES W. ROEDER

A Report on Research Sponsored by

National Science Foundation

Grant CEE-8205260

October 1985

SEATTLE, WASHINGTON

98195

50272-101

REPORT DOCUMENTATION PAGE	1. REPORT NO. NSF/ENG-85055	2.	3. Recipient's Accession No. PB86 163672 /AS

4. Title and Subtitle
Use of Thermal Stress for Seismic Damage Repair

5. Report Date
October 1985

6.

7. Author(s)
C.W. Roeder

8. Performing Organization Rept. No.

9. Performing Organization Name and Address
University of Washington
Department of Civil Engineering
Seattle, WA 98195

10. Project/Task/Work Unit No.

11. Contract(C) or Grant(G) No.
(C)
(G) CEE8205260

12. Sponsoring Organization Name and Address
Directorate for Engineering (ENG)
National Science Foundation
1800 G Street, N.W.
Washington, DC 20550

13. Type of Report & Period Covered

14.

15. Supplementary Notes

16. Abstract (Limit: 200 words)

Different types of damage are described and potential repair methods are noted. It is suggested that most structural steels can be repaired by heat straightening with no significant change to the material properties if a few simple guidelines are followed. An extensive series of experiments are then performed and evaluated. The experiments show that the plastic deformation achieved by heat straightening is very sensitive to temperature, quenching, heat geometry, applied load and restraint conditions. A mathematical model using a finite difference heat flow model with the non-linear finite element method, was developed. The finite element solution is based on a Prandtl-Reuss bilinear plasticity formulation, and the results compare well with the experiments at both the local and global level.

17. Document Analysis a. Descriptors

Thermal stresses	Heating	Steels
Mathematical models	Maintenance	Earthquakes
Steel construction	Damage	Plastic deformation

b. Identifiers/Open-Ended Terms

c. COSATI Field/Group

18. Availability Statement	19. Security Class (This Report)	21. No. of Pages
NTIS	20. Security Class (This Page)	22. Price

(See ANSI-Z39.18) *See Instructions on Reverse* OPTIONAL FORM 272 (4-77) (Formerly NTIS-35) Department of Commerce

USE OF THERMAL STRESSES FOR REPAIR OF

SEISMIC DAMAGE TO STEEL STRUCTURES

by

Charles W. Roeder
Professor of Civil Engineering
University of Washington
Seattle, Washington 98195

Final Report to the Sponsor
National Science Foundation
Grant CEE-8205260

October 1985

Abstract

Thermal stresses are commonly used by welders to introduce camber into steel beams, to repair damage caused by plastic deformation, and to remove distortions caused by welding. A local concentration of heat is applied to the steel. The heated steel expands, but the expansion is resisted by the restraint provided by applied loads, the temperature gradient and the surrounding unheated metal. As a result, large compressive stress develops, while the yield stress and elastic modulus of the steel are reduced by the elevated temperature, and local yielding occurs. This introduces permanent deformations which may be used to curve members or remove unwanted distortions. It is an economical method and it may be useful for repairing damage caused by extreme earthquakes or other dynamic loadings. However, the method is practiced as an intuitive art and is not understood by most engineers. This report is a first step in developing a scientific understanding of the technique.

This report includes a review of existing practice. Different types of damage are described and potential repair methods are noted. A summary of the influence of elevated temperature on the properties of steel suggests that most structural steels can be repaired by heat straightening with no significant change to the material properties if a few simple guidelines are followed. An extensive series of experiments are then performed and evaluated. The experiments show that the plastic deformation achieved by heat straightening is very sensitive to temperature, quenching, heat geometry, applied load and restraint conditions. Some heat patterns such as strip heats are sensitive to residual stress because they cause relatively small plastic strain, while others such as V-Heat cause large plastic strains and are not sensitive to residual stress. The rate of heating and specimen dimensions have a lesser effect on the results. Wide flanges and structural shapes were also tested, and factors such as the P-Δ effect and warping restraint also effect the plastic deformation. Further, the experiments suggest that columns may be heated while supporting large gravity loads.

A mathematical model was developed in response to these experiments. It employs a finite difference heat flow model with the non-linear finite element method. The finite element solution is based on a Prandtl-Reuss bilinear plasticity formulation, and the results compare well with the experiments at both the local and global level.

Acknowledgements

This investigation was sponsored by the National Science Foundation through grant CEE-8205260 with the encouragement and guidance of Dr. J. B. Scalzi. Additional support was provided by the American Institute of Steel Construction Fellowship Program. The author would like to thank NSF and AISC for this support. The conclusions and opinions expressed in this report are those of the author and do not necessarily represent the views of the sponsor.

The author would particularly like to thank four former graduate students who helped in this project. They are Shelley R. Clark, Michael Ehredt, Stephen P. Schneider and Andrew W. Taylor. Mr. Kenneth Moberg was also particularly helpful with this project. He provided continual help and advise during the course of the study, and he lent his valuable experience during the experiments by heating most of the test specimens. Finally, the author would like to thank Ms. Ann Hansen and Ms. Carole McCutcheon for their help in the preparation of this report.

Table of Contents

Chapter IV. ANALYSIS OF EXPERIMENTAL RESULTS

Chapter V. A THEORETICAL MODEL

List of Figures

CHAPTER 1

INTRODUCTION

General

Considerable research has been applied to the seismic behaviour of structures, and a multi-level design approach has evolved [1]. Most buildings are designed elastically for a series of small lateral forces. The forces [2,3] are calculated from an approximate analysis which considers the dynamic properties of the soil and structural system and the regional seismicity. Actual earthquake accelerations produce inertial loadings. Therefore, the actual seismic force experienced by the structure will depend on many additional factors and may be many times larger than the arbitrary design forces. Therefore, structures are expected to remain elastic only during small, frequent earthquakes. During moderate earthquakes, which may occur several times in the life of the structure, limited damage may occur, and significant yielding of the structure may occur during an extreme earthquake which occurs only once or twice in the life of the structure. However, the structure must not collapse nor represent a serious risk to human life during these extreme events. These latter conditions are assured by using ductile structural systems. The ductility dissipates large amounts of energy and dampens the structural response without failure or loss of structural integrity. It is achieved through yielding of the steel and it introduces permanent deformations and deflections into the structure.

This design procedure is simple and economical. Most design engineers perform only standard code design calculations with a linear elastic analysis model. They make no estimate of the plastic deformation or ductility of the structure nor do they estimate when or where damage will occur. Ductility is assured only by using certain well understood structural systems, which are known to provide good elastic and inelastic performance. Steel is a very desirable material for this design, because research and practical experience has shown that properly designed, detailed and constructed steel frames have good strength and ductility.

It is well known that this design procedure will result in structural damage during severe or even some moderate earthquakes. The extent of this damage is non-deterministic, because the intensity of shaking is known only in a probabalistic sense, and structural response may vary greatly with small changes in the acceleration record and structural behaviour. However, it is very clear that during a major earthquake a few structures will be damaged beyond repair. Others will require little if any repair, but many will be prime candidates for damage repair.

This represents a potential problem in seismic engineering practice. Most engineers are knowledgeable in the methods of designing and analyzing steel structures, but they have little experience in designing damage repairs or even in estimating if a repair is possible or economically feasible. Steel is a versatile and ductile material which can frequently be repaired at a small percentage of replacement cost, but clearly a basic understanding of the methods of repair must be available before the full benefit of the properties of steel can be obtained.

Seismic Damage to Steel Structures

Before discussing methods of damage repair for steel structures, it is necessary to understand the types of damage which are expected during an earthquake. Several major framing systems are used frequently for seismic design, and the expected damage is different for each system. Moment resisting frames are perhaps the most widely used framing systems. Research [4,5,6,7] has shown that ductile moment resisting frames dissipate a large quantity of energy through flexural yielding of the beams, and so damage repair requires the reversal of plastic rotations and flange buckling which typically accompanies this rotation as shown in Fig. 1.1. The plastic rotations typically occur in the beams near the beam-column connection, but the rotations may also occur in the columns [6]. Further, some moment frames [4] may develop permanent deflections from shear yielding of the panel zone as shown in Fig. 1.2.

Concentrically braced frames are much stiffer than moment frames, because of the large axial stiffness provided by the brace. Therefore, braces [8,9,10] attract large axial forces and dissipate energy through tensile yielding and plastic rotations occurring during post-buckling deformation as shown in Fig. 1.3. Damage repair would require reversal of these rotations and shortening of the tensile elongation. Some bracing systems such as the K-brace will also induce flexural yielding of beams or other members, and so plastic rotations in the beams may also need repair. Finally, severely buckled braces may also cause local distortion of gusset plates or other connections.

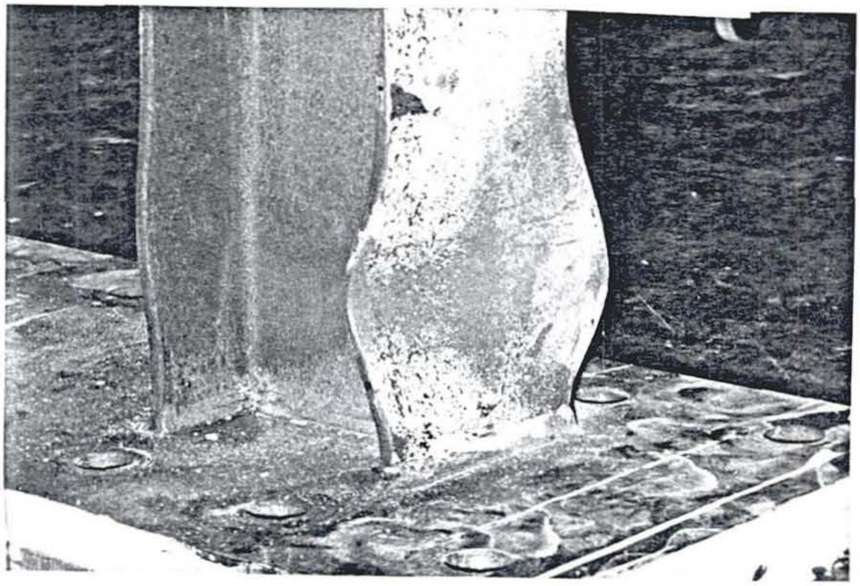

FIGURE 1.1. Photograph of a Plastic Hinge Location with a Flange Buckle.

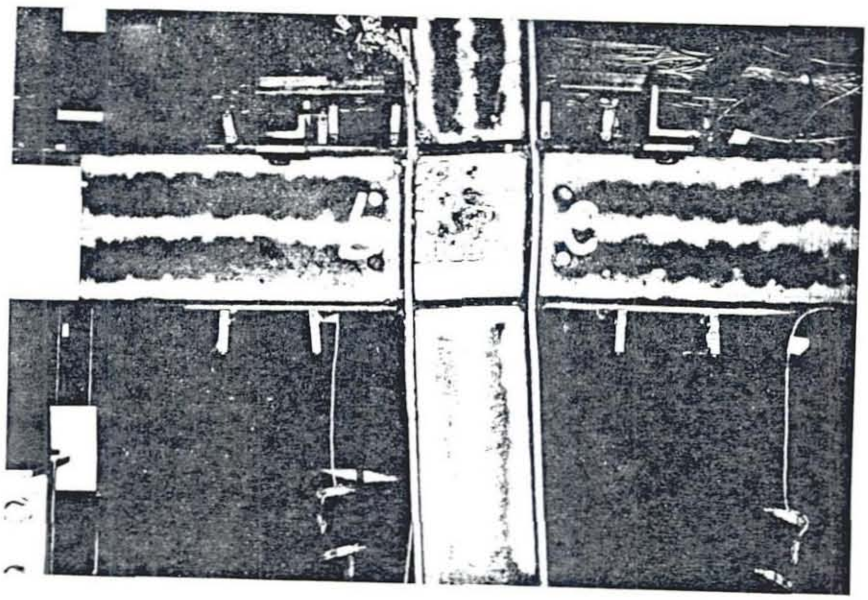

FIGURE 1.2. Shear Yielding of the Panel Zone of a Moment Resisting Frame.

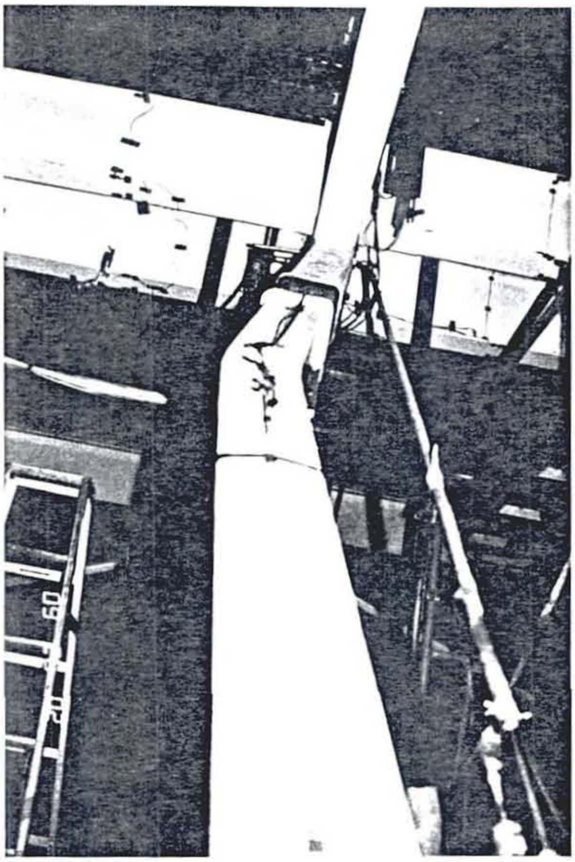

FIGURE 1.3. Photograph of a Buckled Brace

Eccentrically braced frames have also been used in recent years. These structures [10,11] dissipate large amounts of energy through shear yielding of the eccentric link. Flexural yielding may also occur at the ends of the links, and web buckling may accompany this plastic deformation as shown in Fig. 1.4.

Other types of damage may also accompany the above plastic deformations. The frame may be out of plumb, and cracking of the floor slab will likely be observable with the eccentric bracing system and the K-Brace system. Glass, architectural walls and other non-structural elements may be damaged. Lateral-torsional buckling or local web or flange buckling may also accompany yielding of the steel. This additional damage makes it difficult to determine if the structure is repairable. The cost of the structure is typically quite small for most buildings. Structural costs are frequently less than 20% of total cost for taller buildings with foundations, architectural components, and mechanical equipment constituting the bulk of the cost. A building may be regarded as a total economic loss if these non-structural components are heavily damaged even though the structure has sustained only minimal damage. Further, a structure with extensive structural damage may be economically repairable if the non-structural damage is small. However, once it is decided that structural repair is economically feasible, a number of serious technical questions must be addressed. This report will focus on these technical issues.

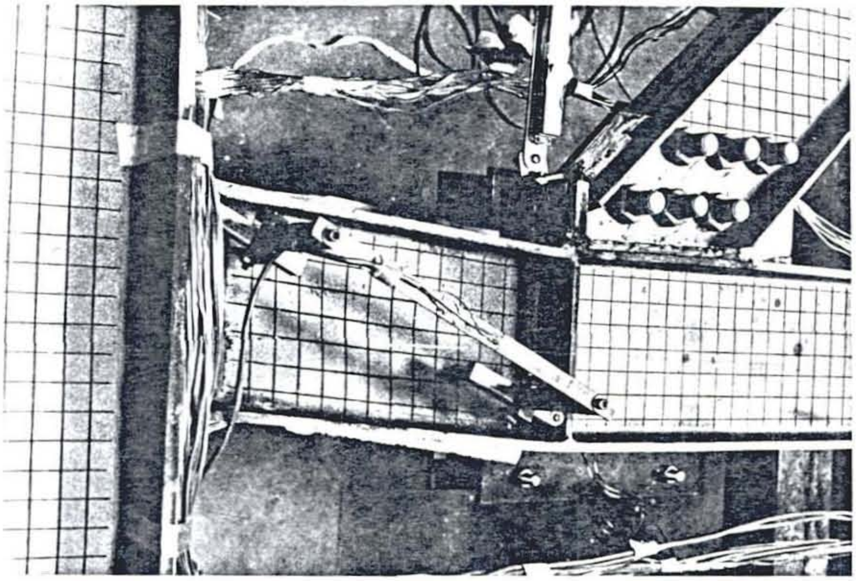

FIGURE 1.4. Photograph of Damages Produced by Cyclic Shear Yielding and Web Buckling of An Eccentric Link.

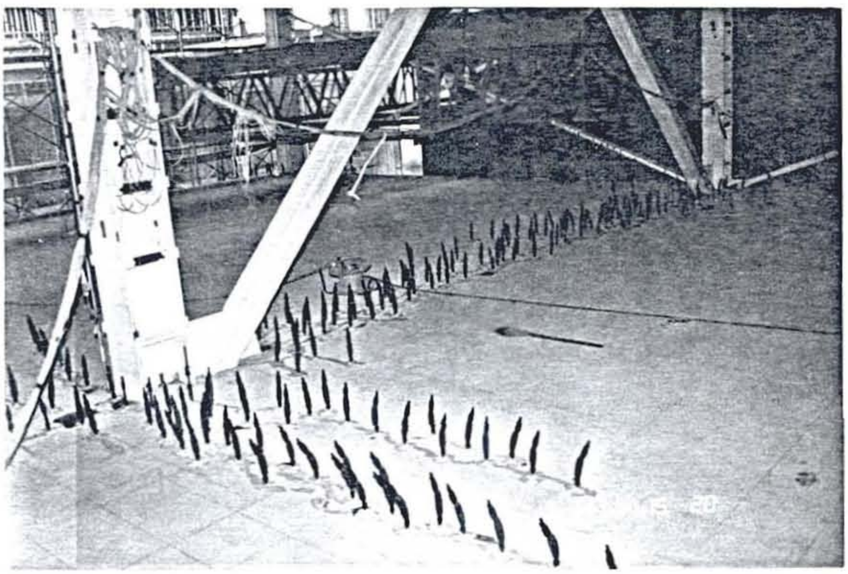

FIGURE 1.5. Photograph of a Floor Slab During Repair by Epoxy Injection

Methods of Structural Damage Repair

Damage to concrete slabs in steel structures may be repaired by one of several methods. Epoxy injection [13,14] has been used to repair reinforced concrete slabs which are extensively cracked as shown in Fig. 1.5, but pieces of loose concrete must typically be removed and replaced. This type of repair may redevelop the composite action and stiffness of the beam [14] if the shear connectors are in good condition, but it will probably be ineffective in redevelopment of shear bond with the metal deck. If the concrete is cracked excessively or shear bond stress or shear connector failure has occurred the concrete slab may require replacement. If the concrete is structurally sound but repair of cracks is desirable for architectural reasons, a thin topping layer may be desirable. Cracking and damage to the slab is likely to be most prevalent in eccentrically braced frames or concentrically K-braced frames. Moment resisting frames are likely to develop large cracks only at large displacements or story drifts.

Damage to the steel frame is usually more important to the structural integrity, but repair sometimes is quite easily accomplished. Several methods of repair have been successfully used for steel structures [15]. The first method consists of removal and replacement of damage steel. This is typically the first repair method to be considered by a structural engineer when developing a program of damage repair, but it is often the least practical or economical repair method. Diagonal braces are sometimes relatively easy to replace, but major beams and columns can be replaced only with very great difficulty [15]. Secondary

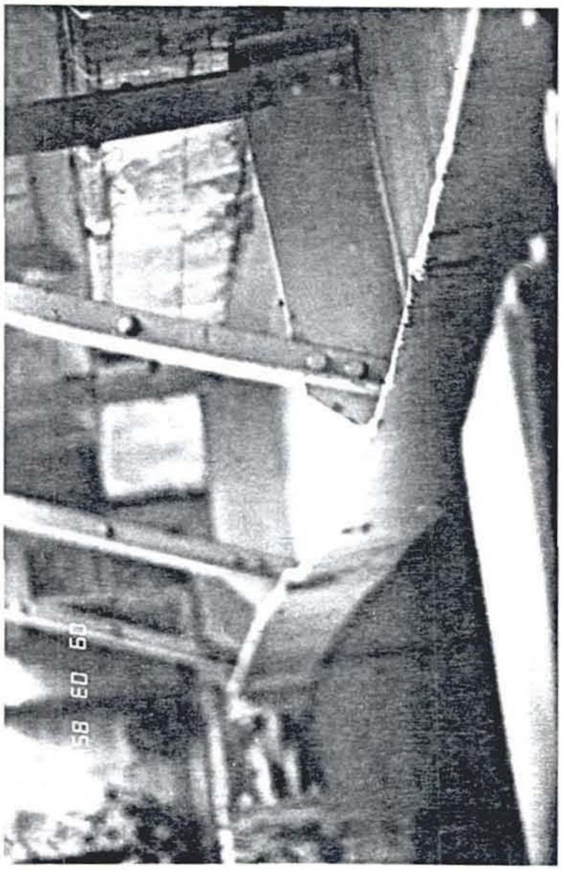

FIGURE 1.6. Photograph of a Cover Plate Attached to a Damaged Steel Girder.

beams and members which support light dead loads often can be replaced with an intermediate level of effort. This repair method is generally very expensive, and will typically not be attempted unless the damage is very slight or isolated in a small part of the structure.

A second method of repair, which is believed to be more economical and has been used more frequently, is to cover the damaged steel with strengthening elements such as cover plates or to insert additional members to strengthen the damaged structure. This method has been used on numerous occasions to repair damage caused by oversized trucks on the lower flanges of bridge girders or at loading docks. The method is likely to be much more economical than complete replacement of the damaged steel, but it also leaves large imperfections and residual stresses on the steel structure. Imperfections cause secondary stress which may seriously weaken the structure. Further, these secondary effects are difficult or impossible to calculate, and so the true strength of the repaired structure is not known. The strengthening elements are also added in places which are sometimes difficult to weld or bolt, and the desired continuity cannot always be achieved. Finally, it should be noted that the damaged steel, which is left in the structure, has a strain history and reduced ductility due to cold working, and may make the steel more susceptible to fracture and fatigue. This repair method illustrated in Fig. 1.6. The photograph shows a damaged steel girder, which was strengthened with a cover plate, but it must be noted that the girder is still crooked and subject to large secondary effects.

The third method consists of plastically deforming (i.e., cold working) the steel to remove the imperfection. This method is commonly used in fabrication shops to camber or curve straight members or straighten member which do not meet erection tolerances. The steel is placed in a loading device and a controlled force or displacment pattern is applied. This cold works the steel and reduces the ductility. However, it is generally assumed that structural steels have great ductility and the reduced ductility and residual stress have no adverse affect on structural behaviour. This assumption is so prevalent that design engineers typically make little or no restriction on the use of this fabrication method. While controlled plastic deformation may be a practical and economical method of accomplishing a repair in fabrication shops, it is far less viable for damage repair in the field. First, it is difficult to develop the controlled loads and deformations needed to reverse the damage without the large fixed frame load equipment available in the fabrication shop. Secondly, the plastic strains caused by seismic or other damage are usually localized, and the cold working needed to reverse the damage would necessarily occur in the same location. This increases the probability of embrittlement of the steel and the likelihood that the steel will crack or fracture during the repair. Finally, it is important to note that many forms of seismic damage occur near the connections where the available ductility is limited, and so it is difficult to apply this method in these areas.

A fourth method is also widely used by fabrication shops, but it is poorly understood by structural engineers. With this method, a local concentration of heat is applied to part of the structure [16]. The heated steel expands, but expansion is resisted by the unheated metal. Therefore, large compressive stress develops in the steel. The yield stress is reduced in the heated area and local compressive yielding and plastic deformation occurs. If the temperature and the heat pattern are carefully selected, damage due to prior plastic deformation can be reversed or initial curvature or camber can be induced. It is used widely by fabrication shops and shipyards to both introduce curvature and repair damage (such as buckled flanges or bent beams) which is encountered during fabrication. It is commonly used by a few state departments of transportation [15] and railroads in the repair of damage in existing bridges. It has also been used in the repair of buildings. For example, in 1956, more than 1400 members of a roof space truss at McChord Air Base were damaged by a fire, and this roof was economically repaired [17]. The repair cost was 14% of estimated replacement cost. There are several advantages with this method. It is not only economical, but it can eliminate some of the problems associated with cold working, since the yielding is accomplished at elevated temperatures. The method requires a minimal work crew with very little equipment, and the repair can frequently be performed while the structure supports the dead load or is in partial service. However, there are several potential problems with this method. First, the method is not well understood by engineers. It is practiced as an intuitive art by skilled technicians, and there is wide variation in the methods used and results achieved by these technicians. Secondly, it uses elevated temperatures. This has the advantage of eliminating cold working, but the elevated temperatures also may change the properties of the steel, introduce embrittlement, cause large residual stresses, and introduce other potential problems encountered with welded structures [18].

A Proposed Program for Damage Repair to Steel Structures

The previous sections briefly described the types of damage expected during moderate or severe earthquakes, and the four potential methods of repair were noted. These methods may be summarized as:

1. Removal and replacement of damaged steel
2. Strengthening of damaged steel with cover plates, additional members, or other methods
3. Reversal of plastic deformation with controlled loads or deformations (Cold Working)
4. Use of thermal stress to reverse plastic deformations (Heat Straightening)

Method 1 is usually the more expensive method, but it is the method which is most well understood by engineers. Method 2 may be quite economical, but it leaves the damage within the structure. This makes estimates of the true strength and stiffness unreliable. Method 3 is economical and practical in a fabrication shop, but is is seldom practical for field repair. Further, the combined effect of multiple cold working of the steel may have serious consequences. Method 4 has been shown to be the most economical and practical alternative for a wide range of damage, but the results are not predictable by the structural engineer. This is a serious failing, because if engineers cannot reasonably predict the cost of a repair and the likelihood of success of the repair method, they will avoid using the method.

It is not likely that Method 4 will be suitable for repairing all damage to steel structures. It will not be adequate for the repair of members which are cracked, torn or have a severely reduced cross-section. Clearly strengthening of the structure or replacement of the damaged steel will be needed in these cases. Further, a few readily accessible members may be more economically repaired, by direct replacement. Therefore, it is likely that the most economical repair program will utilize combinations of these methods. A careful analysis of these options would suggest that a viable repair program should at least consist of the following steps.

Step 1. Determine the locations of damage and measure the degree of damage. Determine the damage in need of repair and find the damage that can be ignored or covered over.

Step 2. For members which are not cracked, torn or excessively deformed, estimate the amount and location of heat needed to affect a repair. Determine the effect of this heating on the material properties and structural performance of the steel. Estimate the cost associated with the repair.

Step 3. Cost estimates should be developed for strengthening of damaged members through the addition of cover plates or other methods.

Step 4. The cost and feasibility of the replacement of damaged steel must also be considered.

Step 5. The total cost and effectiveness of the repair of each member or component can then be evaluated and compared to other structural options, and the most economical combination can be selected. Clearly cracked or torn steel must be replaced or strengthened, but many elements can be economically repaired with thermal stress or heat straightening.

It is likely that a competent structural engineering firm could accomplish Steps 1,3,4 and 5 with reasonable speed and confidence, and an organization with prior experience could do it with alacrity. However, Step 2 could cause some serious problems. First, few structural engineers would be able to estimate a suitable heat program. Secondly, most engineers would not be able to predict the effect of this heating on the properties of the steel or the effect of the heat on the performance of the structure. Finally, most engineers would lack the confidence to specify the critical control parameters to assure that the work is properly done in the field.

Scope and Objective of This Research

This report describes a research program which develops an initial answer to these concerns. A comprehensive state-of-the-art of heat straightening is described, and variations and inconsistencies in present practice are noted. The types and patterns of heat application are also described and their effect on the structure is provided. The present knowledge of the effect of the heat on the permanent material properties and the behavior of the structure under future loads are also summarized.

A series of experiments are then performed to improve our understanding of the heat straightening process. More than 70 experiments are performed, and, when combined with earlier research results, they clearly show how different parameters affect the process and which parameters are most important. A theoretical computer model is then developed to analyze this complex problem. The model is a temperature dependent, plastic finite element solution, which is checked against known plasticity solutions and compared to experimental results. The mathematical model provides a good understanding of the local and global effects of heat straightening. The global behavior is important because it allows the engineer to select the most economical and practical repair method. The local behavior is important because it is needed to evaluate the potential for future problems such as buckling, fatigue and fracture. The analysis is costly, but they can be generalized with a series of nomographs. These graphs would provide the structural engineer with a basis for estimating the deformation produced by heat straightening or curving.

This research is clearly not the total answer to the heat straightening problem. However, it provides a reasonable understanding of the process and gives the engineer a method for estimating the effectiveness of thermal stress in repairing damage and curving steel members.

CHAPTER 2

PRESENT KNOWLEDGE OF THERMAL STRESS BEHAVIOR

Present Practice

Thermal stresses are often used to plastically deform steel. A local concentration of heat is applied to the steel with a torch or other heat source. The heated steel expands, but expansion is restricted by the surrounding unheated metal or other restraint. Therefore, a large compressive stress develops in the heated steel, while the yield stress is reduced by the elevated temperature. The steel yields and this causes permanent deformation which remains after cooling. No stress is introduced in metal which is heated uniformly and is unrestrained against expansion. Nor is stress developed [19,20] in statically determinate beams with a linear temperature gradient over the depth or length. It is the temperature gradient combined with restraint against expansion which causes yielding and permanent deformation. The restraint is usually at least partially developed by the surrounding unheated metal, but often it is enhanced by strategically placed loads or supports. However, it must be emphasized that the yielding is usually compression yielding, and the additional restraint generally is helpful only if it causes compressive stress in the heated area.

Since the temperature gradient induces the plastic deformation, the pattern of the heat is an important parameter in the process. Figure 2.1 shows several typical heat patterns which are commonly used in practice. The V-heat pattern shown in Fig 2.1(a) is used to introduce a plastic rotation into flat bars

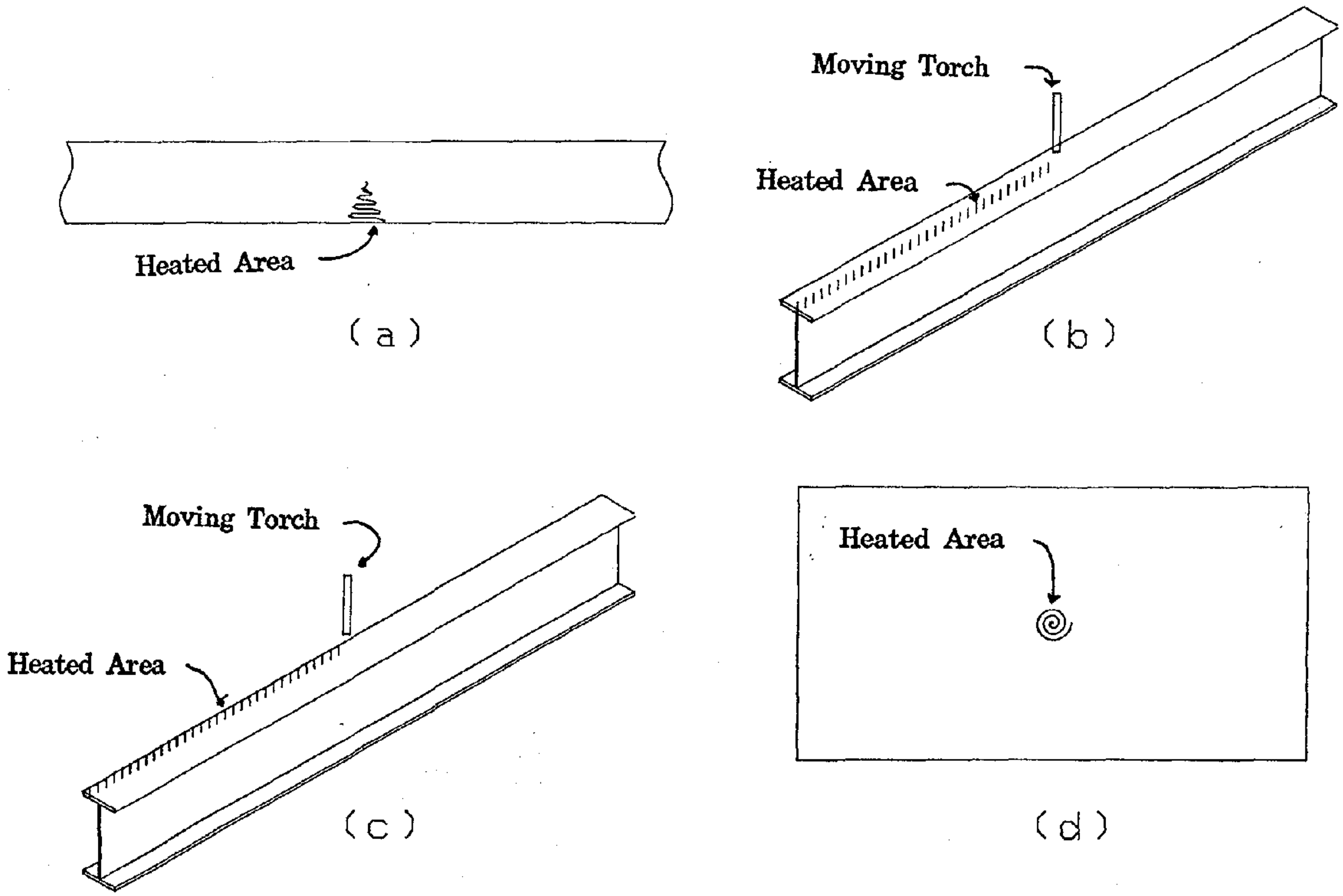

FIGURE 2.1. Typical Heat Patterns Used In Fabrication and Damage Repair

or structural shapes. It is started near the peak of the triangle, and the torch is passed over the triangular area in a serpentine pattern. The duration of heating will vary with geometry of the steel and the heated area, the desired temperature, and the size and settings of the torch, but it will typically require a minimum of approximately 10-15 seconds and a maximum of approximately 10-15 minutes. The longer times are required for thicker steel and larger heated areas. Since plastic rotation is desired in the plane of the heated area, the temperature should have a significant gradient in this plane but be nearly uniform through the thickness of the steel. Therefore, thick plates are often heated from both sides. This target temperature variation must influence the rate of heat application, and so thick steel may require a larger torch size as well as a longer period of heat application than thin steel. The V-heat has been used to induce plastic rotations in both the plane of the flange and the web of structural shapes, and this heat pattern would likely be beneficial in reversing plastic hinge rotations in moment frames, post-buckling deformations in braces, and lateral torsional deformations of beams and columns.

Line heats, strip heats or edge heats as shown in Fig. 2.1(b) and 2.1(c) are commonly used to introduce continuous camber or curvature. Heat applied to the center of the flange as shown in Fig. 2.1(b) cause camber while heat applied at the edge of both flanges as shown in Fig. 2.1(c) causes curvature in the plane of the flange or sweep. Therefore, a temperature gradient is needed either in the plane of the heated surface (Fig. 2.1(c) or normal to the heated surface (Fig. 2.1(b)) depending on the desired deformation. The heat is applied by slowly moving the torch along a given line to attain the target temperature distribution. If a wide strip is to be heated, the torch may follow a zig-zag path along the line. These heat patterns may produce similar results to the V-heat except that the plastic deformation is distributed over a length rather than concentrated. Thus, this pattern is more likely to be valuable in repairing distributed damage or curvature. For example, it may be desirable for straightening braces which are not severely buckled or shear yielding in eccentric links.

The spot heat or surface heat (see Fig. 2-1(d)) is commonly used to introduce curvature in flat plates such as sometimes required in ship hulls or webs of curved girders. Thus, it may be useful for straightening buckled webs and flanges or repair of damage to connection plates. The heat is applied over a surface area which is large compared to the plate thickness and a through thickness temperature gradient may be helpful. Therefore, a slightly more rapid heat application then required for the V-heat may be needed.

Other heat patterns and variations on those shown in Fig. 2.1 have also been used, but these four basic patterns are likely to be the most useful for seismic damage repair. The maximum temperature used with these patterns may affect the plastic deformation since the temperature gradient is increased with higher temperatures. Further, some practitioners quench the steel shortly after heating, because they believe it increases the plastic deformation and decreases the probability of local buckling. However, there is disagreement as to the total effect of quenching. Some engineers [21] believe that peening while cooling the steel increases the plastic deformation attained with an individual application of heat, but this is again a subject of some debate.

In practice, the heat pattern and target temperature are selected by a technician with no reference to theory or understanding of plasticity. This judgement is made primarily on the basis of trial and error and prior experience, and frequent errors occur. Further, discussions with these technicians indicate that there are wide disagreements on how damage repair should be performed and which technique will be most effective for a given application. However, some research has been done in this area, and there is a basis for resolving some differences in opinion.

Influence of High Temperature on Material Properties

It is well known [22,23] that elevated temperatures reduce the elastic modulus and yield stress of steel. This reduction in strength and stiffness has been an important consideration in the design of fire protection for many years, but it is also an important factor in heat straightening. The reduction in yield strength hastens the yielding produced by the thermal stress. The reduction in elastic modulus delays the initiation of yielding and further complicates the mathematical prediction of the resulting deflections. The coefficient of thermal expansion also changes [22] with temperature. Steel expands as heated, and this expansion is the driving mechanism for the development of thermal stress. The temperature dependence of this coefficient also influences the theoretical prediction of the plastic strain produced by heating. However, these are short term effects, and one may ask if there are any more lasting consequences of localized heating of the steel.

The iron-carbon equilibrium diagram [22,24] shown in Fig. 2.2 is an elementary tool [22,24] which may be helpful in evaluating these long term effects. This diagram is generally believed to be valid for all carbon steels (i.e., carbon steel with less than 2% carbon) and most low alloy steels. High alloy steels may have different behavior, but the vast majority of structural steels used in the United States fall into the carbon steel and low alloy category. At normal service temperatures, steel has a body centered cubic molecular structure, and is made up of three major constitutients, ferrite, cementite and pearlite. Ferrite is essentially iron molecules with no carbon attached. Cementite is an iron-carbon compound (Fe_3C), and pearlite is a mixture of 12% cementite and 88% ferrite. Low carbon steels (less than 0.8% carbon) do not have enough carbon to develop a 100% pearlite compound and therefore consist of pearlite with some free ferrite molecules. High carbon steels (carbon greater than 0.8% but less than 2.%) have more carbon than is needed to form pure pearlite, and therefore consists of a pearlite and cementite. Ferrite is soft and very ductile, while cementite is hard and brittle, and so low carbon steels tend to be softer and more ductile than high carbon steels.

Temperatures in excess of 1333^{o}F (723^{o} C) produce a phase change in steel. The iron atoms assume a face centered cubic

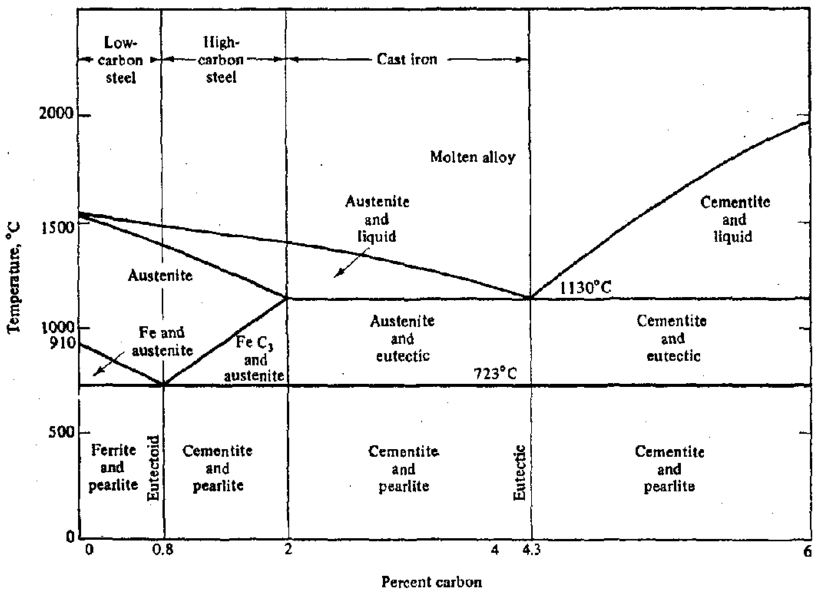

FIGURE 2.2. Iron-Carbon Equilibrium Diagram.

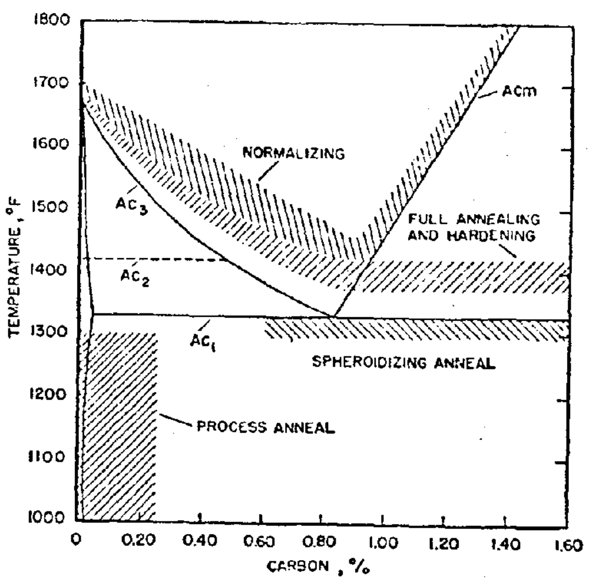

FIGURE 2.3. Temperatures for Normalizing, Annealing and Hardening Carbon Steels.

molecular structure. Carbon atoms easily fit within the voids with this structure and a much larger percentage of carbon will be carried in solution. If carbon steels are heated above the top curve of Fig. 2.2, the steel is molten. In temperatures between the phase change and melting temperatures a wide range of hot rolling and working can occur. When steel is cooled below the phase change temperature, it returns to its normal body centered structure. However, this change requires a limited amount of time, and so very rapid cooling may not permit this change to occur. A very hard, strong and brittle phase called martensite will occur under these conditions. It is sometimes suggested that this is a contributing factor in the loss of ductility sometimes noted with welding and it represents a potential concern in heat straightening. Further, this embrittlement should be more likely to occur in high strength, high carbon steel.

This elementary information serves as a basis for heat treatment of steel and provides a basic understanding of the effects of high temperature on the properties of steel. Figure 2.3 shows the temperature range typically used for annealing, hardening and normalizing of steel. For annealing, the steel is heated to the target temperature and cooled very slowly. This relieves internal residual stresses, softens the metal and refines the grain structure. If work hardening had occurred prior to heating, annealing may also increase the ductility and reduce the yield stress of the steel. Annealing tends to forgive the strain history. The hardening process has a similar target temperature but the surface is cooled quickly by quenching. This forms a hard, brittle, martensite surface structure, while maintaining a soft, ductile interior. Normalizing is typically accomplished by heating and then cooling in a controlled environment but not as slowly as annealing. It tends to refine the grain structure, and it is also used sometimes to increase the notch toughness and decrease the transition temperature of some bridge steels. Tempering and stress relieving are also used to reduce surface hardness or relieve internal residual stress. In these processes, the steel is heated to a temperature less than the phase change temperature, 1333^{0} F (723^{0} C) and cooled by quenching or slow cooling process.

Most structural steels are carbon steel or low alloy steel. Therefore, it is reasonable to expect that most structural steels can be heated to temperatures of 1300^{0} F (704^{0} C) with very little change to the material properties. Residual stresses may be introduced or partially relieved by this heating, and the hardness may be changed slightly. There may also be a slight change in ductility because of the yielding and possible tempering which occurs during heating, but this yield strain will typically be small compared to the minimum required tensile elongation of the steel. Further, the yielding occurs at elevated temperatures, and so there is reason to believe that the loss of ductility is negligible even though the steel is not heated to the annealing temperature. It is likely that quenching can be used throughout this temperature range (particularly with low carbon steel) with no serious consequences since this essentially tempers the steel. Temperatures hotter than 1330^{0} F (721^{0} C) may cause potential problems, particularly for high carbon steels, because the heat is applied locally and rapid cooling may occur. This may result in the formation of martensite and the loss of ductility in the steel. Quenching may be particularly troublesome for these elevated temperatures. Stainless steel, other high alloy steels, or special steel such as A514 require separate consideration because their phase change behavior may be different or because their properties are attributable to prior heat treatment.

These simple concepts have been independently checked by experimental research. Tests have shown [25,26] that mild steel can be heated to temperatures of approximately 1200° F (649° C) with only minor loss in ductility, slight increase in Rockwell hardness, and an increase in Charpy V-Notch impact energy. Tests on A441 steel [27] suggest that there is no change in yield or tensile strength, a slight increase in the notch toughness transition temperature, and a 19% decrease in ductility or strain at fracture when heated to 1200° F. However, the elongation attained after heating was still 56% larger than the minimum required by the ASTM standard. Other researchers have suggested that temperatures as high as 1650° F will cause no adverse effects with mild steel. Pattee and others [28,29] have indicated that low alloy steels with yield stresses in the range of 45-75 ksi can be exposed to temperatures of approximately 1100° F to 1200° F (593 C to 649 C) without significantly affecting material properties. Moberg [30] has indicated that very high strength structural steels such as A514 and A517 will not degrade if temperatures are kept below the 1150° F (621° C) tempering temperature.

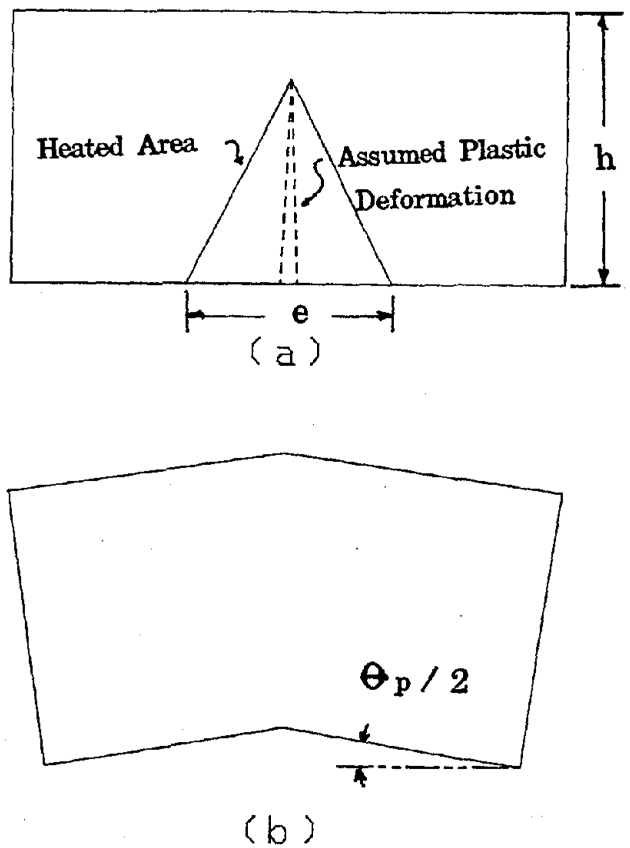

FIGURE 2.4. Geometry used for the V-Heat with the Holt Model.

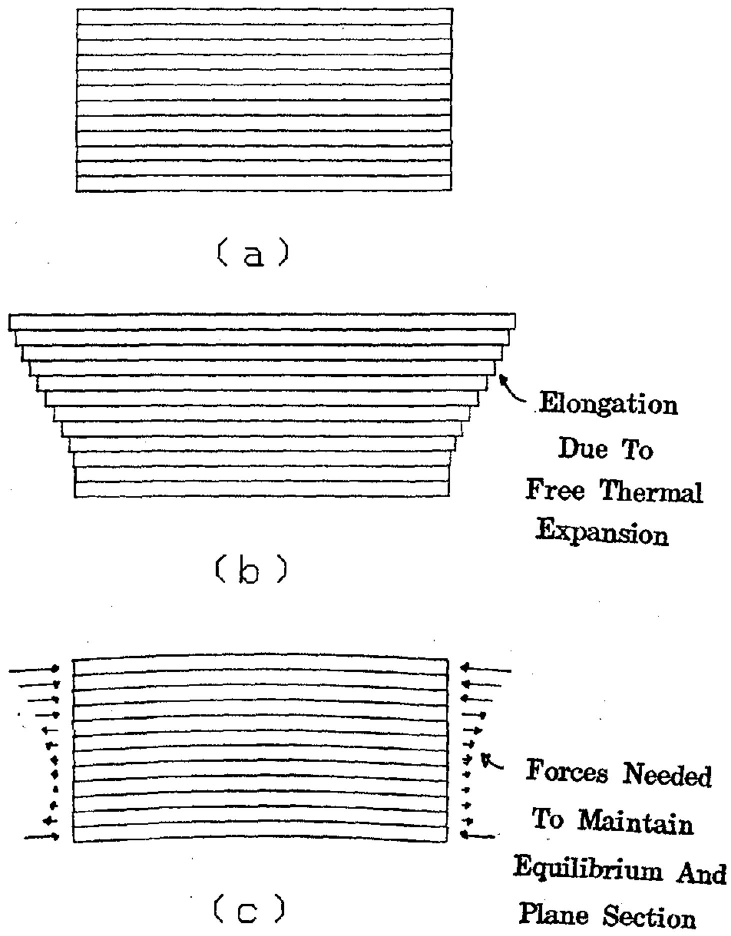

FIGURE 2.5. Assumptions Employed in the Strip Model.

Graham [31] investigated the effect of heat on high alloy steels such as stainless steel. He determined that heat straightening could be performed on stainless steel, but the temperature must be carefully controlled. The yield and tensile strength are lowered with each heat pass if the temperature is too high. He illustrated that proper cooling and mechanical restraint hasten the straightening process, and accomplish the repair with fewer heat cycles at lower temperature.

Prediction of the Plastic Deformation

The previous discussion has described the type of heat patterns required for repair of structural damage, and it has noted the approximate limits on the temperatures which are required to avoid permanent damage to the mechanical properties of the steel. Further, some intuitive guidelines on the use of the heating concept are described. However, before thermal stress can be widely used for damage repair, the method must be somewhat predictable. That is, an engineer (or technician) should be able to make a series of estimates or calculations and obtain a repeatable and consistent prediction of the type and quantity of heat required.

Holt [32] proposed a simple method which is applicable to concentrated applications such as the V-heat. He assumed that the heat was instantaneously and uniformly applied over the heated area with perfect uniaxial restraint. The plastic rotation achieved by a V-heat with geometry as shown in Figure 2.4 is

$$\Theta\rho = \frac{e\left[\int_{T_o}^{T_f} \frac{\alpha\,(T)\,dT}{T_f - T_o} - \frac{F_y\,(T)}{E\,(T)}\right]}{h} \tag{2.1}$$

where α (T), F(T), and E(T) are the temperature dependent coefficient of thermal expansion, yield stress and elastic modulus, respectively. This model is very simple, but it is not always a realistic model since it does not consider the actual time dependent temperature distribution, the true restraint conditions, nor does it meet requirements of strain compatibility.

A similar model [32] has been used to simulate spot heats. The elastic thermal stress distribution caused by a small radially symmetric temperature distribution has been shown [33] to be

$$\sigma_r = \alpha E\left(\frac{1}{b^2}\int_0^b Trdr - \frac{1}{r^2}\int_0^r Trdr\right) \tag{2.2}$$

$$\sigma_4 = \alpha E\left(-T + \frac{1}{b^2}\int_0^b Trdr + \frac{1}{r^2}\int_0^r Trdr\right. \tag{2.3}$$

where α and E are constant. If the temperature is constant, T , within the heated radius, a, and this radius is very small compared to the dimension of the plate, b, then within the heated area

$$\sigma_r = \alpha_H = -\frac{1}{2}E\alpha\,(T_1 - T_o) \tag{2.4}$$

and outside the heated area

$$\sigma_r = -\frac{1}{2} E\alpha (T_1 - T_0) \frac{a^2}{r^2} \tag{2.5}$$

$$\sigma_4 = \frac{1}{2} E\alpha (T_1 - T_0) \frac{a^2}{r^2} \tag{2.6}$$

Holt [32] has noted that yielding will occur within the heated area when

$$\delta_y (T) = \frac{1}{2} E\alpha (T_1 - T_0) \tag{2.7}$$

and this equation can be combined with Eq's 2.5, and 2.6 and strain distribution associated with the elastic solution [33] to estimate the plastic deformation. Holt uses these simple concepts to suggest that the minimum temperature of approximately 310^{o}F and a maximum temperature of 620^{o} F (155^{o} C and 325^{o} C) are needed for this application with A36 steel. However, it should again be noted that this model assumes an idealized heat distribution which may not be valid (particularly for larger diameter heat patterns.) Both Eq's 2.1 and 2.7 suggest that there is an upper limit on the temperature which can be used for heat straightening. Temperatures which are larger than this limit are expected to develop yield reversal on cooling and so they are expected to have increased potential for heat damage without increasing the plastic deformation. However, this conclusion is based on idealized temperature distribution.

Brockenbrough [34] used a strip model known as Duhamel's analogy to predict the curvature and residual stress induced by horizontal curving of members with a neat pattern such as shown in Figure 2.1c. With this method, the structural shape is broken into strips as shown in Figure 2.5(a). The heat pattern is applied and the thermal elongation is computed for each unrestrained strip as shown in Figure 2.5(b). Then compatibility is enforced by assuring that plane sections remain plain as shown in Figure 2.5(c). This induces longitudinal forces (stress) on each strip, and the resulting stress pattern is checked for yielding and equilibrium with the applied loads. It is unlikely that equilibrium will be satisfied after the first step and so this stress distribution is then adjusted by iteration until equilibrium and yield state are both satisfied. Experiments were performed [35] to verify that the model predicted reliable estimates of beam curvature and residual stress distribution.

This model is more complete than the Holt model. It requires an iterative form of analysis, but it allows a realistic time dependent distribution of temperature and ensures compatibility of the strains at specific locations. Further, a step by step solution may be used to increase the accuracy. This method appears to be very reasonable for heat patterns which are independent of length since the basic assumptions of the strip model are applicable. However, other authors [36,37] have also used this method to model concentrated heat patterns such as the V-heat or spot pattern shown in Figure 2.1a and 2.1d, respectively. Experimental comparison with these predictions has been mixed, since the assumption of plane sections is not valid for many of these heat patterns.

Contradictions or Inconsistencies in Present Practice

The prior discussion has focused on topics which have been experimentally verified, have some theoretical basis, or at least are widely accepted by the profession. Many aspects of the art of heat straightening do not enjoy this level of acceptance. Gross inconsistencies can be noted in discussion with different experienced practitioners, and their claims sometimes exceed the bounds of credibility. Further, serious contractions can be noted in the published literature. Examples of these contradictions are:

1. Some practitioners claim that high strength steel is more easily deformed than mild steel. Others correctly note that high strength requires a larger strain (and presumably a higher temperature) to initiate yielding, and so they feel mild steel is more easily deformed.

2. Some researchers suggest that quenching is effective in increasing plastic deformation and controlling local buckling while others doubt this contention.

3. Some authors and practitioners [15] have suggested that a plastic deformation will not increase if the temperature is increased beyond certain limits, (1200^{o} F for V-heats and 783^{o} F for spot heats on mild steel). This is clearly suspicious since unrestrained thermal elongation does not stop at these temperatures.

4. Some authors [30] suggest that very high strength steels such as A514 can be deformed even with the temperature limitations imposed upon quenched and tempered steel. Others [15] dispute this contention.

5. Some authors [26] suggest that peening is helpful in increasing plastic deformation while others [15] contradict this claim.

6. Numerous other inconsistencies can be noted in other topics including the effect of residual stress, the effect of repeated heating, and the effect of added restraint.

CHAPTER 3

EXPERIMENTAL PROGRAM

General Comments

An experimental program was developed to resolve many of the uncertainties and contradictions noted in the review of practice and to improve the engineering understanding of the heat straightening process. These tests were also intended to provide a comparison with later theoretical developments and so extensive data was accumulated. Two series of tests were performed. Series A experiments employed V-heats on simple plate specimens. A large number of these tests were performed so that a broad understanding of the parameters affecting heat straightening could be obtained without excessive duplication of previous research [36, 38]. Extensive measurements of temperature, force deflection and strain were used in these experiments to provide a wide range of comparison between experiment and theory.

Series B was the first step in applying the knowledge gained in Series A experiments to actual structural shapes and practical applications. There were fewer of these experiments and the instrumentation was typically less extensive. Further, both V-heats and continuous strip heats were applied to these wide flange sections. All of the heating for both series of experiments was done by experienced technicians, but several different technicians were used to measure the natural variations expected in practice.

Series A Experiments

A large number of parameters come to mind when evaluating the effect of thermal stress on steel member behavior. They include -

1. Maximum Temperature
2. Time Required to Heat Specimen or Rate of Heat Application
3. Geometry of Specimen
4. Geometry of Heat Pattern
5. Yield Strength of Steel
6. Thermal Properties of Steel (Conductivity, Coefficient of Thermal Expansion, and Emissivity and etc.)
7. Loading on the Steel During Application of the Heat and Restraint
8. Variations in the Residual Stresses Prior to Heating
9. Quenching of Test Specimen.

Sixty-eight test specimens were used to evaluate these parameters. Nine additional test specimens [39] were made and tested as a pilot test program. These pilot tests helped to define the control necessary for the research, but they are not included in this report because the data was necessarily less accurate. The details of the individual tests are summarized in the next chapter. The maximum target temperature was varied from approximately 800^{o} F to 1600^{o} F (427^{o} C to 871^{o} C), and comparison of these results show the effect of increasing temperature on plastic deformation attained during heating. The heat was applied in a typical V-heat pattern as shown in Fig. 3.1

and control of the temperature of the heated steel was provided by the color of the steel. However, independent measurements of the actual temperature were made on both the front and back surface of the steel for all specimens with an Omega OS-2000AS Non-contact Pyrometer, thermocouples and temperature indicating crayons. The pyrometer and crayons were calibrated prior to testing, and it was believed that their measurements were reliable and repeatable to within $\pm$ 50^{o}F. Twenty-one of these specimens also had a grid of thermocouples attached to the unheated side of the steel. The thermocouple temperatures were read at approximately 15 second time intervals with an HP 9816 Computer and HP3497A Data Acquisition System. Typically 10 thermocouples were used and they were attached in a grid as shown in Fig. 3-2. They provided a check of the other temperature measurements, and they also showed the distribution of temperature over the geometry of the specimens and variation of temperature with time.

The specimens were heated with an oxy-acetylene torch with an oxygen pressure of 25, acetylene pressure of 5 and a number 5 tip. These parameters were held constant to maintain a relatively constant heat input for all specimens. The time required to heat each specimen was also measured with a stop watch. It should be noted that the temperature varied through the thickness of the plates, and average through thickness temperature was estimated from the measured values and recorded.

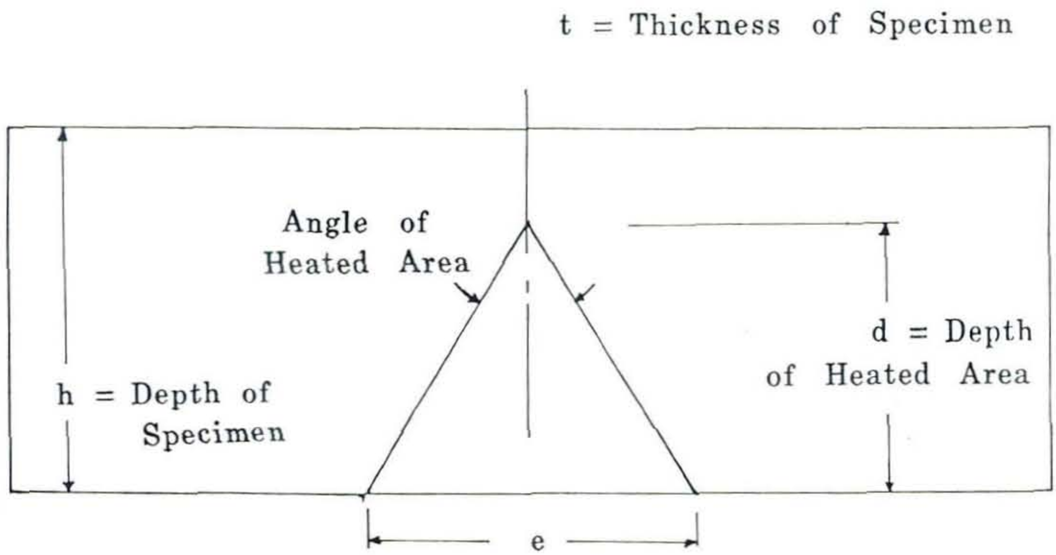

Figure 3.1 Typical Geometry of V-Heats Used in Series A Experiments

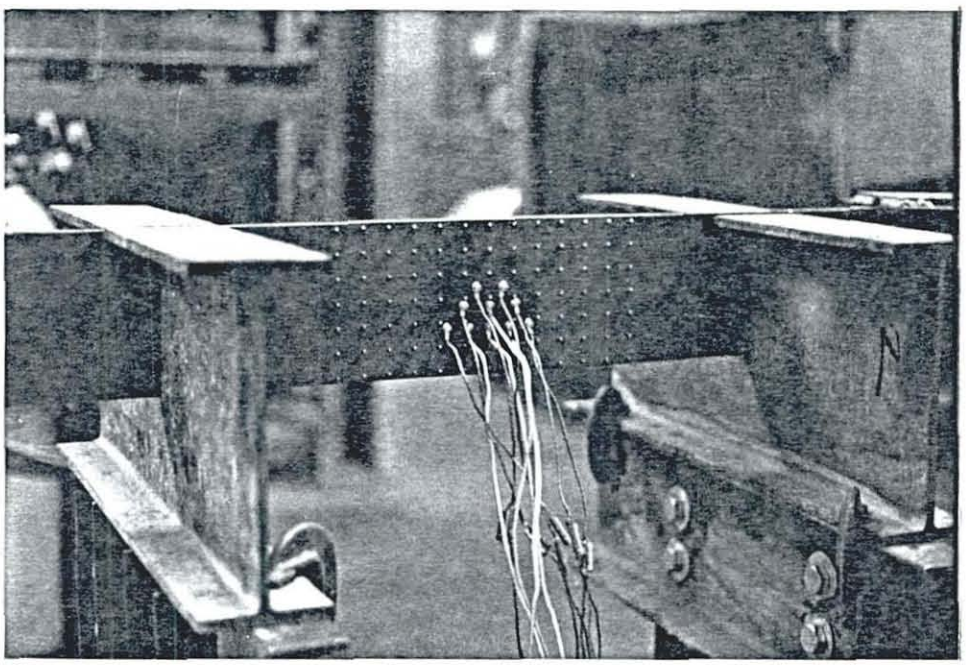

Figure 3.2 Typical Thermocouple Grid for Series A Experiments.

This temperature was invariably larger than the thermocouple measurements. V-heats induce plastic deformation in the plane of the heated surface. Therefore, the heat must be applied slowly enough to minimize through thickness gradient and quickly enough to maximize in-plane temperature gradient. Therefore, thick specimens were heated from both sides.

The geometry of the test specimen affects the rate of application of the heat and the heat flow within the specimen. This may affect the yielding and the plastic deformation which results. All the specimens of Series A were rectangular plate specimens with geometry shown in Fig. 3.1. The h/t ratio is clearly the only geometric parameter for the test specimens, where h is the specimen height and t is the thickness. Most of the plates had nominal dimensions of 3/8" x 6", but four each were tested with nominal dimensions of 1/4" x 8" and 3/4" x 6". This covered h/t values in the range of 8 to 32 and simulates a wide range of practical conditions. Comparison of these test results for different $\frac{h}{t}$ values will illustrate the importance of this parameter on the obtained plastic deformation.

The geometry of heat can be typified by the angle of the heat, Θ, and the depth of the heat, d, as shown in Fig. 3.1. Previous research [36, 38] has shown that increasing the angle of the heat and the depth of the heat increases the plastic rotation if the temperature and applied load are held constant. Fig. 3-3 shows the experimental results obtained for specimens which were heated to 1200°F (649°C). There is no obvious reason to question these results except to note that restraint is necessary to induce compressive stress and yielding, and full-

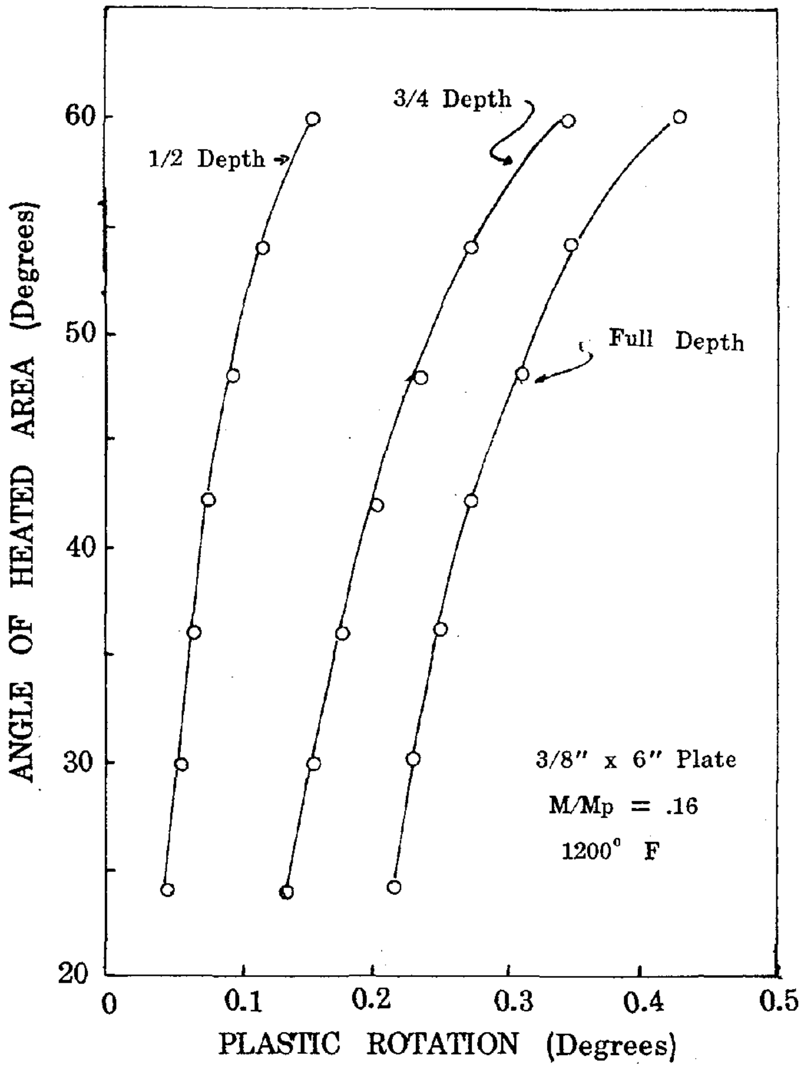

Figure 3.3. Plastic Rotation as a Function of Heat Geometry.

depth heats may lack the necessary restraint under some conditions. Therefore, it was decided to avoid unnecessary duplication of previous experimental results, and, while the heat depth and angle were varied, the variation was not performed in a systematic manner as used for the other parameters. All specimens were heated with a 2/3 or 3/4 depth heat and the heat angles were 45^o, 60^o, or 82^o. The 82^o heat pattern was checked because it was larger than any used in previous research.

There is wide disagreement as to the effect of yield strength of the steel on the resulting deformation and so this parameter was investigated. Most of the specimens were made of mild steel (A36), because this is the steel of most practical importance. The mild steel was purchased from 3 separate orders and came from 3 separate furnace heats. The yield stress at room temperature was measured for each of the steel types and the estimated properties for all of the steel specimens are summarized in Table 3-1. Nine specimens were of a very high strength steel (A514 with nominal yield stress of 100ksi). Comparison of the results of these nine tests with the corresponding mild steel tests will clearly illustrate the effect of yield stress on heat straightening. The thermal properties of steel also vary for different grades of steel. Generally, the thermal conductivity decreases [22] when the alloy content is increased in the steel, but the difference is less important at elevated temperatures. The coefficient of thermal expansion also decreases [22] for high alloy steel. A514 steel is a quenched and tempered low alloy steel, and so it should have a smaller thermal conductivity and coefficient of expansion than mild carbon steel. Therefore, it should require less time for heating to the target temperature and induce larger thermal stress after heating. The bending stress in the steel prior to heating has been shown [38] to be an important parameter in the straightening process. If the V-heat is applied in an area with large compressive bending stress, the steel yields in compression more quickly and larger plastic rotations occur. This is a reasonable and well-documented observation, and so the tests were designed to avoid excessive duplication of previous work. However, the applied moment was varied in these experiments to establish a baseline for comparison to previous research and to extend the results to a wider range of applications.

There is considerable disagreement about the effect of residual stresses on the heat straightening process. Most believe that heat straightening induces large residual stress, and some [15, 35] believe that repeated heating is useless, because of the residual stress which occurs. Other research [16, 32,39] has suggested that residual stress magnitudes or distributions do not seriously affect the results. This is an important contradiction, because residual stresses are induced in fabrication, during the plastic deformation of the steel, and during heat straightening. It is very difficult to make reliable predictions of these residual stresses or to measure them without damaging the structure or specimen, and so the ability to predict the effects of heat straightening will be severely limited if residual stresses are important. Therefore, some of these specimens were devoted to the resolution of this question. These specimens were reheated with identical heat and load patterns used on specimens without prior heating or plastic deformation. If residual stress affects the behavior, considerable difference in plastic deformation should be noted.

Quenching has also been proposed as an aid to heat straightening, and so thirteen of the specimens were quenched and tested with similar heat and load patterns as some unquenched specimens. The quenching was performed with a water mist applied to both surfaces until the steel was cooled below $212^{0}F$.
The volume of water was measured before and after quenching. The difference between these measurements is the volume of evaporated water and this provides an approximate measure of the heat removed by quenching. Quenching was started immediately after completion of the heating in some cases, but in other specimens it was delayed for a period of 15 seconds to 4 minutes. Comparison of these different quench times provides an indication of the effectiveness of quenching and the conditions under which it is most useful.

Series A Set-Up

The previous discussion has described the general parameters evaluated in Series A tests. The primary objectives of the Series A experiments are to provide a better understanding of the heat straightening process, to resolve contradictions and conflicts noted in previous research and practice, and to provide an experimental base for a theoretical model which is discussed later in this report. A wide range of parameters were studied, and therefore, all of the specimens were different. However, there were some basic similarities which should be noted.

The specimens were all heated with an oxy-aceteline torch as noted earlier. The V-heat was applied in a serpentine pattern, on a specimen which was loaded and supported as shown in Fig. 3-4. The heated area was nominally under constant bending moment, and the plate was supported laterally a short distance on each side of the heated area. The support prevented twisting or out of plane movement, but it permitted all in-plane rotation and expansion.

The load was applied by two different methods. Specimen 1 through 32 and H1 through H9 were loaded with a hanging weight as shown in Fig. 3-5. This method provided constant moment, but it was somewhat unstable due to the pendulum motion of the weight when the steel was heated to high temperatures on large areas. This load arrangement caused large out of plane deformation in some of these specimens. The remaining specimens were loaded with a hydraulic ram, as shown in Fig. 3.6. The ram was controlled by a constant pressure valve which was attached to a tank of pressurized nitrogen gas. This control is somewhat analogous to the pressure control used by scuba divers. It eliminated the pendulum effect and potential instability of the specimen, but it meant that the applied load was not absolutely constant during the experiment, because the gas pressure did not respond rapidly to the time and temperature dependent deflections of the plate. This force was monitored over time in these experiments with the computerized data acquisition system and a weighted average was used for the constant load value. The true force was typically somewhat smaller than this value at the start of the test, but larger during the middle portion of the test .

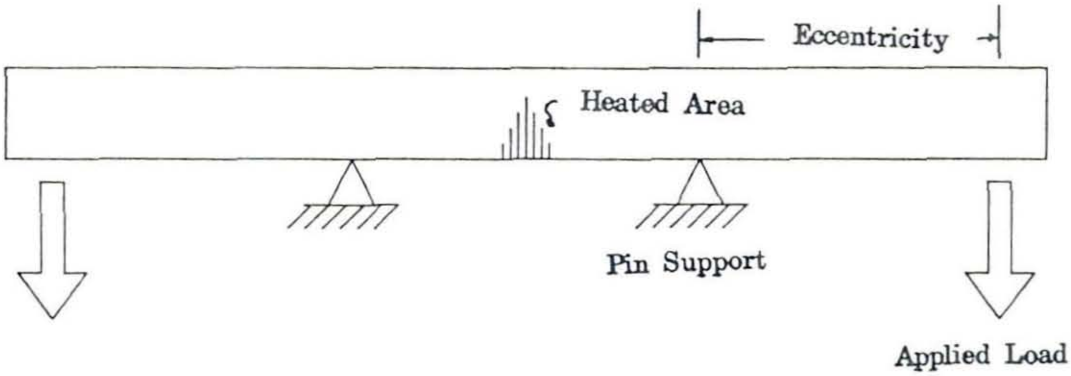

Figure 3.4. Test Set-Up for Series A Experiments.

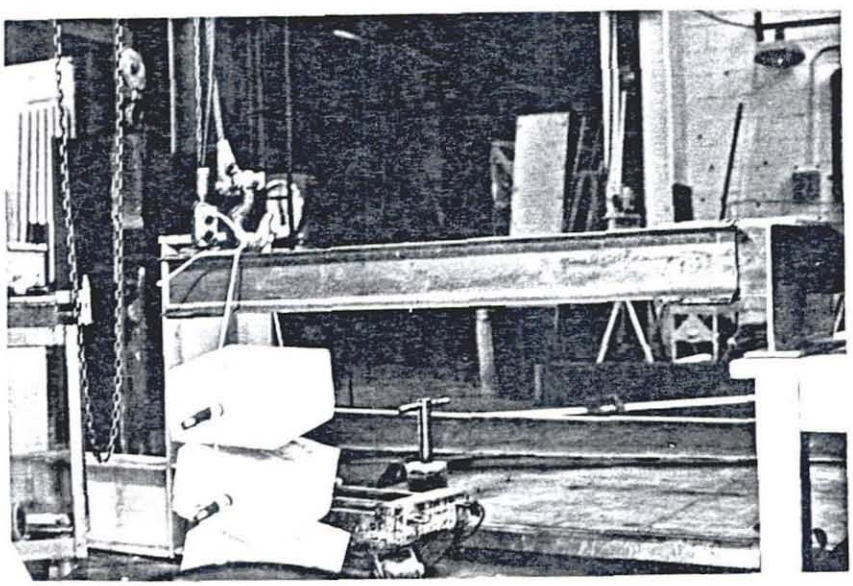

Figure 3.5. Photograph of the Hanging Weight Load Application.

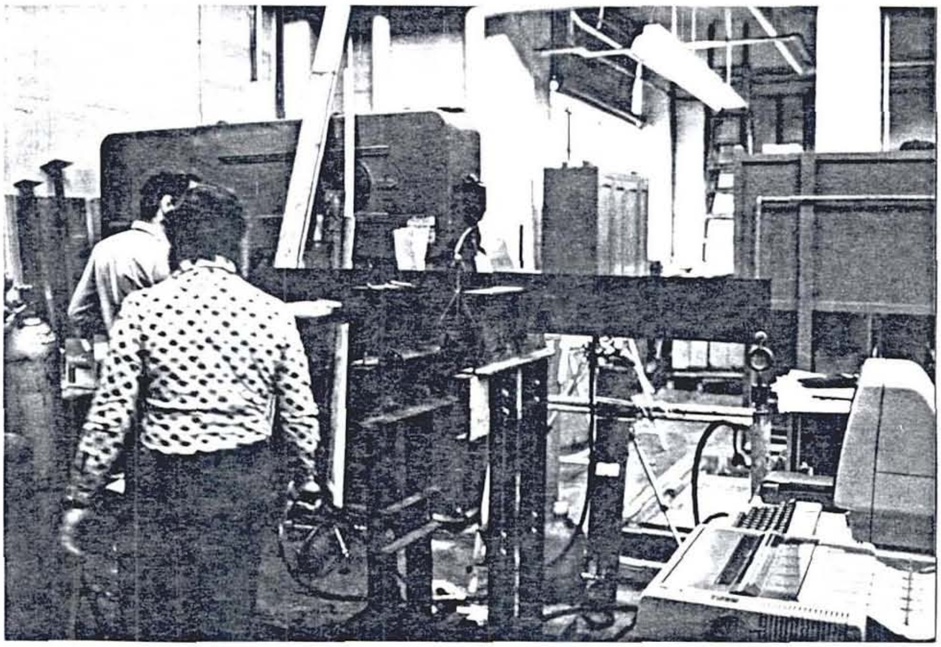

Figure 3.6. Photograph of Hydraulic Ram Test Set-Up.

because of the movements shown in Fig. 3-7. A grid of hardened steel pins was imbedded in each plate for measurement of the plastic rotation and strain distribution due to heating. This grid consisted of 0.125 inch diameter pins inserted into a .123 inch hole for approximately 2/3 the plate thickness as shown in Fig. 3-8. Distances between these pins were measured with a vernier caliper to .001 inch and interpolated to $\pm$.0005 inch to obtain the strain distribution. These surface measurements were found [39] to provide a reliable indication of average in plane deformation if the out of plane deformation was not too large. Measurements for specimans with large out of plane deformation may require an additional correction for this out of plane curvature. Measurements of the distances between pins which were 1, 2 and 3 inches on either side of the plate centerline were also made, and they were used to estimate the plastic rotation due to the heat application and to estimate the validity of the plane sections remain plane assumption. Two independent measurements were taken and if the difference between the two was greater than .001 inch, another independent measurement was taken. These measurements were taken both before heating and after cooling to determine the plastic strains caused by the heat.

Out of plane deformations were measured with a steel straight edge before heating and after cooling. The steel straight edge was placed on a set of milled blocks, and deflections were measured at the quarter points with the aid of a depth gauge. If the out of plane deflection was excessive, this measurement was then used [39] to correct the in-plane measurements.

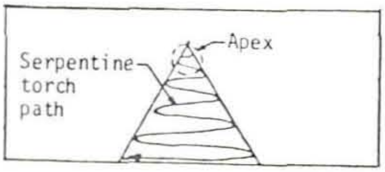

a. Torch path

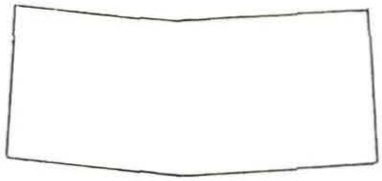

b. Exaggerated shape of the plate when hot

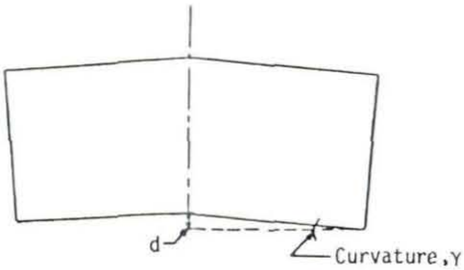

c. Exaggerated shape of the plate when cool

Figure 3.7. Time and Temperature Dependent Deflections of the Heated Plate.

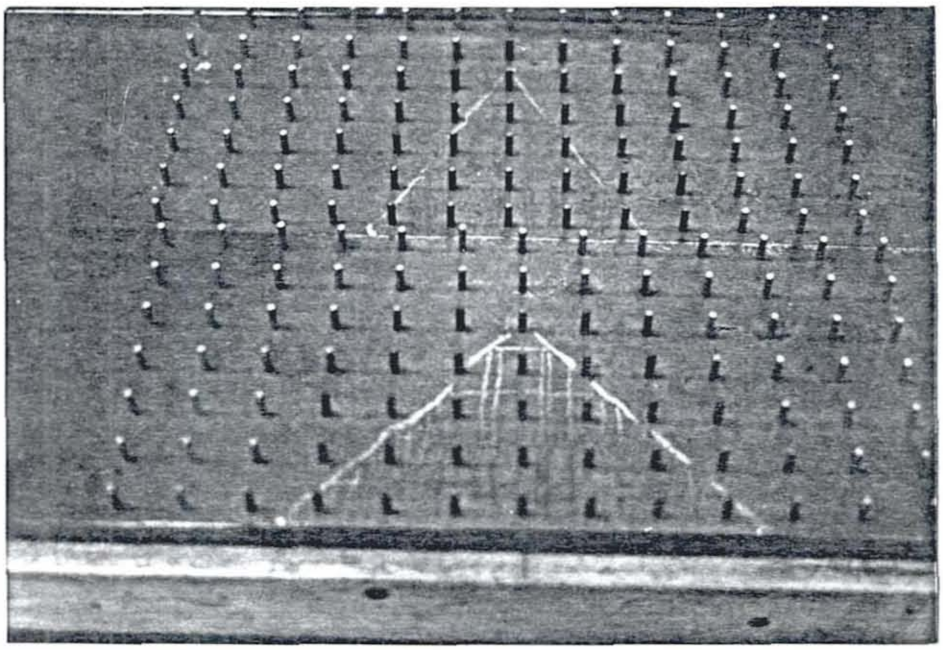

Figure 3.8. Photograph of the Grid Used for Strain and Rotation Measurements.

measurements.

Series B Experiments

The Series B experiments were the first step in applying the knowledge gained in the Series A experiments to structural shapes and practical applications. This series was divided into two parts. The first part, Series B-1 consisted of wide flange columns which were heated with V-heats on a single flange while supporting a compressive load as shown in Fig. 3.9. This heat pattern would typify the repair method needed to produce a lateral-torsional deformation of the column. Eight specimens were tested and the general parameters used in each test are summarized in the next chapter. All specimens were W6x25 wide flange sections of A36 steel. This shape was chosen because its flange size (b = 6.08 and t = .32 inches) closely approximated the 3/8" x 6" plate size used in many Series A experiments. Two of the specimens B1-1 and B1-2 had no axial force or other loading during heating. Hardened steel pins were installed in the heated flange of these two specimens as used in series A, and the results of these two experiments were compared to Series A experiments. This comparison shows the influence of the web and unheated flange on the test results, and it provides a general indication of the applicability of the Series A plate test results to structural shapes.

The remaining six specimens of Series B1 were designed as simply supported columns for weak axis buckling with weak axis $\frac{kl}{r}$ values varying between 60 and 120. A compressive load between 40% and 80% of the AISC [40] design service load was

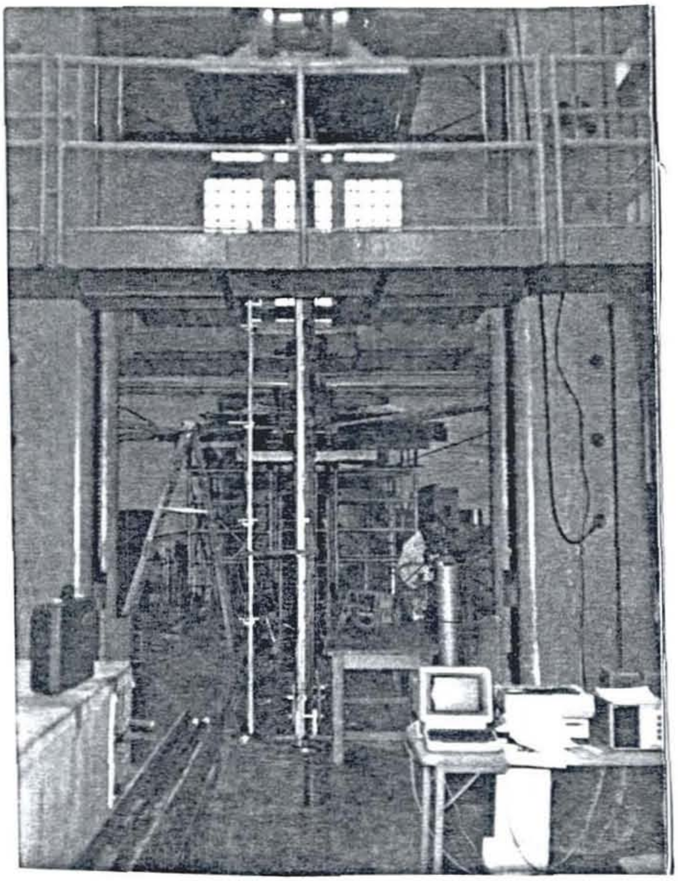

Figure 3.9. Photograph of Test Set-Up for Series B Column Tests.

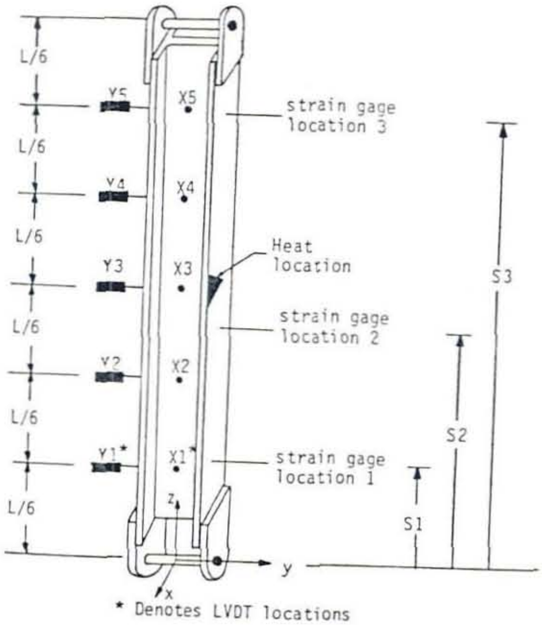

Figure 3.10. Placement of Strain Gages and LVDT's in Series B Column Tests.

applied and maintained constantly during the experiment. This load was applied to evaluate the effect of compressive load on plastic deformation attained during heating and to determine if the elevated temperature introduces any tendency toward buckling of the column. This later consideration is important in the repair of seismic damage, because gravity loads must be supported during the repair. Elevated temperatures dramatically reduce the modulus of elasticity and yield stress of steel, and thus the ultimate buckling load will be smaller. If this reduction in strength does not exceed the reserve strength or margin of safety of the column, it may be possible to repair the damage with minimal added bracing or support.

Deflections were measured with linear voltage displacement transducers (LVDT's) on both direction at points along the axis of the columns as shown in Fig. 3.10. Strain gauges were mounted in sets of five as shown in Fig. 3.11 at 3 locations as shown in Fig. 3.10. These strain gauge locations were out of the heat affected zone, and provided a measure of the time and temperature dependent forces and moments in the column. Temperatures were measured with temperature indicating crayons, and a non-contact pyrometer as used in Series A. All strains and deflections were measured with the electronic data acquisition system described in Series A. The measurements were taken at 15 second time intervals from just prior to application of compression load until the specimen had reached thermal equilibrium. The heat was applied with the same torch size and settings as used in Series A experiments.

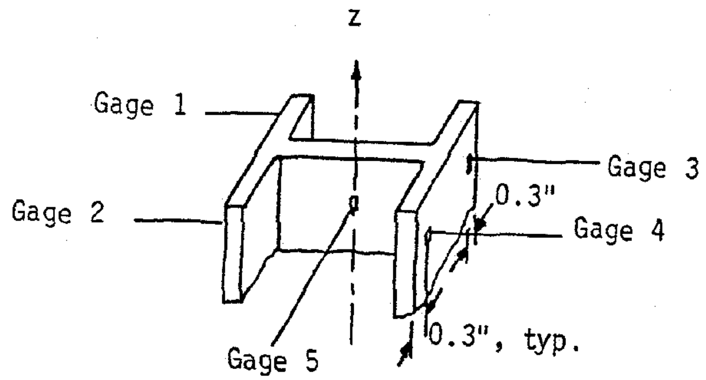

Figure 3.11. Distribution of Strain Gages over the Cross-Section in Series B Column Tests.

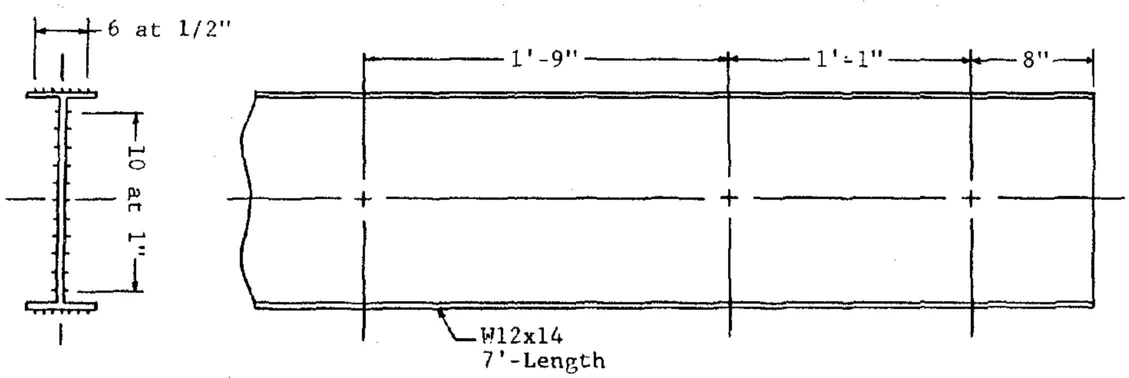

Figure 3.12. Whittemore Gage Strain Measurement Locations for Series B Beam Tests.

Series B-2 consisted of two W12x14 sections which were heated with a continuous strip heat on a single flange as shown in Fig. 2.1(b). This heat pattern is typically used to introduce a distributed curvature (or camber) to a beam section. The strip heat pattern is quite different than the V-heats used in the other experiments, since it has a greater symmetry. Every segment along the length of the member experiences a similar time and temperature history. However, the yielding is caused by the compressive stress developed through restraint provided by the unheated steel as in the Series A experiments. The ends of the beam cannot develop this restraint, and so local end effects may be expected. Series B-2 provided a measure of the curvature and strain distribution produced by the strip heat and an indication of the effect of the end boundaries on the resulting strain distribution. The beam was supported as a 7' simple span with no load (other than its self weight) applied. The top flange was heated to 1200^{o}F (649^{o}C) with a medium size torch. The beam was drilled and punched for a 10" Whittemore Gage at the center span, quarter span, and near the end as shown in Fig. 3-12. The longitudinal distance between punch marks were carefully measured before heating and after cooling. The temperatures were monitored at points along the length of the specimen with a grid of temperature indicating crayons.

Summary of Experimental Program

This chapter has provided a description of the Series A and B experiments. The experiments are not totally unique, since limited experimental work [37, 38, 39] has been performed in earlier research. However, these experiments will provide both a broader and more in-depth understanding than is available from the existing research. The detailed strain measurements used in Series A and B-1 will provide an accurate measure of curvature and distribution of plastic strain. The deformation measurements are more accurate than those used in previous research, and the greater accuracy will be helpful in development of a mathematical model. They will serve as a baseline for comparison to theoretical calculations described later in this report and will provide a check of the validity of assumptions such as plane sections remain plane. The temperature measurements will show both the magnitude of the peak temperature but also the distribution of the temperature over time and position. Research which has been performed to date used relatively simple measurements of deflection to estimate curvature and strain, and the peak temperature was typically assumed to be constant over the heated area, while the unheated area is assumed to remain at room temperature.

This experimental study also broadens the understanding of thermal stress behavior, through the wide range of parameters evaluated in Series A. These experiments help to resolve many of the inconsistencies noted in the literature, and it begins to sort the substantiated facts from the unsupported opinions.

CHAPTER 4

ANALYSIS OF EXPERIMENTAL RESULTS

Series A Experiments

The Series A experiments were performed [41] and the results for mild steel are summarized in Table 4.1. The results for high strength steel are summarized in Table 4.2. This chapter will provide a description and analysis of these results. The evaluation will focus on the important parameters and contradictions in present practice noted in the earlier chapters.

Distribution of Strain and Curvature

These experiments provide a valuable contribution to the understanding of heat straightening since they are the first experiments to provide a reliable measure of the distribution of strain in the deformed member. This is an important step in the development of a mathematical model for predicting the heat straightening effect. A series of steel pins were attached to the steel specimen as shown in Fig. 3.8, and comparison of the distances between pins provides a measure of the strain produced by thermal yielding. Longitudinal strains were measured for all specimens, but transverse and diagonal distances were also measured for the majority of test specimens. Figures 4.1 and 4.2 show the typical constant strain contours for longitudinal and transverse strain, respectively. These typical measurements were

TABLE 4.1

EXPERIMENTAL DATA FOR MILD STEEL SPECIMENS

SPECIMEN #	SPECIMEN CODE	SPECIMEN THICK. (IN)	SPECIMEN DEPTH (IN)	HEAT DEPTH RATIO	HEAT TEMP. (F)	HEAT ANGLE (DEG)	HEAT TIME (MIN)	LOAD RATIO	ANGLE PLASTIC ROTATION (DEG)	NET ELONG-ATION (IN)	CORRE-LATION COEFF.
1	S 4	.375	5.90	.67	1150	82	4.08	.23	.56	-.015	.996
2	S 7	.375	5.90	.67	1200	82	3.65	.23	.58	-.014	.989
3	S 5	.375	5.90	.75	1150	82	5.75	.23	.67	-.017	.990
4	S 1	.375	5.90	.75	1200	82	5.55	.23	.76	-.016	.991
5	S 2	.375	5.90	.67	1250	45	3.03	.23	.54	-.014	.999
6	S11	.375	5.90	.67	1125	82	4.78	.16	.66	-.017	.993
7	S 3	.375	5.90	.75	950	82	3.67	.16	.39	-.009	.991
8	S 9	.375	5.90	.67	1000	45	2.00	.13	.25	-.007	.992
9	S12	.375	5.90	.67	925	60	2.22	.09	.21	-.005	.994
10	S 8	.375	5.90	.67	975	60	2.62	.25	.35	-.006	.984
11	S13	.375	5.90	.75	1075	60	2.73	.16	.42	-.011	.993
12	S10	.375	5.90	.67	700	82	3.25	.16	.17	-.002	.996
13	S14	.375	5.90	.75	700	82	2.28	.16	.16	-.002	.986
14	S 6	.375	5.90	.75	725	60	1.27	.16	.08	-.001	.976
15	S28	.375	5.90	.67	1025	82	4.83	.09	.52	-.011	.992
16	S27	.375	5.90	.67	1025	60	3.12	0.00	.40	-.011	.998
17	S26	.375	5.90	.67	1275	45	3.00	.16	.67	-.016	.999
18	S21	.375	5.90	.67	975	45	2.25	.25	.47	-.007	.997
19	S20	.375	5.90	.67	1050	60	2.08	.23	.35	-.004	.991
20	S19	.375	5.90	.67	950	82	2.95	0.00	.22	-.004	.989
21	S18	.375	5.90	.67	1025	82	2.75	-.23	-.03	.001	.819
22	S25	.375	5.90	.75	1000	60	4.10	.16	.39	-.003	.998
23	S24	.375	5.90	.75	700	60	1.53	.16	.15	-.001	.982
24	S23	.375	5.90	.75	950	82	5.15	.16	.52	-.008	.995
25	S22	.375	5.90	.75	700	82	2.73	.16	.29	-.002	.988
26	S15	.375	5.90	.67	1450	82	7.75	.16	.74	-.017	.992
27	S16	.375	5.90	.75	1500	82	7.70	.16	.93	-.021	.995
28	S17	.375	5.90	.75	1475	60	6.92	.16	.87	-.021	.997
29	S29	.375	5.90	.67	1200	45	2.75	-.25	0.00	-.001	.091
30	S26	.375	5.90	.67	1150	45	2.28	.23	.60	-.011	.999

TABLE 4.1 (Continued)

SPECIMEN				HEAT							
#	CODE	THICK. (IN)	DEPTH (IN)	DEPTH RATIO	TEMP. (F)	ANGLE (DEG)	TIME (MIN)	LOAD RATIO	ANGLE PLASTIC ROTATION (DEG)	NET ELONG- ATION (IN)	CORRE- LATION COEFF.
31	S13	.375	5.90	.75	1200	60	3.27	.23	.69	-.015	.999
32	S11	.375	5.90	.67	1200	82	3.17	.23	.60	-.014	.995
33	S33	.375	5.90	.67	1260	60	2.50	.16	.38	-.010	.996
34	S34	.750	5.90	.67	1240	60	2.13	0.00	.15	-.007	.999
35	S35	.750	5.90	.67	1240	60	2.10	.09	.22	-.009	.998
36	S36	.750	5.90	.67	1240	60	2.35	.16	.34	-.012	.999
37	S37	.750	5.90	.67	1250	60	2.45	.23	.41	-.012	.998
38	S38	.250	7.90	.67	1220	60	1.77	0.00	.25	-.012	.993
39	S39	.250	7.90	.67	1240	60	2.33	.09	.41	-.018	.991
40	S40	.250	7.90	.67	1200	60	1.78	.16	.33	-.014	.992
41	S41	.250	7.90	.67	1180	60	1.97	.23	.37	-.011	.992
46	S46	.375	5.90	.67	1000	60	1.92	.16	.28	-.007	.995
47	S47	.375	5.90	.75	1260	60	2.33	.16	.46	-.012	.999
48	S48	.375	5.90	.75	1175	60	2.50	.16	.33	-.009	.999
49	S49	.375	5.90	.75	1125	60	2.17	.16	.26	-.007	.999
50	S50	.375	5.90	.75	820	45	1.25	.16	.08	-.001	.975
51	S51	.375	5.90	.75	925	45	1.42	.16	.17	-.004	.998
52	S52	.375	5.90	.75	1150	60	2.08	.16	.40	-.011	.994
53	S53	.375	5.90	.75	1230	82	3.83	.16	.73	-.022	.996
54	S54	.375	5.90	.75	1490	60	8.13	.16	1.17	-.032	.999
55	S55	.375	5.90	.75	1400	82	8.40	.16	1.16	-.036	.996
56	S56	.375	5.90	.75	780	45	1.33	.16	.08	-.001	.999
57	S57	.375	5.90	.75	1000	45	1.83	.16	.20	-.005	.998
58	S58	.375	5.90	.75	1180	60	2.60	.16	.34	-.009	.999
59	S59	.375	5.90	.75	1110	82	2.83	.16	.42	-.010	.994

TABLE 4.2

EXPERIMENTAL DATA FOR HIGH STRENGTH STEEL

SPECIMEN				HEAT							
#	CODE	THICK. (IN)	DEPTH (IN)	DEPTH RATIO	TEMP. (F)	ANGLE (DEG)	TIME (MIN)	LOAD RATIO	ANGLE PLASTIC ROTATION (DEG)	NET ELONG-ATION (IN)	CORRE-LATION COEFF.
91	H 1	.375	5.90	.75	1100	82	3.53	0.00	.15	.002	.995
92	H 2	.375	5.90	.75	1100	60	3.10	0.00	.21	-.004	.996
93	H 3	.375	5.90	.75	700	82	2.02	0.00	0.00	.002	.334
94	H 4	.375	5.90	.75	750	60	1.17	0.00	-0.00	.001	.203
95	H 8	.375	5.90	.75	750	82	1.97	0.00	.01	.001	.264
96	H 9	.375	5.90	.75	675	45	1.05	0.00	-.01	.003	.408
97	H 5	.375	5.90	.75	725	60	1.37	0.00	0.00	.002	.280
98	H 6	.375	5.90	.67	675	60	1.20	0.00	-.01	.003	.809
99	H 7	.375	5.90	.75	675	45	1.42	0.00	-.01	0.000	.538

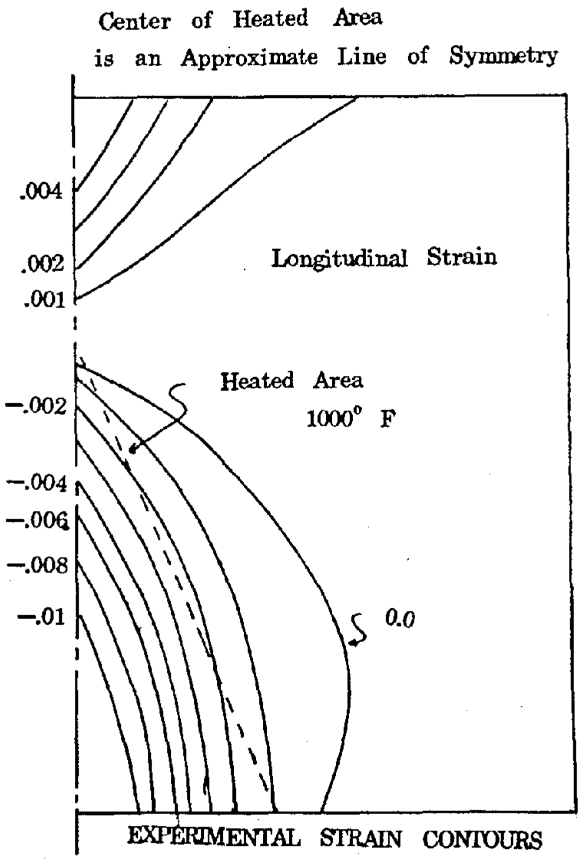

Figure 4.1. Constant Strain Contours for Longitudinal Strain of Typical Specimen.

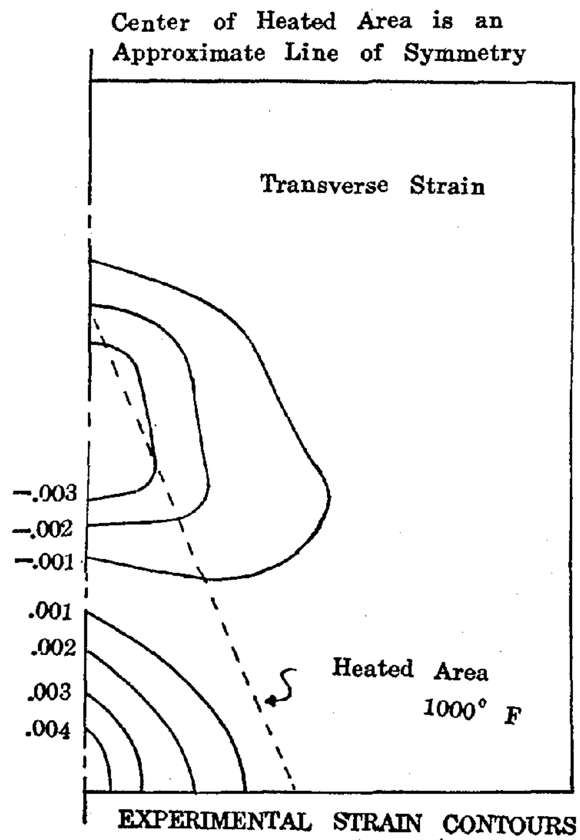

Figure 4.2. Constant Strain Contours for Transverse Strain of Typical Specimen.

taken from Specimen 8. The magnitude of the measured strains varied for different test conditions, but several general observations could be noted. First, most but not all of the yielding occurred within the heated area. This is an important observation, since most mathematical models assume all yielding is confined to the heated area. Second, large transverse strains were noted within the heated area. The combined effect of these observations was that the heated plates developed a plastic rotation with a bulge as noted in Fig. 4.3. Most longitudinal residual strains are compressive strains (i.e., longitudinal shortening) while transverse strains are typically in elongation in the heated area and in compression in other areas. Further, the magnitude of the transverse strains was typically one half of that observed in the longitudinal strain. It is frequently suggested that plates with tensile stress in the heated area will yield in tension rather than compression. Specimens 21 and 29 were heated with a negative moment (i.e., the moment introduced tensile bending stress in the heated area), and no significant yielding was noted. The maximum compressive residual strains were usually in the order of 1 or 2%, and larger strains were noted for specimens heated to hotter temperature and specimens with larger plastic rotations.

The plastic rotation produced by the V-heat was measured by two methods. The first method was used in previous research [36], and it employed a depth gauge and straight edge to measure deflections along the bottom edge. The rotation was then inferred by assuming a concentrated plastic rotation at the center of the member. The bulging effect noted in Fig. 4.3 and

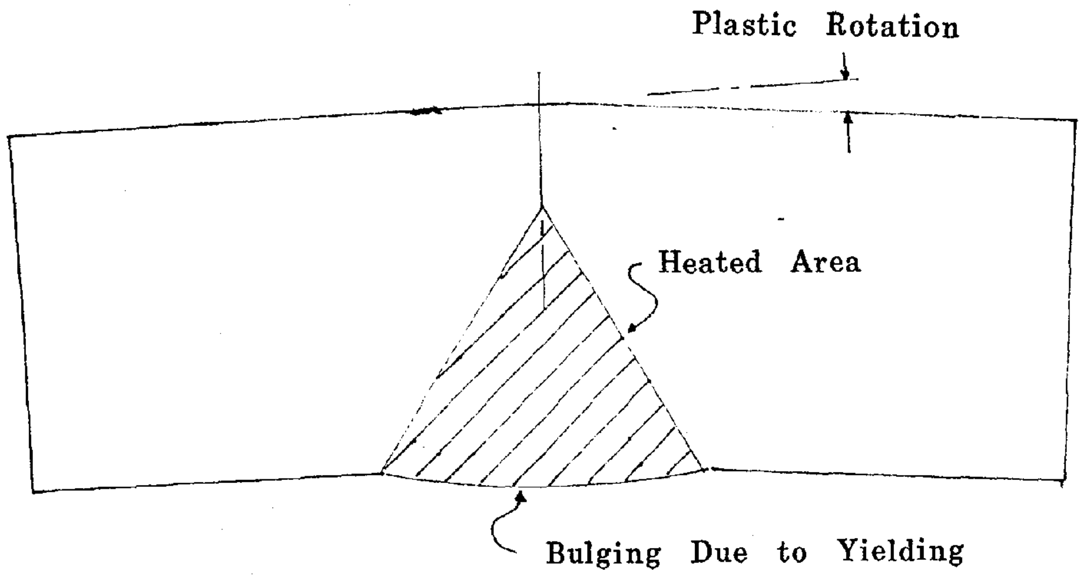

Figure 4.3. Bulging of Heated Specimen Caused by Transverse Strain.

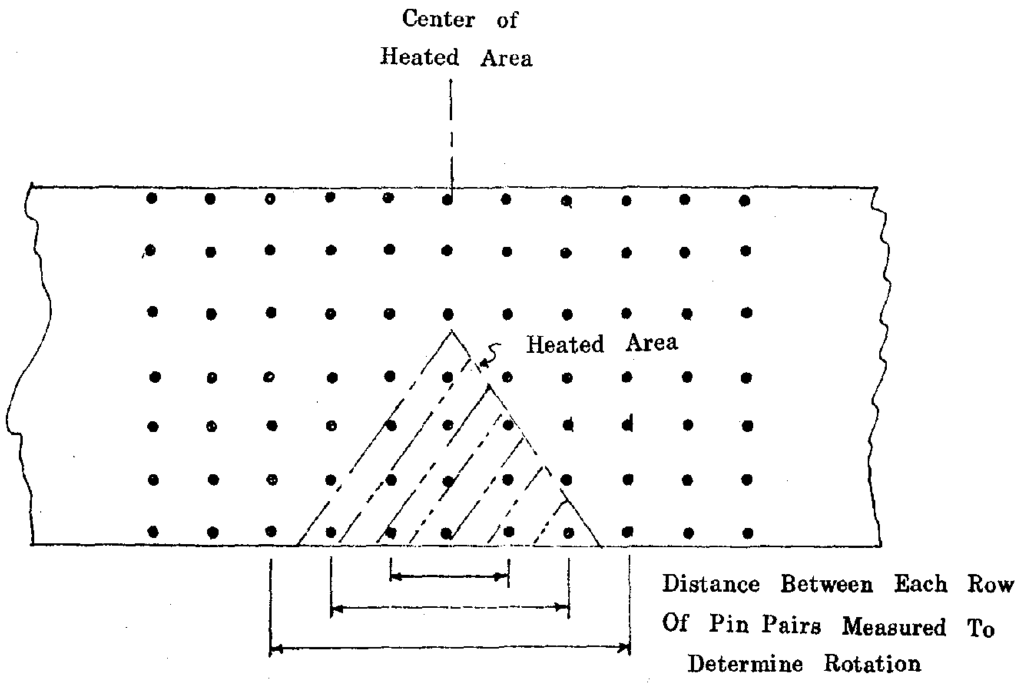

Figure 4.4. Pin Measurements Used for Determination of Plastic Rotations.

the small deflections measured made these rotations relatively unrepeatable and inaccurate. Therefore, a second method was used. This method [39, 41] used measurements between vertical lines of pins which were symmetric about the heated zone as shown in Fig. 4.4. The measurements were made before heating and after cooling, and the differences between these results were analyzed by the least squares method to determine rotations. This second method provided a much more accurate and repeatable measure of rotation and these rotations are used throughout this report. It should be noted that the first method generally overestimated the plastic rotation, because the center of plastic rotation (and neutral axis) was not at the center of the member as assumed by the method. This occurred because all members except one became shorter during the heating process. This is an important observation, because damaged members typically elongate during plastic deformation.

The method shown in Fig. 4.4 was used for rotation measurements, but it also provides a measure of the reliability of the assumption of plane sections remain plane. The plane sections assumption is used in the analysis of many structural members to satisfy strain compatibility conditions. It is therefore reasonable to expect that the assumption may be useful in developing a mathematical model for predicting the deformation produced by thermal stress. The hypothesis was checked by performing a statistical correlation [42] study. It was found that plane sections clearly do not remain plane within the heated area. The statistical correlation was invariably less than .5 or clearly satisfied a short distance outside the heated area since a correlation coefficient larger than .99 was attained in this region. Several specimens did not provide good correlation with the hypothesis. However, they all had essentially zero plastic deformation and the poor correlation occurs because of the limitations in the accuracy of the measurements.

Effect of Temperature

The temperature of the heated area is probably the most important parameter in heat straightening. Figure 4.5 shows the plastic rotation as a function of the average measured temperature of the heated area for all mild steel specimens. There is considerable scatter in the data, because many of the other parameters were varied during the tests. However, it is clearly evident that plastic rotation increases with temperature, and there is no limiting temperature as suggested in one previous work [15]. This effect is more precisely illustrated in Fig. 4.6, where all of the parameters are held constant and most of the experimental scatter is eliminated. While the temperature is extremely important, it is also difficult to accurately define. All of the heating was performed by technicians, and they judged the temperature by the color of the heated steel. In addition, actual measurements of surface temperature were made on the front and back of the specimen (as described in Chapter 3) to obtain the average temperature. Even the most experienced practitioners made relatively poor estimates of this average temperature, since they commonly misjudged it by $\pm$ 100^{o}F ($\pm$ 55^{o}C) and sometimes misjudged it by more than $\pm$200^{o} F (110^{o} C). Further, different

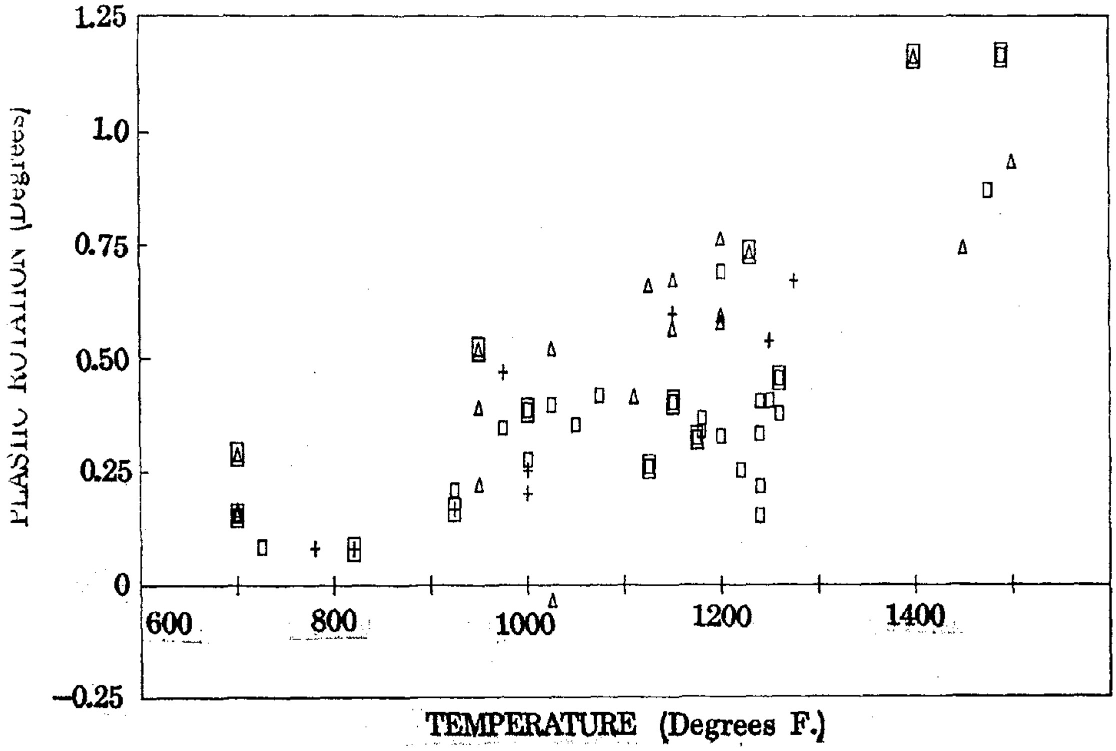

Figure 4.5. Plastic Rotation as a Function of Temperature for All Mild Steel Series A Specimens.

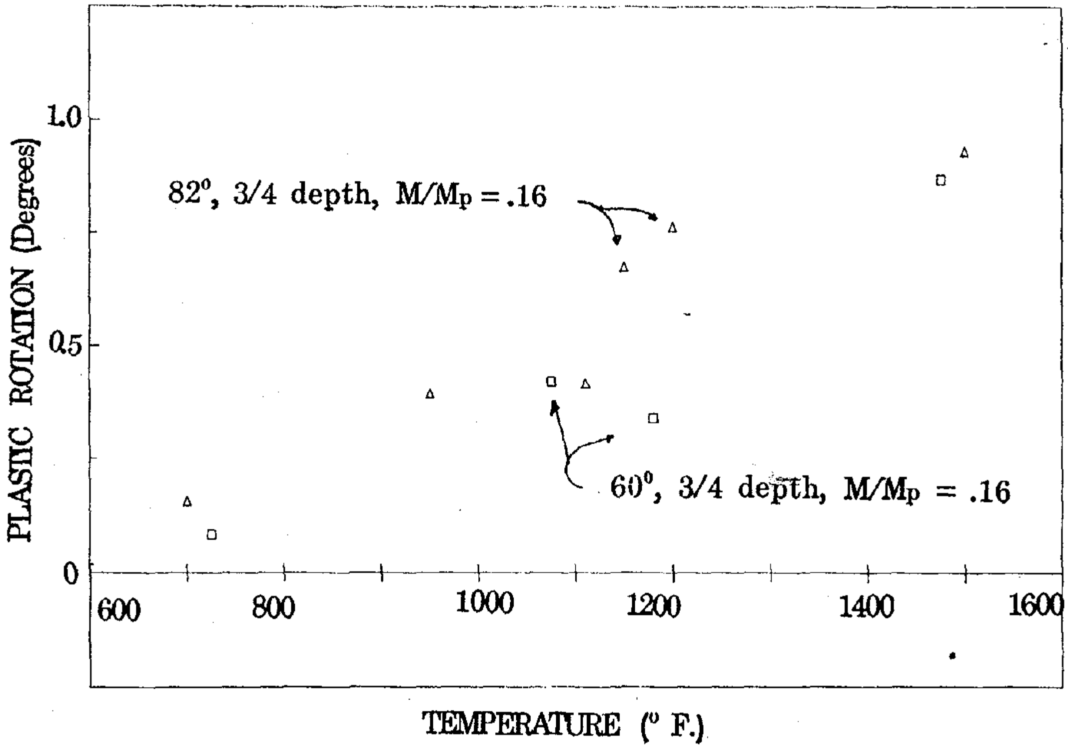

Figure 4.6. Plastic Rotation as a Function of Temperature for Mild Steel Series A Specimens with 60° and 82° V-Heat at 3/4 Depth.

technicians apply the heat differently and this likely contributes to the scatter noted in the figures. For example, some practitioners use a tight pattern with a more rapid torch movement as shown in Fig. 4.7(a) while others use a coarse mesh with slow torch speed as shown in Fig. 4.7(b).

This human variation in the application of the heat is further illustrated in Fig. 4.8. The torch tip and gas pressure were held constant for all experiments, and so the heat flux should be approximately constant for all specimens with differences introduced only by human variation in the application of the heat (i.e., the height and angle of the torch and torch speed). If the heat flux is constant, the time required to heat the specimen should vary approximately linearly with the temperature for a unit volume of heated steel. Fig. 4.8 is a plot of time required to heat a unit volume as a function of temperature. The relationship is approximately linear, but there is considerable scatter because of human variations in the use of the torch. In view of this variation, small differences in plastic deformation must be expected for different individuals.

Higher temperature results in larger plastic rotations for a given heat pattern and load condition. However, there is a minimum temperature below which no plastic deformation can be expected. This minimum temperature varies with load but is the order of 600°F (315°C) for mild steel and 1000°F (540°C) for T-1 steel. It should be noted that these minimum temperatures are higher than those suggested by a perfect uniaxial restraint analysis. Since higher temperature produces larger plastic rotation, it is tempting to use the hottest possible temperature,

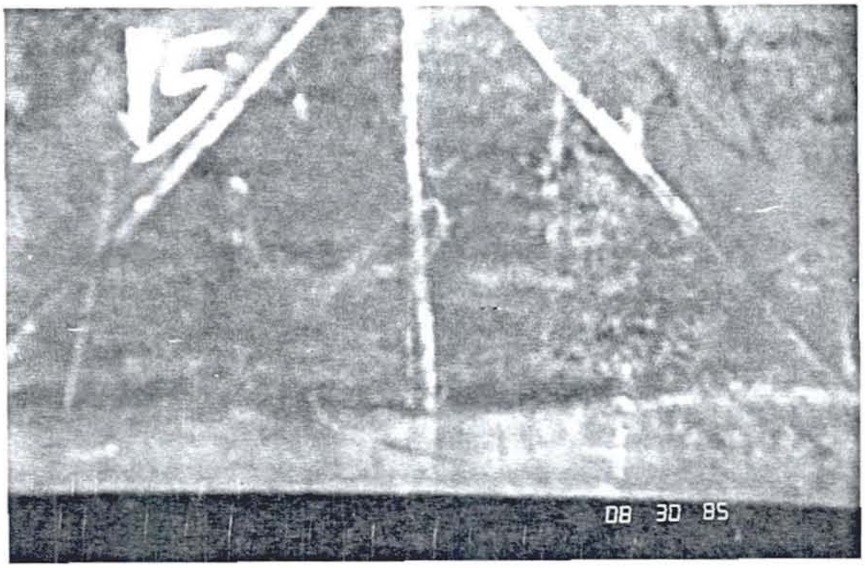

Figure (a)

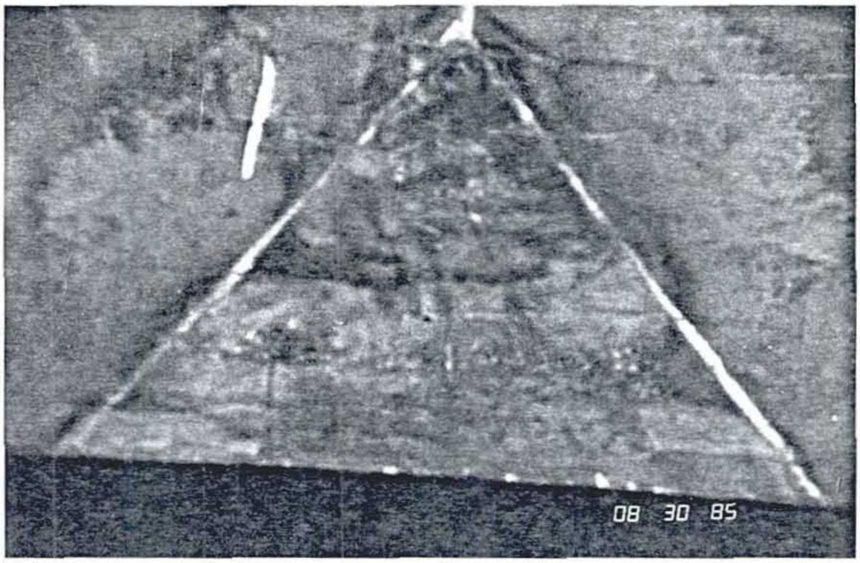

(b)

Figure 4.7. Photographs of Different Heat Patterns Obtained by Different Technicians.

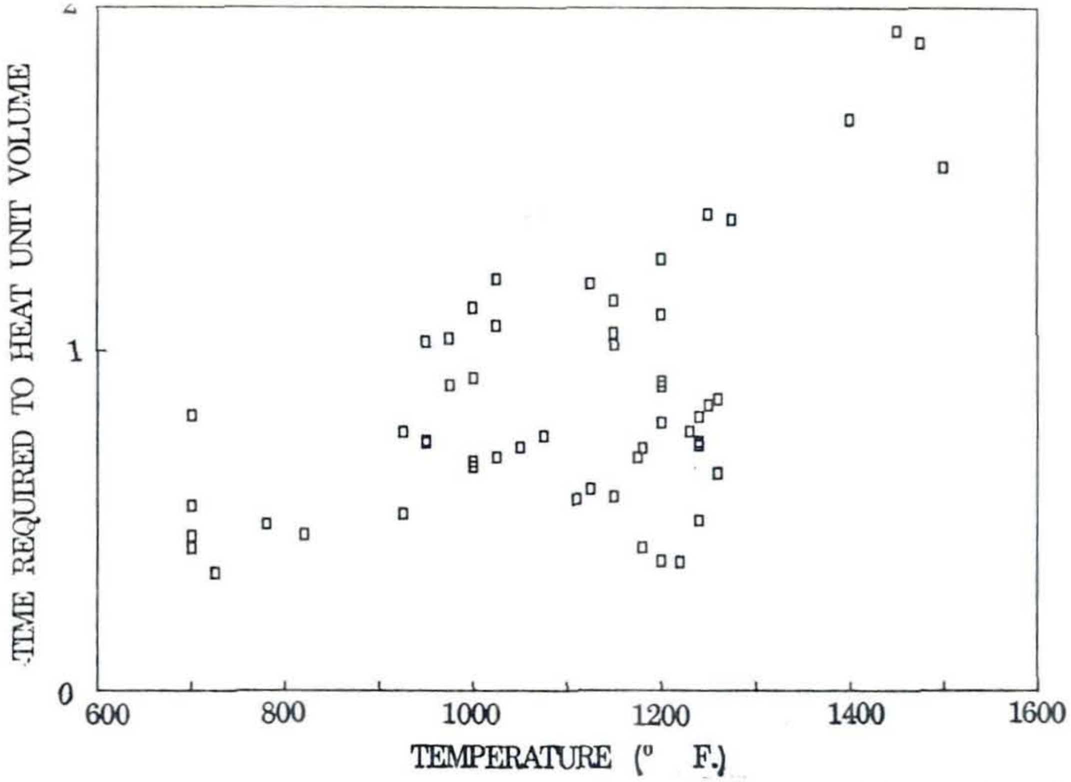

Figure 4.8. Time Required to Heat a Unit Volume of Heated Steel to the Target Temperature.

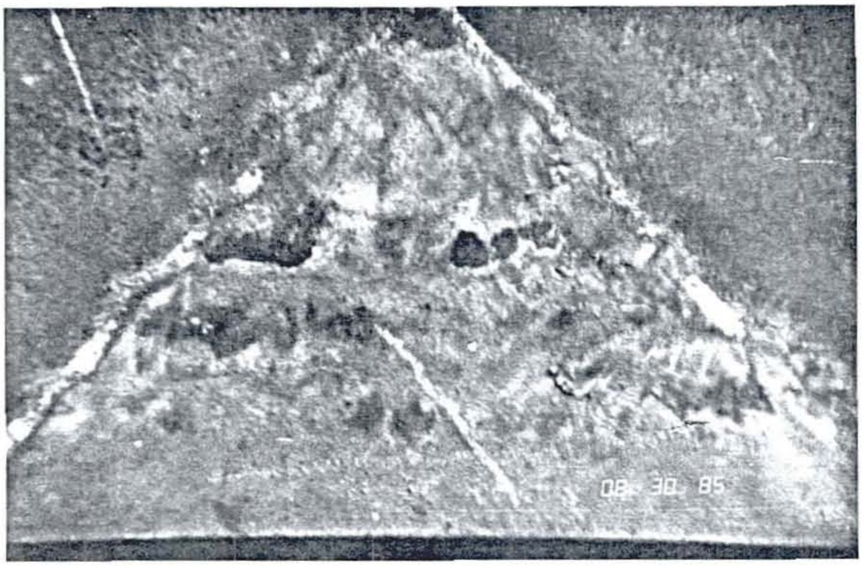

Figure 4.9. Photograph of Surface Damage Caused by Temperatures in Excess of 1400°F.

but caution must be exercised. Previous discussion has indicated that structural steel should not be heated to a temperature greater than approximately 1300^{o}F without better information as to the effect of the temperature on the material properties. Since most technicians cannot consistently estimate the temperature with greater accuracy than $\pm$100^{o}F, 1200^{o}F is a practical limit on temperature. Second, while all of the specimens supported the applied load without buckling during these tests, test specimens had an inclination toward out-of plane distortion and possibly plate buckling with increased temperature. Finally, Series A experiments showed that pitting and surface damage to the steel occurred when the surface temperature exceeded approximately 1400^{o}F (760^{o}) as shown in Fig. 4.9.

Effect of Applied Load

Previous research [36, 38, 39] has shown that an applied load which introduces compressive stress into the heated area will increase the plastic rotation. The series A results support this conclusion as illustrated in Fig. 4.10. The specimens were loaded with a constant moment in the heated area as shown in Fig. 3.4. The ratio of the applied moment to the plastic moment capacity at room temperature, M_p, is plotted against the plastic rotation for the specified heat geometry and temperature in this figure. The elevated temperature reduces the plastic moment capacity while it introduces a thermal moment. The thermal moment required to reach M_p is smaller if M/M_p increases, and so it is very logical to expect that increasing applied load

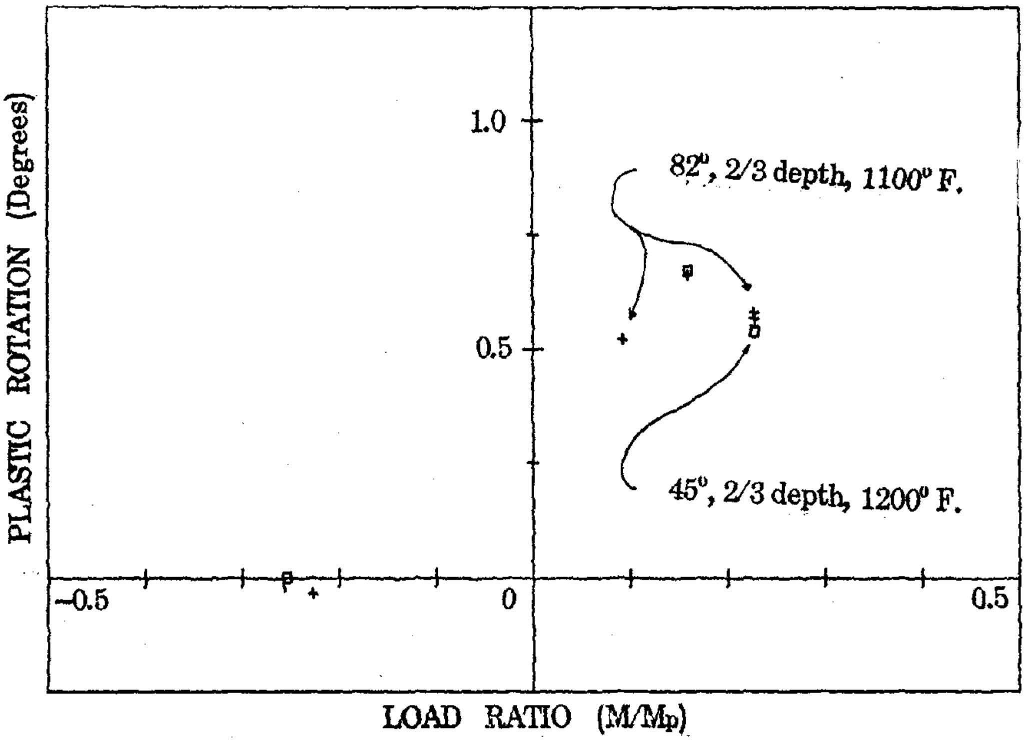

Figure 4.10. Plastic Rotation as a Function of Loading.

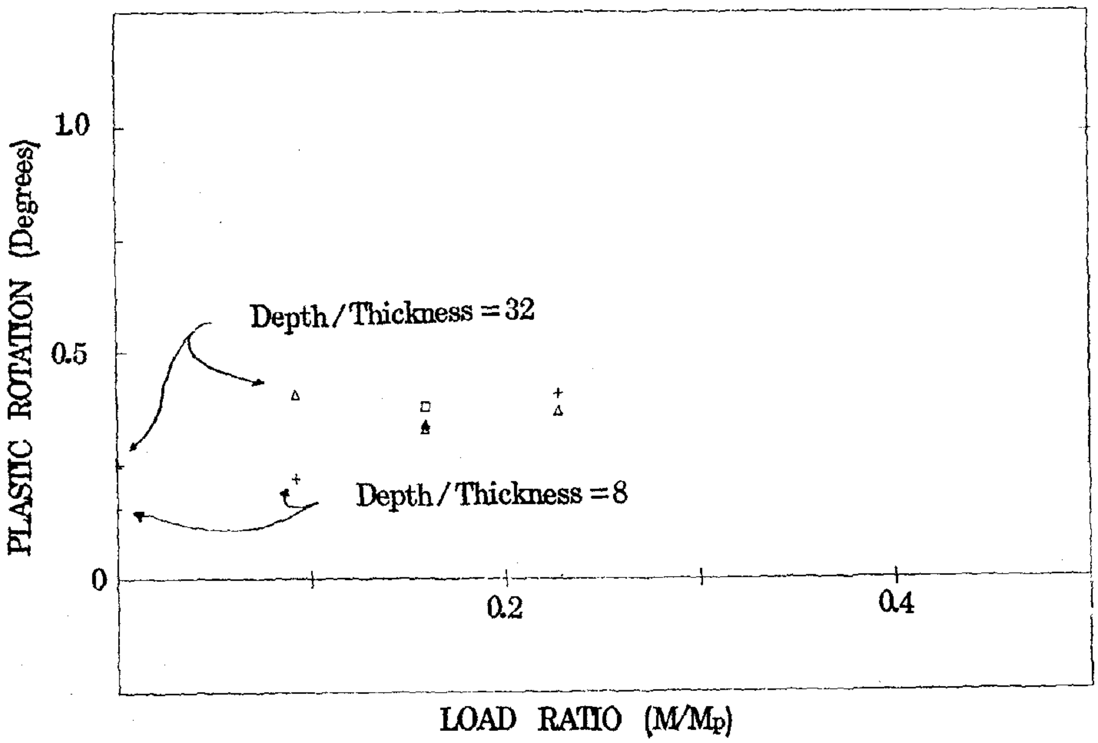

Figure 4.11. Plastic Rotation Achieved by Different Specimen Geometry with Similar Heat Pattern and Load Conditions.

will increase the plastic rotation.

Effect of Residual Stress

It is frequently suggested that residual stress has a major impact on plastic rotation achieved in heat straightening. If this is correct, different plastic rotations must be expected for virgin specimens, specimens which have been damaged due to prior loading and specimens which were deformed during earlier heating, since the residual stress will be quite different for each of these conditions. Specimens 30, 31, and 32 were reheated and were compared to similar control tests. Test 32 is comparable to 1 and 2 while 30 and 31 are comparable to 5 and 11, respectively. The plastic rotation does not vary significantly for the reheated specimens, and so it is reasonable to conclude that residual stresses do not affect the plastic rotation significantly. This conclusion can be rationally explained because it is well known [43] that the plastic moment capacity, M_p, is not affected by residual stress if all forms of buckling are prevented. Residual stress must be self-equilibrating, and so they cause no net force or bending moment. Residual stress may induce early or delayed yielding, but the full plastic rotation can be achieved only after the applied moment reaches the critical value required for the given temperature profile.

Effect of Specimen Geometry

Three different specimen geometries were evaluated in Series A. They covered a range of depth to thickness ratios of from 8 to 32. Figure 4.11 shows the plastic rotation attained for different specimen geometry as a function of M/M_p where the temperature profile is similar for all specimens. This figure suggests that there is a geometric effect, but the precise influence is not clearly defined. For small values of M/M_p, thick, shallow specimens resulted in significantly larger plastic rotations. For larger load ratios, narrow, deep specimens had slightly larger plastic rotations, but the difference was not great. The reason for this variation is not totally clear, but many factors affect the behavior. Thermal stress is very sensitive to the temperature gradient, and two dimensional heat conduction [20] depends on the depth of the specimen. However, the time required for heating depends upon thickness as well as the depth, and therefore a greater relative quantity of heat flow can be expected for shallow, thick specimens. This causes variations in the temperature gradient as a function of time and modifies the yield pattern. The problem is further complicated by the fact that the thick plate was heated from both sides. Therefore, the deformation will vary with plate geometry for similar heat patterns, but the variation appears to be related to differences in heat conduction flow and the resulting thermal gradient rather than other fundamental differences.

Effect of Quenching

Some of the specimens were quenched with a water mist after heating. Quenching was usually started 30 seconds after completion of heating, but some experiments were started immediately after heating while others were delayed for 2 to 4 minutes. The mist was sprayed on both sides of the specimen until the steel was cooled to 212°F (100°C). The weight of the evaporated water was measured, since it is an approximate indication of the heat removed by quenching. Table 4.3 summarizes some of the quenched test results and provides a comparison of the quenched tests to similar unquenched specimens. Most specimens showed a significant increase (typically 20% to 80%) in plastic rotation with quenching, but there were several notable exceptions. Specimens 48, 49, and 51 showed a reduction of plastic rotation with quenching, and 22 and 50 showed little effect of quenching. However, special circumstances can be associated with these specimens. Specimen 48 and 49 used a delayed quenching, and delayed quenching reduces the plastic rotation as shown in Fig. 4.12. This figure shows the plastic rotation attained for different specimens with different delay times for quenching and similar heat patterns and loading ratios. Specimen 22 and 51 are compared to unquenched specimens with somewhat hotter temperatures, and elevated temperatures cause increased rotation as noted in Figs. 4.5 and 4.6. Quenching is clearly most effective when a large quantity of heat can be dissipated, since Table 4.3 shows that specimens with the largest weight of evaporated water also had the largest increase in rotation. In view of these observations, it is logical to conclude that quenching will consistently increase the plastic rotation if the quenching is performed shortly after heating, but quenching should be used with great care at temperatures in excess of 1200^{o}F (650^{o}C), since sudden cooling may affect the material properties as noted in Chapter 2.

TABLE 4.3

TEST DATA FOR QUENCHED SPECIMENS

QUENCHED SPECIMEN								UNQUENCHED COMPARISON			
#	DEPTH RATIO	HEAT ANGLE	LOAD RATIO	TEMP. (F.)	ROTATION ANGLE	DELAY TIME	WGT. WATER	#	TEMP. (F.)	ROTATION ANGLE	COMP. RATIO
22	.750	60.	.1587	1000.	.3876	30	156	11	1075	.419	.925
23	.750	60.	.1587	700.	.1543	30	101	14	725	.084	1.833
24	.750	82.	.1587	950.	.5203	30	236	7	950	.394	1.320
25	.750	82.	.1587	700.	.2894	30	195	13	700	.157	1.847
47	.750	60.	.1587	1260.	.4560	0	56	58	1180	.340	1.340
48	.750	60.	.1587	1175.	.3251	120	38	58	1180	.340	.955
49	.750	60.	.1587	1125.	.2619	240	30	11	1075	.419	.625
								58	1180	.340	.770
50	.750	45.	.1587	820.	.0795	30	67	56	780	.082	.971
51	.750	45.	.1587	925.	.1672	30	88	57	1000	.202	.827
52	.750	60.	.1587	1150.	.4046	30	127	11	1075	.419	.965
								58	1180	.340	1.189
54	.750	60.	.1587	1490.	1.1658	30	284	28	1475	.869	1.341

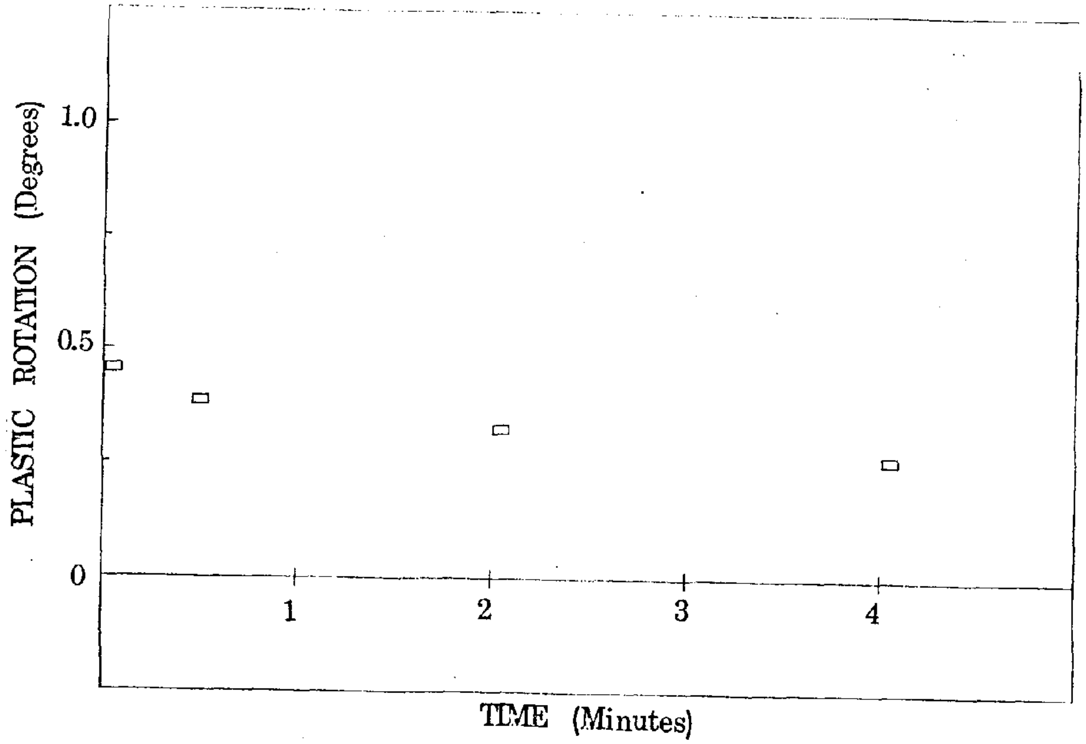

Figure 4.12. Effect of Time Delay of Quenching on Plastic Rotation.

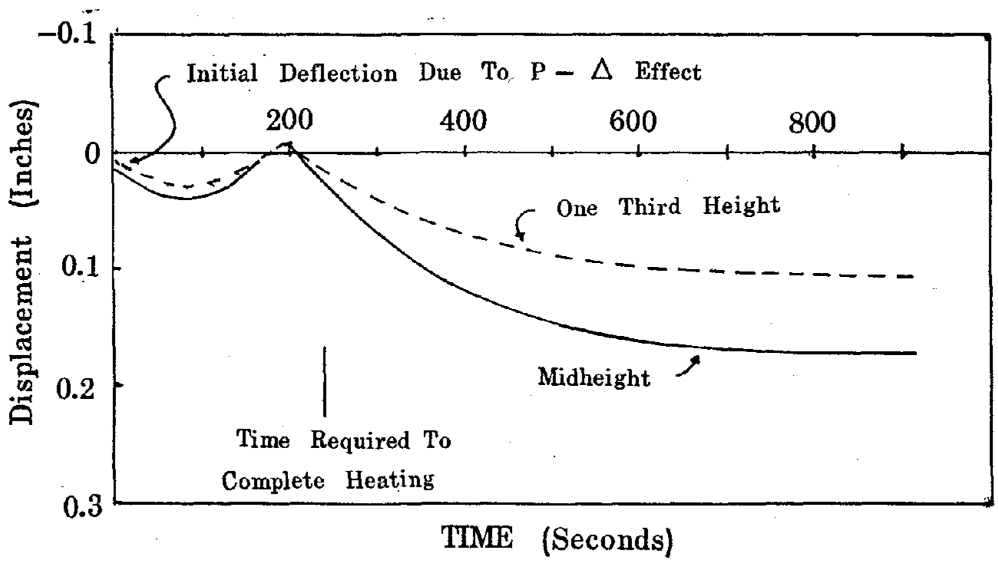

Figure 4.13. Time Dependent Deflections of Specimen B3

Effect of the Geometry of the Heated Area

Previous research [36, 38, 39] has shown that increasing the depth of the heat and the angle of the V-Heat increases the plastic rotation, and these conclusions are supported by the Series A experiments. Figure 4.5 shows that increasing heat angles generally results in increased plastic rotations even for heat angles as large as 82°. The effect of heat depth can be seen by comparing specific data points (such as Specimens 1 and 2 compared to 3 and 4) in Table 4.1. However, full depth heats may be less effective unless the heated steel is restrained by a compressive stress or bending moment, because it is approaching the unrestrained thermal expansion condition. While increasing heated area increases the plastic rotation achieved with a given temperature, the Series A experiments show that increases in heated area also increase the out of plane deformation and the probability of local buckling.

Effect of the Yield Strength of the Steel

Increased yield strength reduces the plastic rotation achieved with a given heat and load pattern. This contradicts the opinions held by some practitioners, but it can be clearly seen by comparing the data of Table 4.2 with that shown in Fig. 4.5. Increased yield stress increases the plastic moment capacity, M_p, and this reduces the effectiveness of an applied loading, since the load ratio is reduced. Thus, a larger temperature increase is needed to cause initial yielding. It is tempting to apply larger restraining loads, but this increases the probability of buckling, because the elastic modulus does not increase for high strength steel. However, most structural steels are carbon or low alloy steel will yield strength no greater than 50 or 60 ksi (345 or 415 MN/m^2), and so while high strength structural steels may require more effort to repair, it is not likely to be an insurmountable problem for most practical conditions. Quenched and tempered steel such as A514 probably can be repaired or cambered by heat straightening, but it may not be an economical procedure. A514 steel apparently does not deform plastically unless heated to temperatures in the order of $1000^{o}F(540^{o})$ or higher and the maximum temperatures will likely be limited to the tempering temperature of the steel (approximately $1150^{o}F$), because higher temperatures may change the material properties of the steel. These constraints seriously reduce the effectiveness of the method.

<u>Effect of Time and Variations in Thermal Properties</u>

Time and temperature were the most difficult parameters to control during these experiments, because they may vary dramatically with minor changes in the style of the operator. If the torch was held closer to the steel, at an angle to the steel, or was moved at a different rate or in a different pattern, the time required to heat the specimen will change as seen in Fig. 4.8. Further, as time elapses, conduction of heat within the metal and radiation and convection heat losses become more important, and and this further complicates the process. Table 4.4 helps to understand the effect of time. It compares the plastic deformations obtained for specimens with similar geometry, loading and heat profiles but with different heat times. Plastic rotation changes with the time required to heat the specimen, but there is no obvious, consistent relationship between the two. Further, the time dependent variation is relatively small compared to the variations observed with other parameters such as applied load and temperature. In fact, the differences seen in Table 4.4 in plastic rotation could also be explained by minor differences in temperature. In view of these observations, it is believed that the time required to heat the specimen is of secondary importance to the straightening process. That is, very large time differences are needed before significant differences in plastic rotation will occur. This is believed to be valid because time enters primarily through the conduction heat flow in the steel. The time required to heat a specimen must be long enough to assure a minimal temperature gradient through the thickness of the steel, and short enough to have favorable in plane time dependent temperature profiles. As long as the time remains within these limits, relatively small differences in plastic deformation are expected.

Series B Experiment

The Series B experiments were performed as the first step in extending the knowledge gained in Series A to more complex structural shapes and practical conditions. Two types of tests were performed. Eight W6x25 sections of A36 steel were tested, while simulating column loading. Two W12x14 sections were tested while simulating the cambering action (shown in Fig. 2.1(c)) commonly used for wide flange beams.

TABLE 4.4

COMPARISON FOR TIME REQUIRED TO HEAT SPECIMENS

HEATED SPECIMEN							COMPARISON SPECIMEN				
#	DEPTH RATIO	HEAT ANGLE	LOAD RATIO	TEMP. (F.)	ROTATION ANGLE	HEAT TIME	#	TEMP. (F.)	ROTATION ANGLE	HEAT TIME	COMP. RATIO
1	.670	82.	.2270	1150.	.5648	245	2	1200	.578	219	.978
							32	1200	.595	190	.949
2	.670	82.	.2270	1200.	.5776	219	32	1200	.595	190	.971
3	.750	82.	.2270	1150.	.6735	345	4	1200	.764	333	.881
33	.670	60.	.1587	1260.	.3794	150	36	1240	.336	141	1.131

Column Tests

The results of the column tests are summarized in Table 4.5. Two of the specimens (B1 and B2) were simple stubs of steel section, which were heated with no applied load. The heat was applied on a single flange, and the geometry of the flange closely simulated the 3/8" x 6" plates used in Series A. The rotations for Specimen B1 and B2 were measured with steel pins as in Series A experiments and they are rotations of a single flange rather than the total section. As a result, Specimens B1 and B2 are somewhat comparable to Series A specimens 16, 20, and 34. The rotation obtained for B1 and B2 appear to be smaller than would be consistent with the Series A test results. This indicates that the stiffness of the web and unheated flange reduces the plastic rotation over that occurring in flat plates. This reduction appears to be in the order of 25-30%, and it must be considered when evaluating the effect of thermal stress on structural shapes.

Specimens B3 through B8 were columns with $\frac{kl}{r}$ values of either 60 or 118 and they were loaded with an axial load which was 40% or 80% of the AISC allowable compressive load. The heat was applied on a single flange with heat patterns as used for B1 and B2. This heat pattern induces lateral motion and twisting of the wide cross section. Centrovidal deflections were measured at intervals during the heating and subsequent cooling, and they were used to determine plastic rotations. The weak axis rotation is the rotation of the centroid of the cross section and it is approximately one half that occurring in the heated flange. A strong axis rotation was also noted, but it was too small to be

TABLE 4.5

SUMMARY OF COLUMN EXPERIMENTAL RESULTS

	SPECIMEN DATA					HEAT DATA				PLASTIC ROTATION	
#	LENGTH (IN)	$\frac{Kl}{r}$	AISC P_{all}	APPLIED LOAD	LOAD RATIO	ANGLE OF HEAT	DEPTH RATIO	TEMP. (F.)	TIME (MIN.)	STRONG AXIS	WEAK AXIS
B1	UNLOADED COLUMN STUB					60	.67	1240	5.36	N/A	.19
B2	UNLOADED COLUMN STUB					82	.67	1225	5.33	N/A	.20
B3	179.4	118	76.6	61	.80	60	.67	1210	3.83	***	.22
B4	179.4	118	76.6	30	.40	60	.67	1250	3.35	***	.09
B5	91.2	60	127.5	102	.80	60	.67	1210	3.38	***	.16
B6	91.2	60	127.5	51	.40	60	.67	1200	3.59	***	.11
B7	91.2	60	127.5	102	.80	82	.67	1210	4.50	***	.21
B8	91.2	60	127.5	102	.80	45	.67	1210	2.92	***	.13

accurately measured. Fig.4.13 shows typical time dependent displacement records for specimen B3. It illustrates the classic behavior noted for heat straightening. That is, the specimen deflects in one direction during heating as shown in Fig. 3.7. Yielding occurs in the heated area and the contraction caused by cooling reverses the deflection to obtain the permanent rotations and deflections seen Fig. 4.13 and 3.7.

The above behavior illustrates an important consideration in the development of heat straightening programs for compression members. Initial heating of the steel increases the damage deflections of compression members. These deflections cause increased P-Δ moments while decreasing the strength and stiffness. This means that columns are more prone toward buckling while being repaired. One important objective of experiments B3 through B8 was to evaluate this tendency toward buckling. None of the columns exhibited a strong tendency toward buckling. They all supported the applied compressive load during the heating process.

Since the P-Δ effect reduces the compressive stress while the steel is hot and increases the compressive stress during cooling, the plastic rotations were smaller than if P-Δ deflections were prevented. This suggests that the addition of restraint, which restricts lateral deflection and limits the P-Δ moment, will be particularly effective for compression members. The experiments were further complicated by the warping stiffness of the columns. The heat pattern causes rotations about the longitudinal axis in addition to lateral movement. The pinned end boundary conditions (see Fig. 3.10) permits free rotation for the weak axis and fixes the strong axis. Since the pin essentially enforces the same rotation for both flanges, it also introduces a warping restraint. This warping effect was analyzed [41] and it was found that the warping restraint also reduces the plastic rotations obtained by a given heat pattern. These factors had considerable impact on the experimental results for specimens B3 through B8. The plastic rotations for these six specimens were relatively small compared to B1 and B2, when the increase in compressive stress is considered, and they are even smaller when compared to the Series A experiments. Increased axial force (and compressive stress) increased the plastic rotation, but the increase was limited by the P-Δ effect and warping restraint. Columns with low slenderness ratios, $\frac{Kl}{r}$, have larger working stresses but develop smaller plastic rotations for the given axial compression, because of their greater stiffness under compressive load. It must be again emphasized that the weak axis plastic rotations for specimens B3 through B8 should be doubled when compared to B1 and B2 and Series A experiments, because these are plastic rotations of the centroidal axis rather than rotations of the heated flange.

Beam Experiments

Two W12x14 beam specimens were heated [39] with a continuous strip heat pattern down the center of the flanges as depicted in Fig. 2.1(b). This pattern is frequently used to introduce camber into beams and girders. They were heated to approximately 1200^{O}F and the curvature and strain distribution were measured with a

Whittemore Gage at the mid-span, quarter-span and near the end. The specimen had no loading other than its own self weight. Table 4.6 summarizes some of the more important results of these tests. Fig. 4.14 illustrates a typical maximum temperature distribution over the steel cross section, and Fig. 4.15 shows typical strain or curvature distribution near the end of the specimen and at mid-span. It should be noted that the heat was continuous over the length. The assumption that plane sections remain plane appears to be satisfied within the flanges and web, although there is some twisting due to warping torsion. However, no compressive stress develops at the ends of the beams during heating, and so the plastic strain distribution is fairly constant over the length in the interior portions of the beam and it is smaller near the ends.

While the heat pattern was approximately constant over the length and symmetric about the plan of the web, significant transverse curvature was noted. That is, the beam also deflected normal to the plane of the web. This can be clearly seen from the strain distribution in Fig. 4.15, and it apparently was caused by residual stress in the beam and the narrow flanges of a deep section. The beam specimens had been previously used in a series of lateral-torsional buckling experiments, and so residual stresses should vary over the flange because of local yielding due to warping torsional stress. Residual stress is important for the Series B beam experiments but it is unimportant for the Series A experiments, because the plastic strains were much larger in the V-heated specimens. Figure 4.16 shows a typical elasto-plastic moment curvature relationship for a steel beam

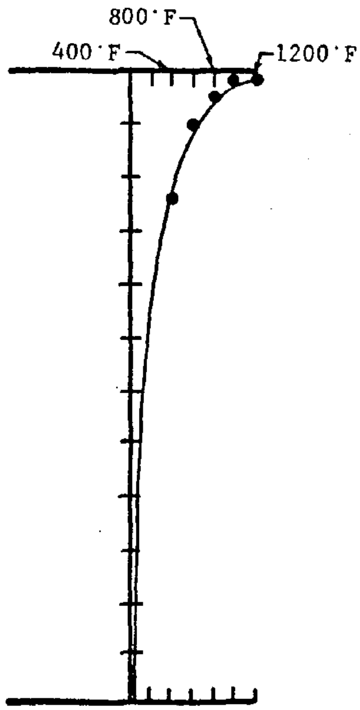

Figure 4.14. Typical Distribution of Maximum Temperature in the Wide Flange Beam Experiments.

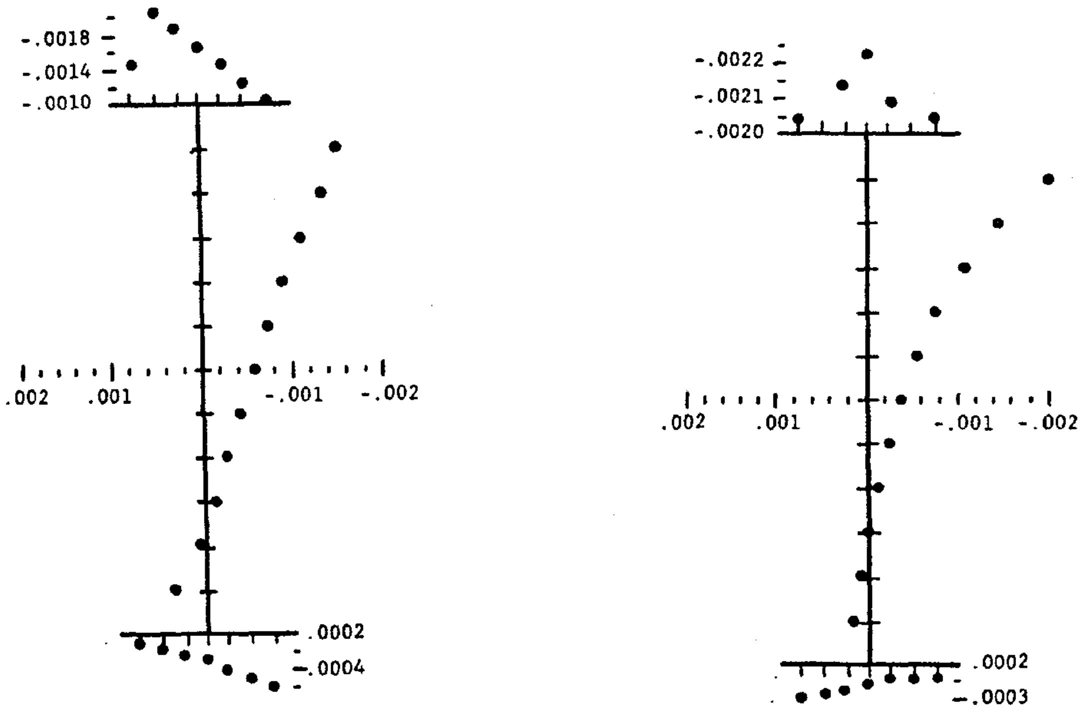

Figure 4.15. Residual Strain Distribution at Midspan and Near the End of the Beam Speciman.

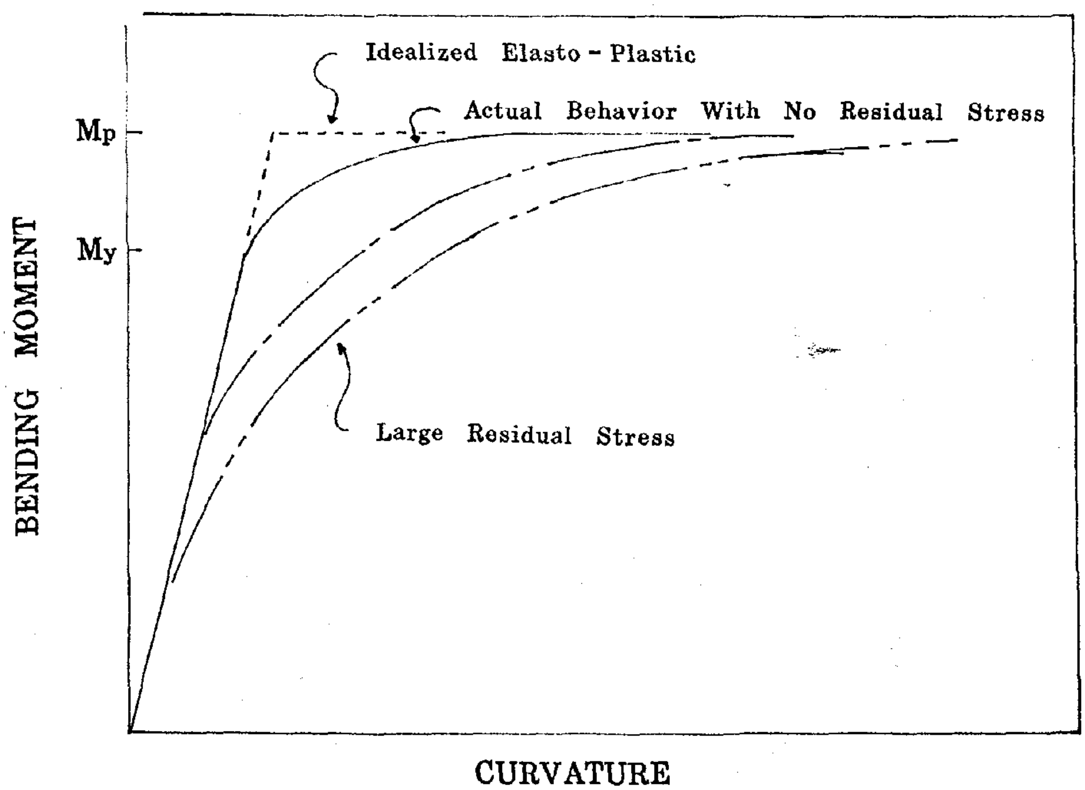

Figure 4.16. Typical Elasto-Plastic Moment-Curvature Relationship for a Steel Beam with and without Residual Stress.

with no residual stress, moderate residual stress and large residual stress. Residual stress has no impact on the ultimate plastic moment capacity of the beam, but they greatly influence the initiation of yielding. Therefore, if the thermal stress induces large internal moments (i.e., the elastic thermal moments would be large compared to the M_p of the section), the full plastic moment will be achieved, large plastic strains will develop, and the plastic rotation will not be influenced greatly by residual stress. However, if the yielding is marginal (i.e., the elastic thermal moment is small or at least not large compared to M_p), the plastic strains will be small, and the residual stress will have considerable impact on the plastic deformation. V-Heats typically use deep heat patterns with relatively high temperatures and this induces large thermal moments and plastic strains. Plastic strains in the order of .01 or .02 were commonly observed with V-heats, while the strip heats develops plastic strains which are an order of magnitude smaller. A V-Heat with low temperatures, small heat angle, or shallow depth would not develop these large internal moments and so residual stress would be more important. The strip heat used in the beam experiments causes marginal yielding, and residual stress becomes more important. This is clearly seen by comparing the maximum plastic strains seen in Fig. 4.15 with those seen in Figs. 4.1 and 4.2.

Summary

This chapter has provided a brief description of the Series A and B experiments, and an analysis of these results. It has shown how different parameters influence thermal stress and heat straightening. There is considerable scatter in the test results. This scatter occurs because it is not possible to precisely control the time and temperature in the experiments, and further it is not possible to precisely measure temperature or temperature distribution. However, the general conclusions are well supported and documented. Further, they seem to form a rational theoretical framework. In the next chapter a theoretical model will be developed and compared to these results. This is an important step because the model is needed before reliable predictions of heat straightening deformations can be achieved. The experiments provide an essential baseline for this model, since they help determine the reliability and validity of the calculations.

CHAPTER 5

A THEORETICAL MODEL

General Comments

The development of an analytical model for predicting the effects of heat straightening is essential to the development and utilization of heat straightening for damage repair. The results of a heating program must be predictable before engineers can specify its use in practice. As noted earlier, several models have been proposed. Holt [16,32] prepared a simple model for V-heats and spot heats. The model has given fair agreement with some but not all experimental results [30], but some serious anomalies can be noted. The model does not satisfy strain compatibility conditions for the V-heat, and it uses an unrealistic temperature distribution. It suggests that there is a maximum temperature for heat straightening, but this clearly is contradicted by experimental results. Further, it does not provide a realistic estimate of the effect of restraint and the effect of the depth of heating.

Brockenbraugh [34] has proposed the use of a strip model for continuous heats on steel shapes. Compatibility conditions are enforced by the application of the plane sections assumption. Experiments have shown that this assumption is severely violated within the heated area of concentrated heat patterns such as V-heats. The assumption is realistic outside the heated area and it is approximately maintained with continuous strip or edge heats. Other authors, [37,38] have attempted to extend this model to concentrated heat patterns, such as the V-heat or spot heat despite the compatibility problems with mixed results. This model is an iterative model and therefore more difficult to use than the simple model suggested by Holt. It eliminates some of the irrational predictions which may result from the simple model. It also permits the use of a realistic time dependent temperature distribution, but this is done at the cost of increased load steps and iterations. However, the model may provide a good indication of global behavior, if these refinements are introduced. It can never predict local behavior, and it will sometimes oversimplify the problem and produce erroneous results.

Therefore, another model was developed. The objective of this model was to predict both the local and global behavior of the heated member. The understanding of local behavior is essential, because local effects tend to influence important failure modes such as buckling, fracture and fatigue. The model must consider the time variant temperature distribution of the steel, and it must include the temperature dependent elastic-plastic strain and deformation. The heat flow and elastic deformation are theoretically coupled phenomenon [19], but this coupling effect is not significant unless the temperatures change very rapidly. Heat straightening appears to be well outside this critical range, and so the heat flow and plastic deformation problems are separated. The time dependent temperature profiles are first computed with a finite difference model. A series of time independent temperature distributions are generated from the heat flow analysis, and these are used as load steps for an non-linear finite element analysis. The temperature history is considered in all phases of the analysis, and the temperature dependent properties of the steel are included.

Heat Flow

A finite difference heat flow model [44] was developed for rectangular plate specimens such as those evaluated during Series A experiments. The plate was broken into a rectangular grid and a simple thermal energy balance was applied to each element.

$$\frac{\Delta T \rho C p \Delta V}{\Delta t} = q_k + q_c + q_r + q_f \quad . \tag{5.1}$$

ΔT and Δt are the incremental temperature and time, and ΔV is the volume of the element. The thermal mass is ρC_p, and q_k, q_c, q_r, and q_f are the rate of heat flow by conduction, convection, radiation and torch input flux, respectively. The thermal conductivity between adjacent elements is discretized by

$$q_k = K_n A_k \frac{T_a - T_e}{d_{ae}} \tag{5.2}$$

where A_k is the conduction surface area between elements, K_n is the thermal conductivity, d_{ae} is the centroidal distance between elements, and T_e and T_a are the respective element temperatures. Note that this simple model assumes the element is always of a uniform temperature. The convection and radiation heat transfer between the steel and the surrounding air are computed by the Newton equation,

$$q_c = A_c \kappa (T_e - T_a) \tag{5.3}$$

and the Stefan-Boltzman equation,

$$q_r = A_r F_e Fa \tag{5.4}$$

A_c and A_r are the areas for convection and radiation, respectively. F_e and F_a are the emissivity factor and the shape factor, and is the coefficient of convective heat transfer. Note that convection heat loss is not considered while the torch is heating a given element. Neither convection nor radiation have a significant effect on the element temperatures until the cooling cycle is started.

The input flux is a critical parameter in the development of a realistic time-temperature profile. The elements are sequentially heated to a target temperature with the pattern of a V-heat shown in Fig. 5.1. This pattern simulated the serpentine pattern shown in Fig. 2.1(a), but it assumes the temperature profile is symmetric about the centerline. While the heat flux was directed toward a single element, the spreading of the flame of the torch shown in Fig. 5.2 heats adjacent elements. Previous research [37] has shown that this spreading effect can be modeled with the equation

$$q_f = G(r)A \tag{5.5}$$

and

$$G(r) = ae^{-br} \tag{5.6}$$

where a and b are experimental parameters and r is the radial distance from the center of the torch. The parameters a and b vary with the size and placement of the torch and likely they require calibration for different welders.

The parameters a and b were selected to provide reasonable

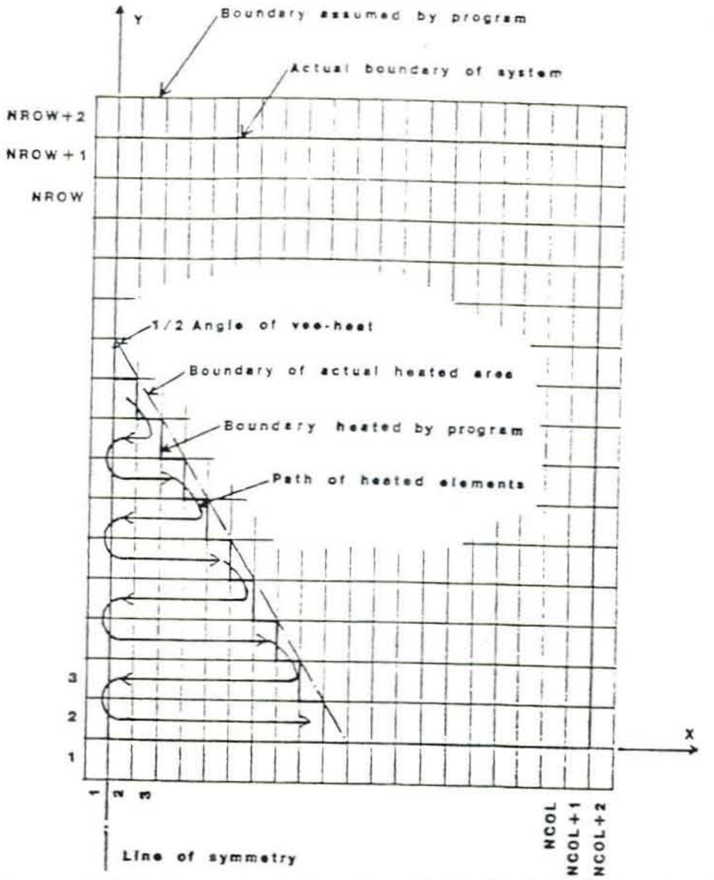

Figure 5.1. Sequential Heat Pattern Used To Model V-Heats in the Heat Flow Analysis

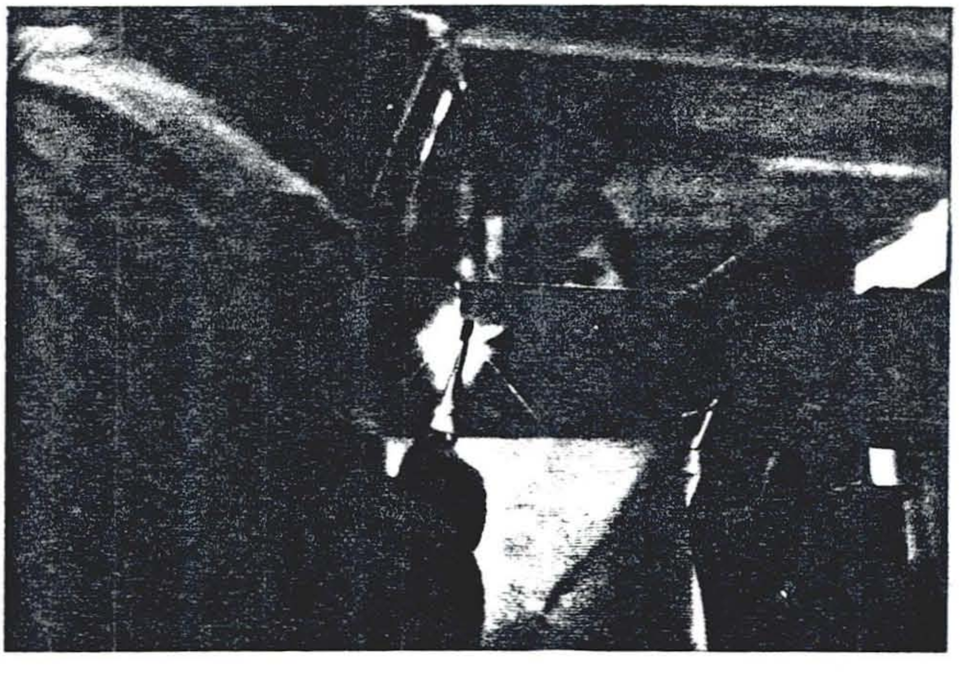

Figure 5.2. Photograph of Spreading of the Flame From Torch.

correlation with the temperatures observed during the experiments. The combination of equations 5.1 through 5.5 can then be solved to determine the time dependent temperature profile. Steady-state temperature profiles require the assumption of an initial temperature profile, and the correct temperature distribution is determined by iteration. However, the transient solution can be determined by direct step-by-step solution if the time step size is sufficiently small. The step size must be carefully selected to assure that the solution will be stable. This method was used for different temperatures and V-heat patterns, and the solution was obtained with a computer program developed on the Hewlett Packard HP 9816 Computer System. The program was written in HP Basic 2.0 and Appendix A provides a listing of this program with input instructions. Figs. 5.3 and 5.4 provide a typical comparison of these computed temperatures with experimentally measured results. Good correlation can be obtained with this mathematical model, but these results must be modified before they can be used in the non-linear stress-strain analysis. Therefore, a number of temperature profiles were selected at specific time intervals throughout the time history. The time intervals were selected to assure that the incremental temperature change for any element was not too large, (typically less than 150^{O}F) and 30-60 load steps were typically needed to simulate the heating and subsequent cooling program.

Non-Linear Finite Element Analysis

The time independent temperature profiles obtained from the

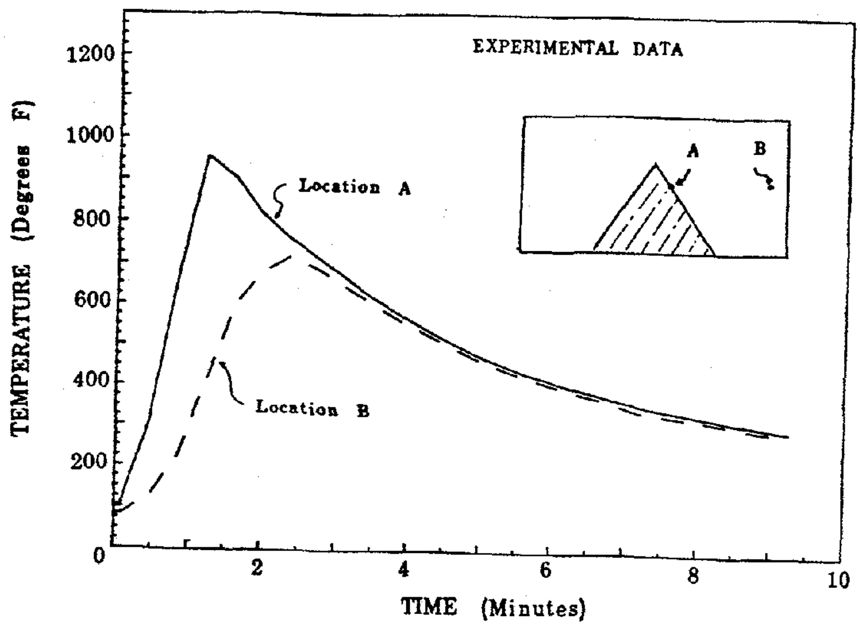

Figure 5.3. Measured Time-Temperature Profiles for a Typical Specimen.

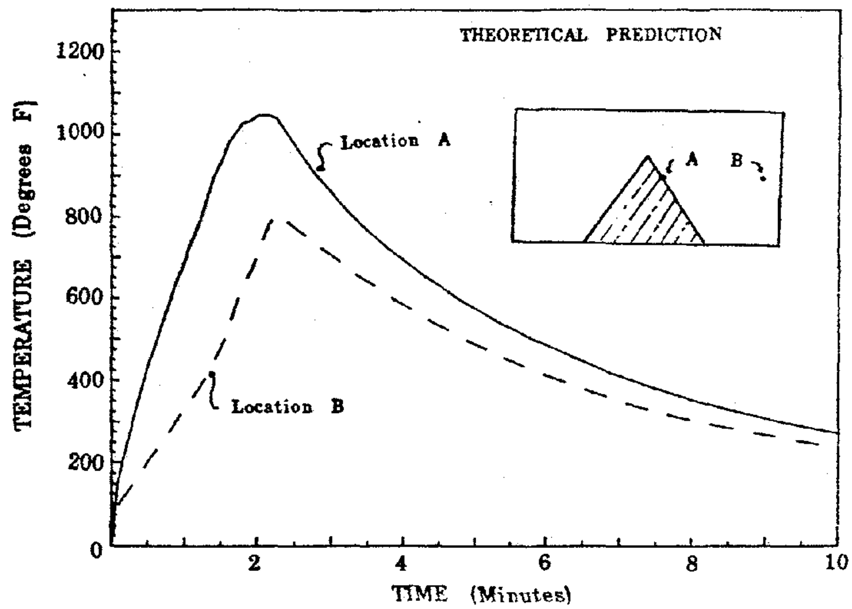

Figure 5.4. Computed Time-Temperature Profiles for the Typical Specimen Used in Figure 5.3.

heat flow analysis were then used as applied incremental loads for a non-linear finite element analysis. The finite element method was used to analyze V-heats and other concentrated heat patterns where the temperature gradient is large in the plane of heating but negligible through the thickness of the steel. Therefore, a plane stress isoparametric finite element was used. The elastic stiffness and properties of this element were derived by usual matrix formulation and variational methods [45]. The change in temperature for each load step and the temperature dependent coefficient of thermal expansion provided the applied loads for each step. It should be noted an elastic material with an incremental change in temperature and perfect biaxial restraint develops an internal stress.

$$\sigma_x = \sigma_z = \frac{\alpha \Delta T E}{1-\nu} \tag{5.7}$$

and so the coefficient of thermal expansion, α and the incremental temperature change provide an equivalent body force to the element.

Non-linearity is introduced through yielding of the steel the temperature dependence of the yield stress E and α. Figs. 5.5, 5.6 and 5.7 show the variations of these parameters used in the analysis. The Von Mises yield criteria was used as the yield surface. This criteria depends only upon the deviatoric component of stress, and yielding occurs when

$$J_2' - k^2 \geq 0 \tag{5.8}$$

where J_2' is the second invariant of the deviatoric stress tensor and k^2 is the yield constant.

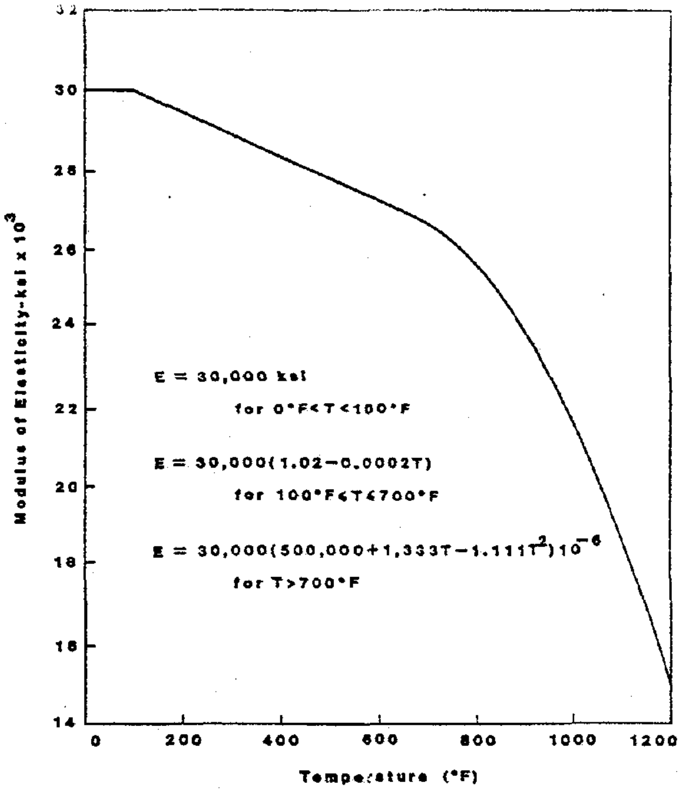

Figure 5.5. Elastic Modulus as a Function of Temperature Used in the Finite Element Analysis.

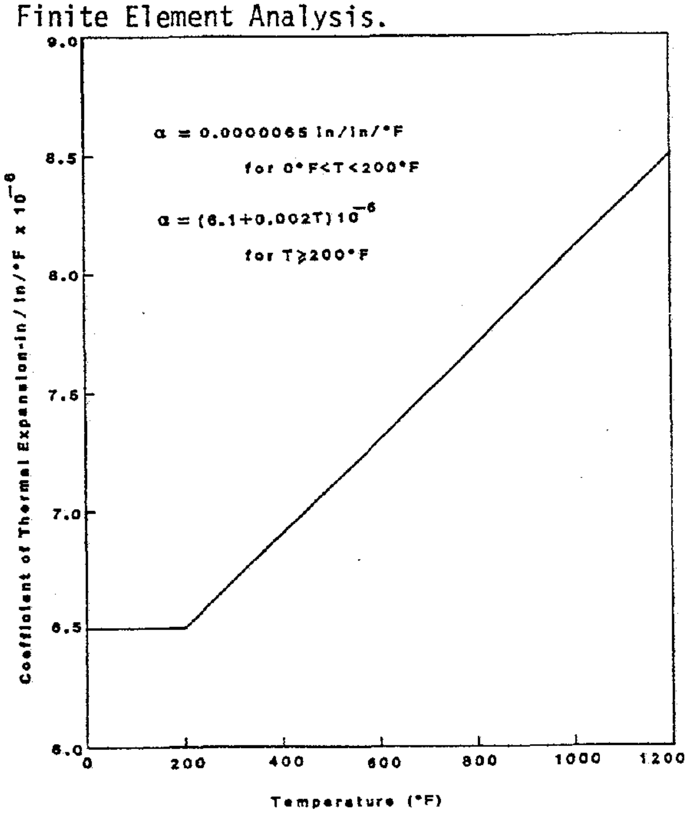

Figure 5.6. Coefficient of Thermal Expansion as a Function of Temperature Used in the Finite Element Analysis.

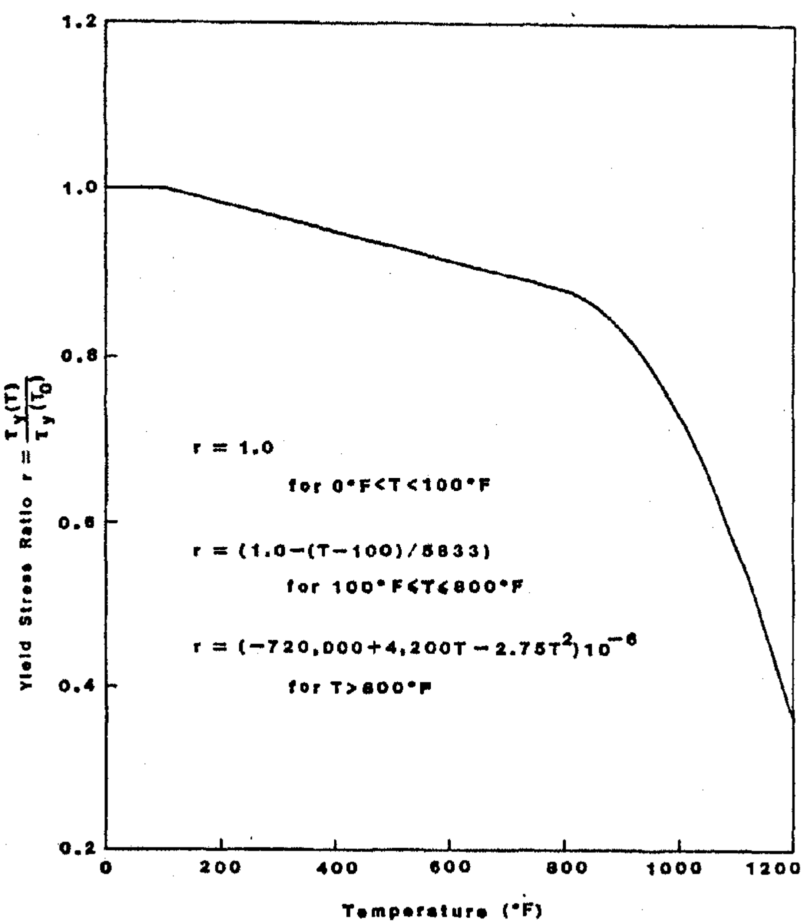

Figure 5.7. Normalized Yield Stress as a Function of Temperature.

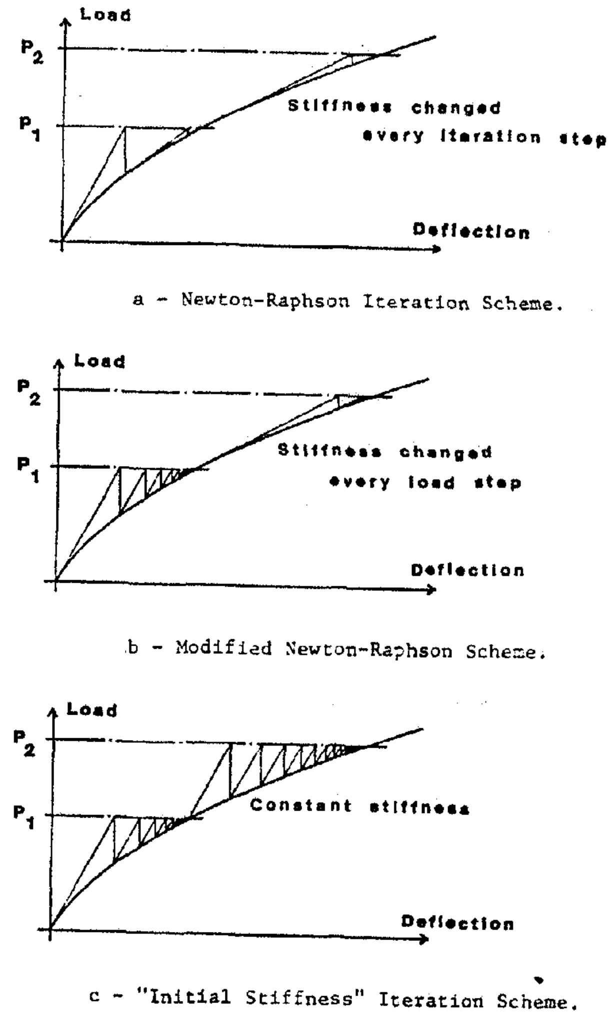

Figure 5.8. Iterative Methods Used to Adapt the Linear Elastic Finite Element Method to Non-Linear Solutions.

$$J_2' = \frac{1}{2} \sum_{i=1}^{3} \sum_{j=1}^{3} T_{ij}' \, T_{ij}' \tag{5.9}$$

$$T_{ij}' = T_{ij} - \frac{1}{3} p \, \delta_{ij} \tag{5.10}$$

$$p = \sum_{i=1}^{3} T_{ii} \tag{5.11}$$

and

$$k^2 = \frac{1}{3} F_y^{\,2} \tag{5.12}$$

The stress components, T_{ij}, and the yield stress of the steel under uniaxial tension F_y, are the only variables in the yield surface calculation, but the size of the yield surface changes with temperature because of the yield stress variation shown in Fig. 5.7. The calculation of stresses and strains after initial yielding requires a plastic flow rule, and the Prandtl-Reuss bilinear flow rule was used with a small amount of isotropic strain hardening [46, 47]. With this model the plastic component of strain, $de_{ij}^{\,p}$, is computed by

$$de_{ij}^{\,p} = T_{ij} d\lambda \tag{5.13}$$

where $d\lambda$ is a scalar multiplier dependent on the stress state.

$$d\lambda = \frac{3}{2} \frac{d\,\bar{\sigma}}{\bar{\sigma}\,H'} \tag{5.14}$$

The term, $\bar{\sigma}$, is the equivalent uniaxial stress for the given stress state, and H' is the hardening ratio with respect to plastic strain [46].

Convergence and Stability of Non-Linear Solution

These forms of the yield surface and flow rule are well known and documented in many references. Therefore, they may be easily programmed into a finite element analysis. The non-linearity is introduced into the linear finite element method by a series of incremental step-by-step linear solutions. Fig. 5.8 illustrates three commonly used methods. The tangent stiffness (or Newton-Raphson) method shown in Fig. 5.8(a) changes the stiffness after each load step and iteration. A linear elastic analysis is performed with each iteration, and the computed response is used to compute changes in state, a new stiffness, and the unbalanced load vector which are passed on to the next iteration. Iteration is continued until the unbalanced load is reduced to an acceptable limit. Fig. 5.8(c) illustrates the constant stiffness iterative method. The structural stiffness is always kept constant, but the yield criteria and flow rule are applied to the computed strains to accurately determine the state of stress and unbalanced load vector. Fig. 5.8(b) illustrates one of several possible combinations of these two methods. Here a new stiffness matrix is formed and solved at particular points such as the beginning of each load step or after a specified number of iterations.

Each of these non-linear solution methods have advantages and disadvantages. An intuitive observation would suggest that the tangent modulus method should converge with the smallest number of iterations, but each iteration will be costly since a new stiffness matrix must be formed and analyzed for each iteration step. Further, difficulties may be expected on cooling or unloading, because this method may not respond equally well to stiffening and softening behavior. The constant stiffness method requires many more iterations, but the iterations require much less computer time, because only back substitution of the stiffness solution is required. Combined methods such as depicted in Fig. 5.8(b) would appear to offer the best of both methods, but it is difficult to devise a modified method which accommodates load reversal and thermal stiffening as well as normal yield behavior.

However, the thermal loading used in the finite element analysis severely complicates the selection on appropriate method. Plastic stiffness models, which are based on an associated flow rule such as the Prandtl-Reuss bi-linear model, employ isothermal plasticity models. Stable solutions result with these models for a wide range of conditions. However, Drucker's postulate for stable plastic flow requires that only positive total work can be done by applied loads during yielding. Temperature dependent behavior results in reduction of yield stress and stiffness when temperature is increased and increases when temperature is decreased. Therefore, it is possible that temperature dependent plasticity may violate the conditions of stable plastic flow. In any case, the Newton-Raphson method and Modified Newton-Raphson methods produced quick and accurate solutions with plastic flow with no thermal effects, but these methods usually diverged with the addition of thermal effects. The constant stiffness method appears to invariably converge for all cases, but the convergence was frequently extremely slow. Many solutions required more than 20,000 iterations over 30 to 60 load steps for adequate convergence.

Determination of an appropriate convergence criteria was difficult for nonlinear thermal stress solutions. After numerous trials of alternate convergence criteria, a dual criteria was selected. Both criteria are based on the strain energy of the system since this energy contains a measure of both the strains or deflections and the unbalanced force or stress in the body. The primary convergence criteria, C11, compares the energy for the given iteration to the summation of all for previous iterations of that load step. The second criteria, C22, is compared to the magnitude of the energy for that iteration. This second criteria is intended to prevent excessive iteration on a load step with very small loads or deformation, since it may not be possible to achieve normal convergency under these conditions. Figure 5.9 illustrates the variation in solution resulting from different convergence criteria for a typical thermal stress solution. Generally, better accuracy and faster convergence of the non-linear solution were obtained with less restrictive convergence criteria if the applied load was greater than zero but not too large. Large applied loads result in large plastic deformation and greater instability of the solution. Extremely small applied loads resulted in small plastic deformations, and consequently the convergence errors were relatively larger. Figure 5.9 shows that the solution was somewhat erratic if C22 is less than 10^{-8} regardless of the value of C11. Further, the solution is not dramatically improved when C11 and C22 are reduced below 10^{-3} and 10^{-9}, respectively. These criteria were used for all heat straightening analysis described in this

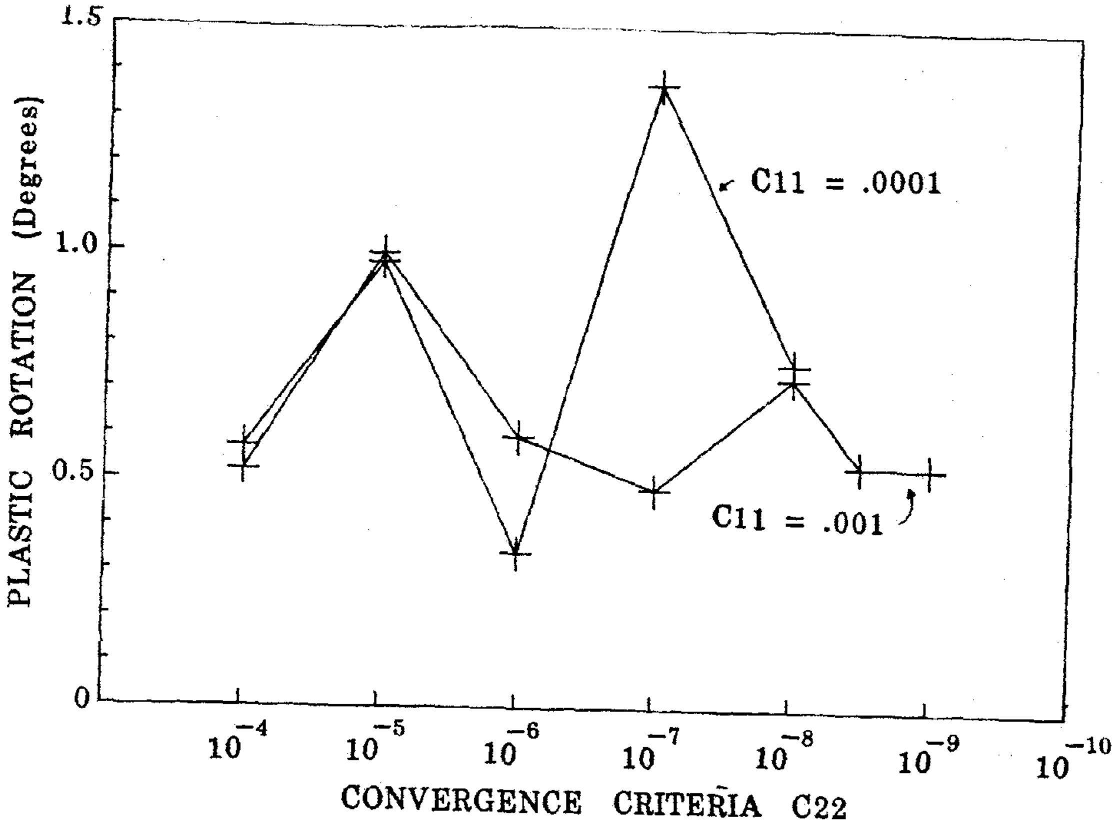

Figure 5.9. Effect of Variation of the Convergence Criteria on the Solution of a Typical V-Heat Analysis.

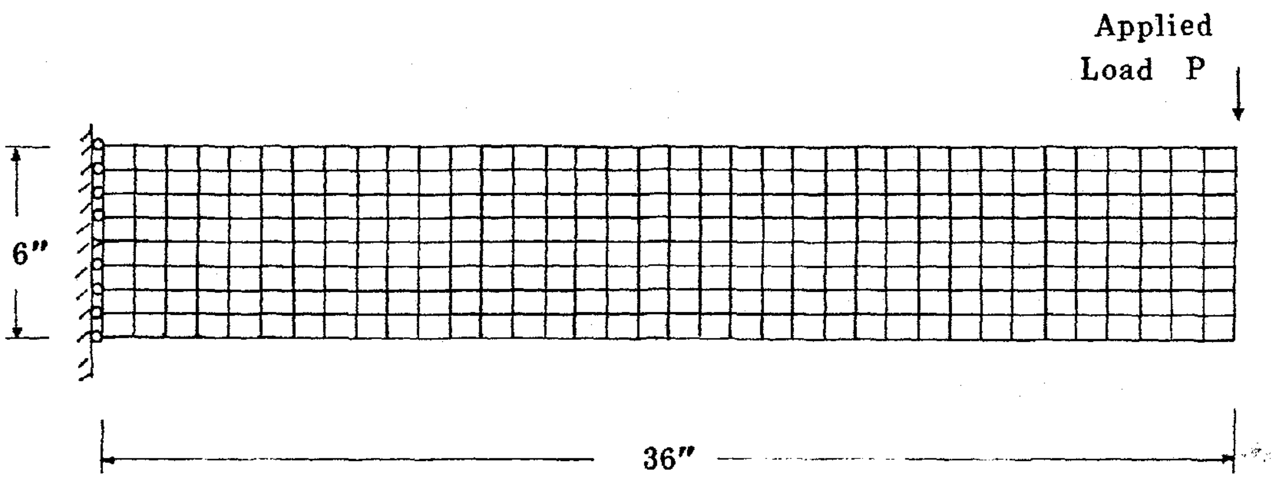

Figure 5.10. Finite Element Model of a Cantilever Beam with a Point Load.

report. These criteria are believed to be acceptable for most problems of practical importance , but C22 could be reduced further when $M/_{Mp}$ is less than 0.05 or greater than 0.4. The solution is less stable when $M/_{Mp} > 0.4$ because the plastic rotations are large, and it is relatively unstable if $\frac{M}{M_p} < .05$ because the plastic deformation is nearly zero.

Validity of the Solution Method

Appendix B contains a listing of the computer program for the finite element analysis and input instructions for using the program. A series of calibration runs were made to determine the validity of the method, before it was used for heat straightening analysis. The first of these calibration runs considered a rectangular cantilever beam with a point load applied at the free end as shown in Fig. 5.10. The beam was broken into a rectangluar grid as shown in the figure and the load P was gradually increased until 75% of the section yielded at the fixed end and then slowly removed. The results of the finite element analysis were then compared to an exact solution [48]. Fig. 5.11 shows a comparison of the force-deflection behavior of the beam, and Fig. 5.12 shows a comparison of the longitudinal strain distribution at the maximum load for the finite element and exact solutions. Finally, Fig. 5.13 shows a comparison of the residual stress after the load is removed. Comparison between the two solutions is good both at the global and local level, and convergence was achieved with tolerences much larger than those required for thermal solutions. A slight difference between the solutions can be noted at the fixed end boundary, but this difference is caused by incorrect modeling of the finite element

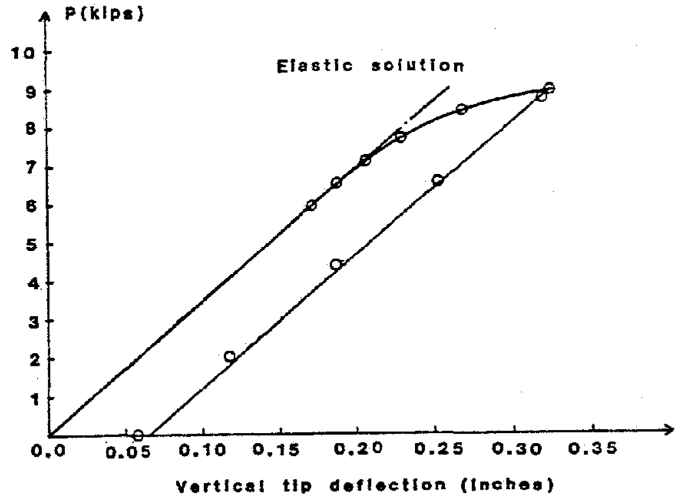

Figure 5.11. Comparison of the Force-Deflection Behaviour Obtained by Non-Linear Fine Element Solution With the Exact Solution for the Cantilever Beam.

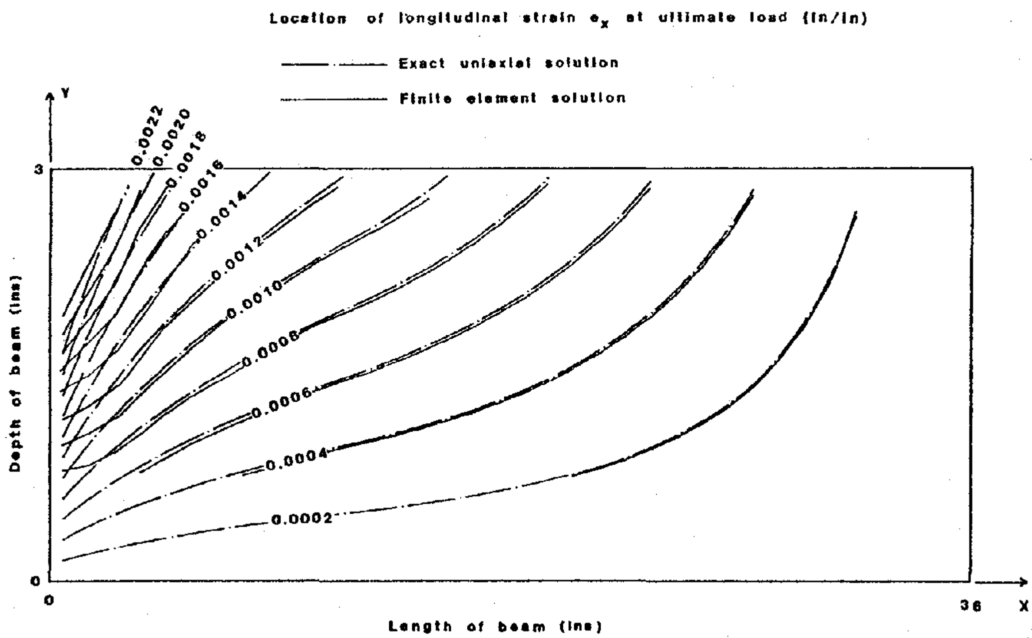

Figure 5.12. Comparison of the Strains at Maximum Load Obtained by Non-Linear Finite Element Solution with the Exact Solution for the Cantilever Beam.

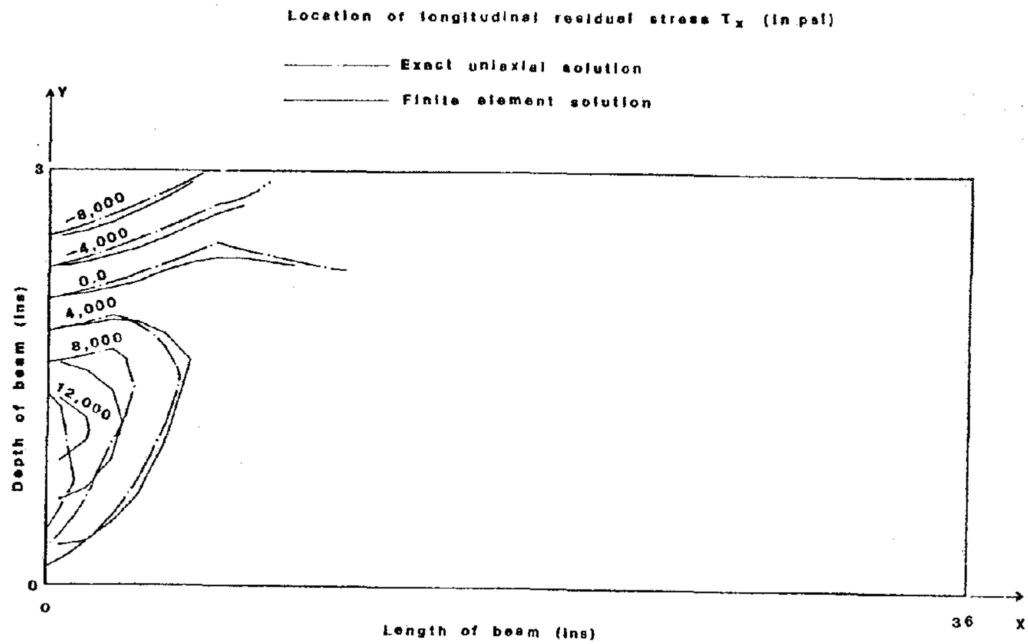

Figure 5.13. Comparison of the Residual Stress Obtained by the Non-Linear Finite Element Analysis with the Exact Solution for the Cantilever Beam.

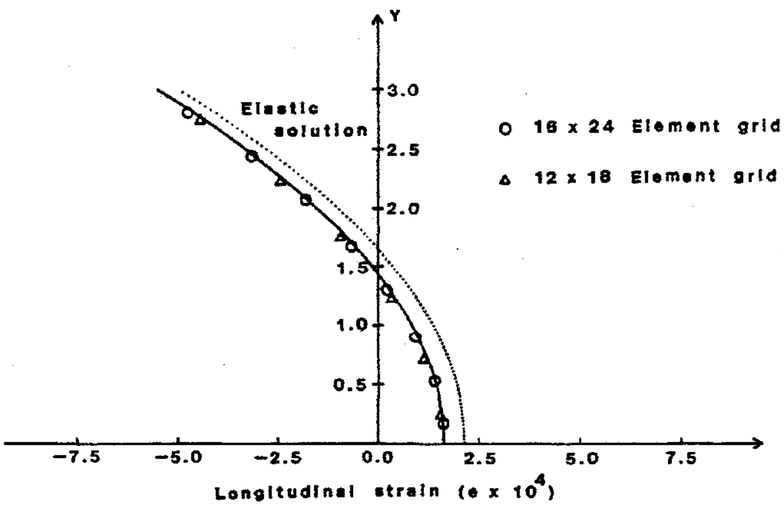

Figure 5.14. Comparison of the Strains Obtained by the Finite Element Method with the Exact Solution for A Beam with a Parabolic Temperature Distribution.

solution boundary condition rather than a problem with the solution method. The finite element boundaries shown in Fig. 5.10, result in a local variation in shear distribution at the fixed end, because all shear force is transferred through the central node. Other variations in the finite element boundaries were tried and similar local variations at the fixed end were noted because of variations in shear stress distribution or pinching of the elements due to restriction of transverse strain. Simple finite element boundaries simply do not provide an accurate simulation of clamped end boundaries used in exact beam solutions.

The preceeding analysis was an isothermal analysis. Verification of the thermal problem was also needed but there are very few exact solutions of plastic, thermal stress problems [19]. If the thermal properties of the material are constant, no elastic stress is induced in an unrestrained cantilever beam subjected to a temperature profile which is constant or linear over the length or depth. A parabolic temperature distribution results in elastic thermal stress, and ultimately yielding will occur. Figures 5.14 and 5.15 show the stress and strain distribution for the inelastic finite element analysis and the exact elastic and plastic solutions. The dotted line is the exact elastic solution and the solid line is the exact plastic solution. The shape of the strain distribution is similar for both elastic and plastic solutions as would be expected. The inelastic finite element solution correlated well with the exact plastic solution at convergence criteria which were less restrictive than those used in heat straightening analysis.

Heat Straightening Analysis

The non-linear, temperature dependent finite element model was then used to calculate the response to a large number of V-heats similar to those used in Series A experiments. As noted earlier, the convergence of some of these solutions was quite slow, but the accuracy of the final solution was good. Large plastic strains were observed in the heated areas. Longitudinal strains in the order of 1% were typical and plastic strains as large as 2% were not uncommon. Outside the heated area some plastic deformation occurred, but the magnitude of these strains was an order of magnitude smaller. Large transverse plastic strain and bulging also were noted in the heated areas. The distribution of strain and magnitudes of strain obtained in the finite element solution agreed well with the measured experimental results. This can be observed by comparing the computed longitudinal strain contours shown in Fig. 5.16 with the measured values for a comparable specimen in Fig. 4.1. Slight local differences can be noted near the boundaries, but the general results are very similar.

The plastic rotation and plane sections hypothesis were evaluated at various location with a least squares analysis of the computed nodal displacements. Plane sections clearly do not remain plane within the heated area, but a short distance outside the heated area the plane sections assumption is very reasonable, since statistical correlation coefficients in excess of .99 were typically obtained. Again these observations agree very well with experimental data.

The overall plastic rotations and deflections of the beams

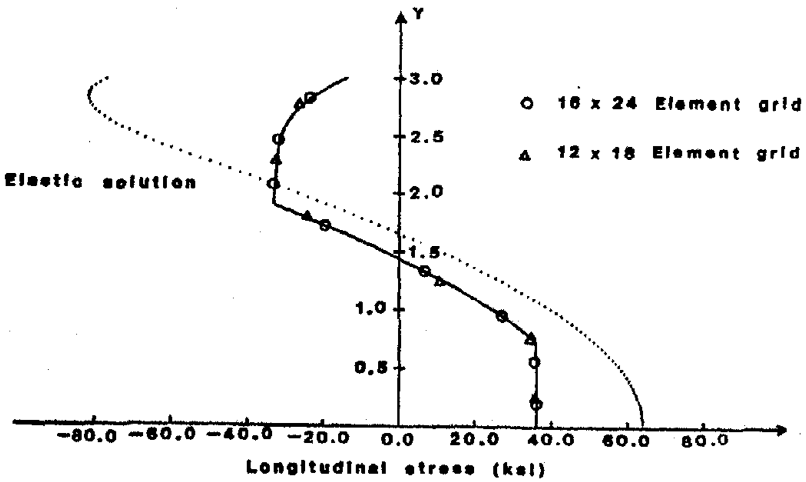

Figure 5.15. Comparison of the Stress Obtained by a Nonlinear Finite Element Solution With the Exact Solution for an Elastic Beam with a Parabolic Temperature Distribution.

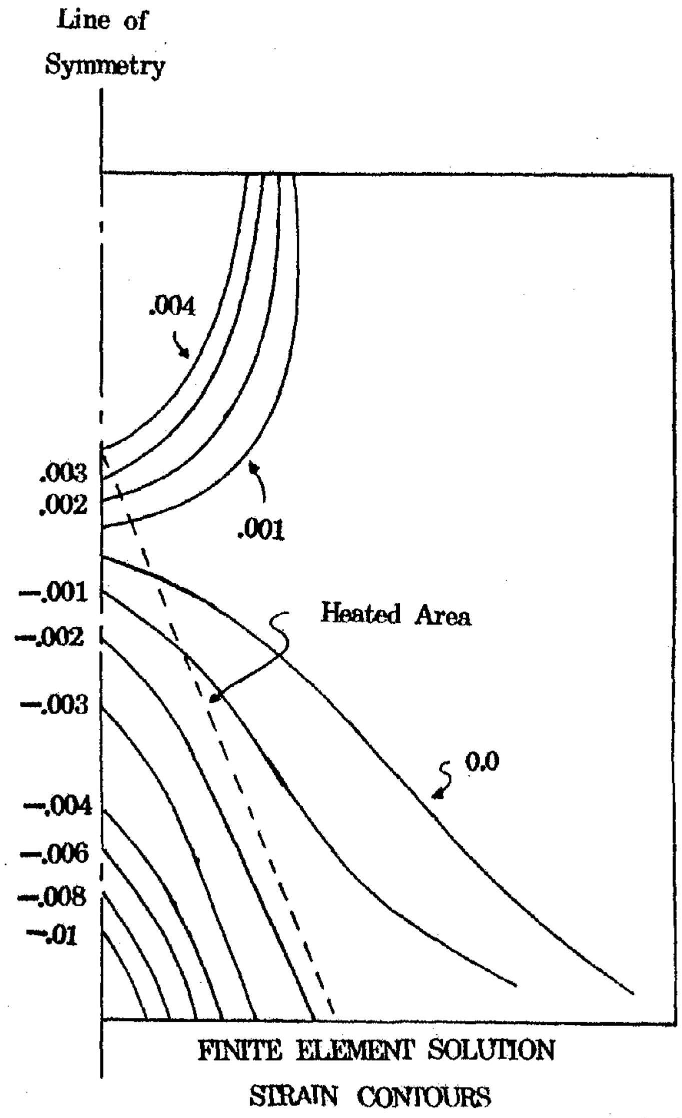

Figure 5.16. Typical Residual Strain Distribution Computed by Finite Element Analysis for V-Heat.

also agreed well with experimental observations if the solution had properly converged. The good global and local comparison of the computed experimental results are extremely important. Global accuracy is needed to predict the plastic deformation and the number and location of heat applications required to repair a measured damage pattern. However, local accuracy is needed to estimate the plastic strains and residual stress induced by the heating. These local effects may be extremely important in evaluating the future potential for brittle fracture and fatigue. Further, the residual stress is on important parameter in the determination of the buckling capacity of repaired members. The heat straightening (or cambering) process induces large residual stress, and these residual stresses are predicted by the finite element analyses. Fig. 5.17 is a typical longitudinal residual stress contour obtained from the computer analyses. Note that this analysis is comparable to the experimental results shown in Figs. 4.1 and 4.2. It should be noted that residual stress is extremely difficult to accurately and reliably measure in experiments, and so these calculated stress values cannot be verified experimentally. However, in view of the good general comparison between measured and computed strains and deformations, it is likely that the computed residual stress is approximately correct. The computed residual stress distribution of Fig. 5.17 shows that large compressive residual stress occurs at the extreme fiber of the heated specimen. This causes early yielding in compression members and may result in a dramatic loss in local bending stiffness. The tangent modulus buckling theory [49], which is used to predict the inelastic buckling capacity of

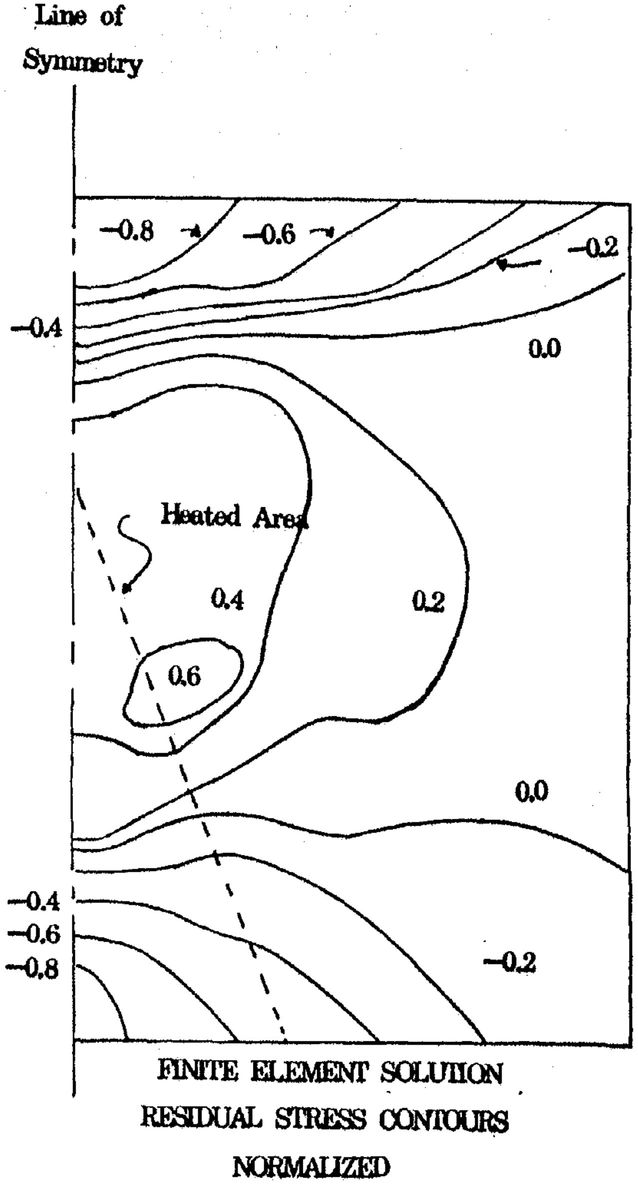

Figure 5.17. Typical Residual Stress Distribution Computed by the Finite Element Method.

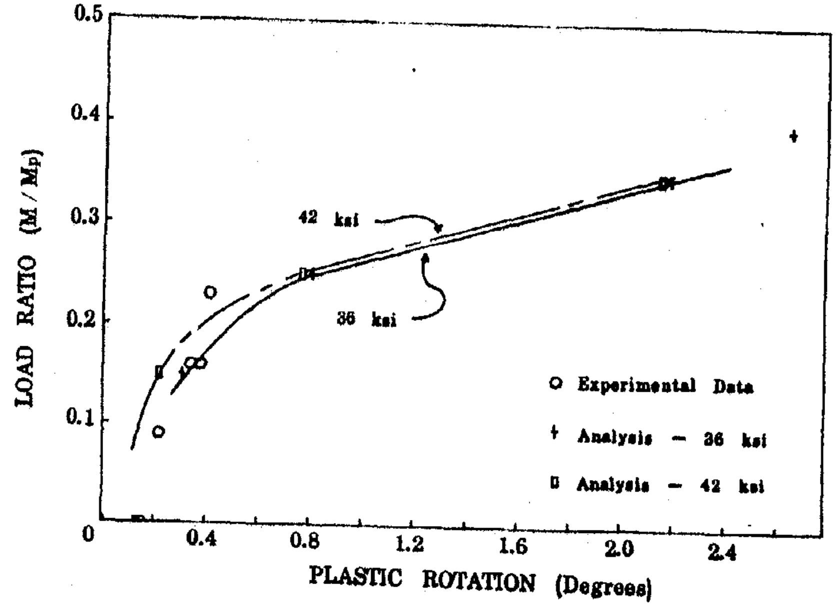

Figure 5.18. Effect of Applied Load on the Computed Plastic Rotation.

columns, indicates that this reduction in stiffness may reduce the buckling load of a straightened member. However, the compressive residual stress occurs only over a short length, and this reduction in stiffness may also have insufficient length to influence the buckling capacity. This clearly is one area where more research is needed.

Further Comparison of Theoretical Predictions with Experimental Results

The mathematical model also provided good correlation with the experimental results on a global level. Fig. 5.18 shows the computed plastic rotation for 1200° V-heat with a 60° heat angle and 2/3 depth for A36 steel. Increased yield stress results in decreased plastic rotations as observed in the experiment. For example, a 16% increase in yield stress resulted in 29% and a 5% reduction in plastic rotation if the load ratios were .15 and .25 respectively. Series A experimental results with reasonably comparable heat conditions also are plotted on this curve. Note that there is some scatter in the comparison, because the temperature could not be precisely controlled in the experiments and the yield stress of the steel in the Series A experiment exceeds 36 ksi. Figure 5.19 illustrates the effect of heat angle and temperature on the predicted plastic rotation. The figure shows that increased plastic rotation occurs when the angle of the heated area is increased. However, this effect does not become significant until the temperature exceeds approximately $1000^{\circ}F$ ($540^{\circ}C$). Comparable experimental results are also plotted on this curve. The mathematical model also predicts that the

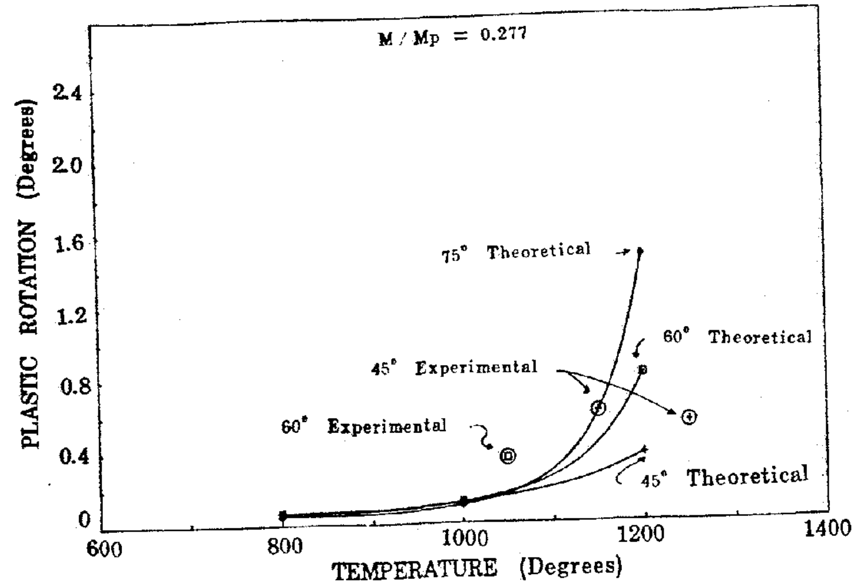

Figure 5.19. Effect of Heat Angle and Temperature on Computed Plastic Rotation.

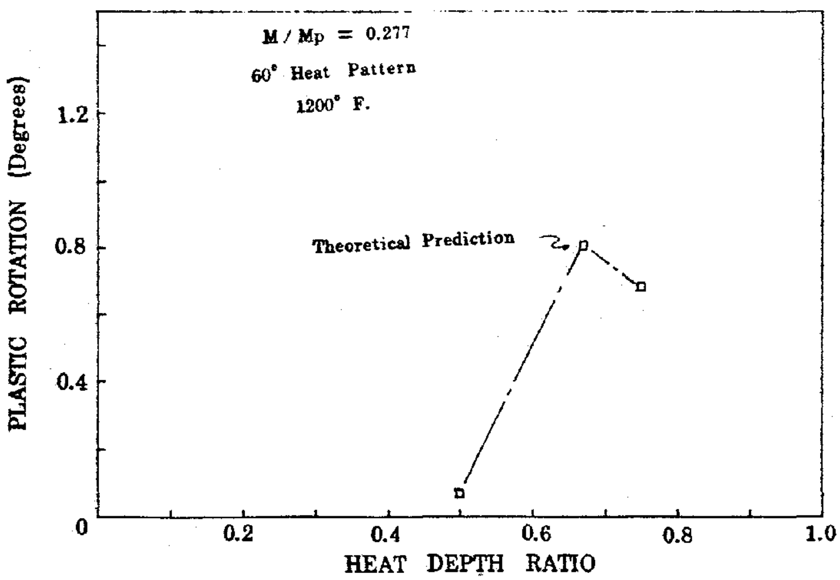

Figure 5.20. Effect of the Depth of Heat on Computed Plastic Rotation.

plastic rotation increases with increasing temperature as noted earlier. This is also consistent with experimental observations. Figure 5.20 shows the computed effect of heat depth on the plastic rotation. Increased depth generally results in increased plastic rotation as observed in the experiments. The 3/4 depth heat resulted in a slight reduction in plastic rotation and an attempted analysis for a full-depth heat did not converge. This may indicate that a more refined convergence criteria is needed for these conditions. However, it may also be suggesting that deep heat patterns have less restraint provided by the surrounding unheated metal, and so smaller rotations may occur. Figure 5.21 shows the effect of the time required to complete the heating on the plastic rotation. The plastic rotation is influenced by variation in time, but the sensitivity is clearly less than that seen for temperature and applied loads. This again agrees with intuitive observations. No stress is developed without a thermal gradient, and so smaller plastic rotations must be expected with extremely slow heating.

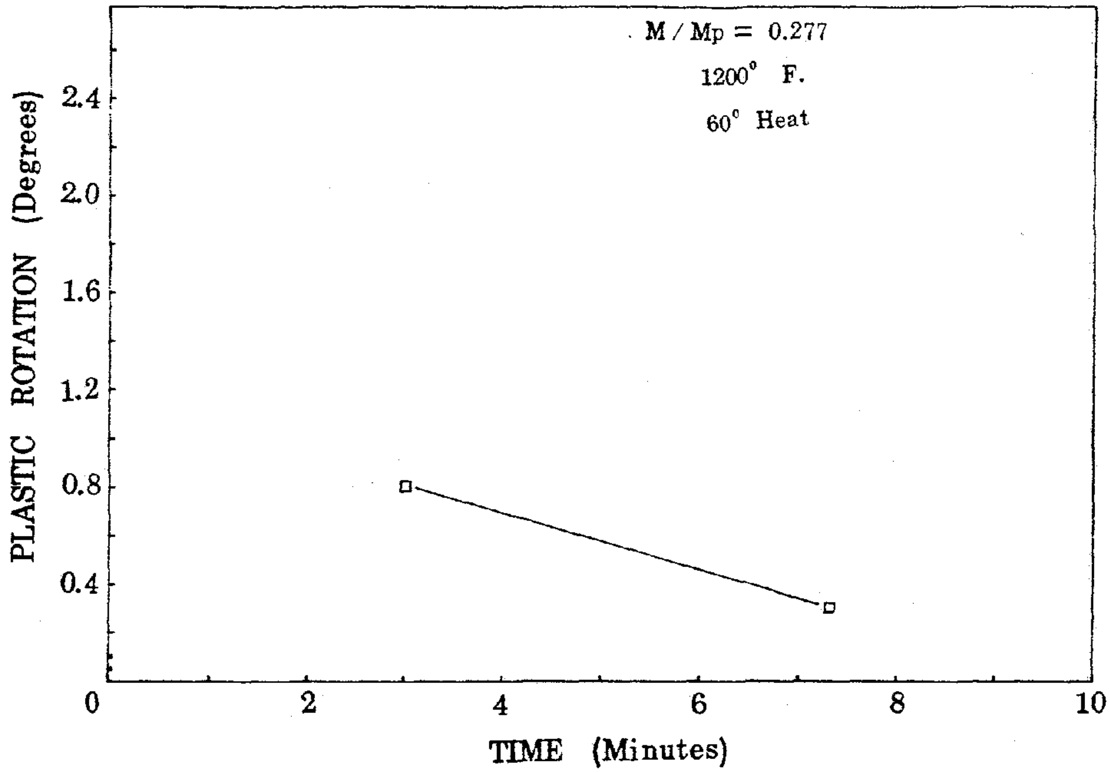

Figure 5.21. Effect of the Time Required to Heat Specimen on the Computed Plastic Rotation.

CHAPTER 6

SUMMARY AND CONCLUSIONS

Summary

This report has described a study into the use of thermal stress or heat straightening for seismic damage repair. It has shown that heat straightening is an economical method for repairing damaged steel which has not been cracked, torn or excessively deformed. A local concentration of heat is applied to the structure in one of several well defined patterns, and a temperature gradient is developed. The heated steel tries to expand, but expansion is restricted by the surrounding unheated metal and any additional restraint which is applied. Further, the yield stress and elastic modulus decrease in the heated steel, and the steel yields primarily in compression. This yielding causes permanent deformations which remain after the steel has cooled, and the deformations can be used to curve or straighten members.

While heat straightening has been shown to be an economical method for repairing members which are not fractured or excessively deformed, the method is not understood by most structural engineers. This is an important limitation, because the selection of the best repair method is necessarily an economic decision where the cost of heat straightening must be compared to the cost of replacement or strengthening of the damaged elements. However, the determination of the cost of heat straightening requires a reliable estimate of the amount and placement the heating needed to repair the damage and a determination of the effect of the heat on the properties of the steel. Structural engineers must be prepared to make this assessment before the method can be widely used in practice. This report is the first step in development of a method for making this assessment.

Conclusions of this Research

Most structural steels are carbon or low alloy steels which go through a microstructure phase change at approximately 1333°F. As long as the steel is kept below this temperature, heating should induce only minor changes to the material properties of the steel. These changes may include a slight reduction in yield strength and ductility and an increase in notch toughness. Since welders cannot precisely determine the temperature of the steel during heating, 1200°F is a practical upper limit for these carbon steels. High alloy steel, quenched and tempered steels, or steels with strength developed by cold working or other heat treatment may require lower temperature limits. Quenching or slow cooling will both be acceptable for most structural steels heated within these temperature limits.

Temperatures greater than 1200°F will increase the plastic deformation achieved by the heat, but they should be used only when the effect on the material properties is understood. Further, temperatures greater than approximately 1400°F cause surface damage to the steel.

V-heats can be used to introduce a concentrated plastic deformation. Increasing temperature introduces increasing plastic deformation. Further, an increase in heated area (i.e., the depth and/or angle of the V-heat) will also increase the plastic rotation, but increases in temperature and heated area also increase the out-of-plane deformation and the tendency toward local buckling. The plastic deformation is caused by the in-plane temperature gradient, and the primary yielding is yielding in compression. The addition of loads or restraint which induce compressive stress in the heated area increases the plastic deformation. Quenching of the heated steel may increase the plastic deformation by 20% to 80%. It is particularly effective if quenching is started immediately after heating, since more heat is removed and a larger temperature gradient and differential is created. There is also evidence that quenching may also reduce the tendency toward buckling if properly employed. However, quenching quickly cools the steel and increases the probability of embrittlement if the steel is heated above the phase change temperature.

V-heats cause large plastic strains within the heated area, and minimal plastic strain outside the heated area. This results in considerable cross section warping within the heated area, but plane sections remain plane outside the heated area. Maximum longitudinal strains of .01 to .02 in compression are typical, and transverse strains of one-half this magnitude are common. These large plastic strains indicate that significant yielding occurs, and the plastic deformation is not sensitive to residual stress. High strength steel is more difficult to deform, since it requires higher temperature with increased restraint to achieve a specified deformation. Little if any plastic deformation is achieved with V-heats on mild steel with temperature less than 600°F or on A514 steel with temperature less than 1000°F.

The plastic deformation achieved by heating is somewhat sensitive to the geometry of the steel. However, it is believed that much of this effect can be attributed to differences in rate of heating and heat flow. When the heat is applied to a single flange of a wide flange section, the stiffness of the web and unheated flange reduced the plastic deformation by approximately 25-30%. The column tests have shown that straightening can be accomplished on columns while they are supporting service loads, but the secondary moments due to gravity loads and end restraint at the boundaries reduce the plastic deformation. The addition of restraint should be particularly effective with columns.

Line or strip heats cause much smaller plastic strains than concentrated yield patterns such as V-heats. Maximum plastic strains were an order of magnitude smaller than those observed on the V-heats, and so strip heats are affected by the magnitude and distribution of the residual stress.

A mathematical model has been developed to predict the global and local effects of heat straightening. The model consists of a finite difference solution to the heat flow problem combined with a non-linear finite element solution. The finite element analysis considers the temperature dependence of the elastic modulus, yield stress, and coefficient of thermal expansion. A series of time independent temperature profiles are generated by the finite difference solution and used as a series of load steps in the finite element analysis. This analysis compares very well with the experimental results at both the global and local level. Good global comparison is useful in the development of models for predicting the deformation which will be achieved by heat straightening, and good local comparison is helpful in the prediction of failure modes such as buckling, fracture and fatigue. The model is presently applicable only to rectangular plates, but it can be readily extended to structural shapes and structural systems. Further, there is some human variation in the application of heat to the steel, and so the analysis requires calibration to the human variations. An accurate analysis requires many iterations, and is therefore quite expensive.

Future Research Needs

This research should enhance the understanding of the use of heat straightening in the repair of structural damage. It provides guidelines on how to accomplish a repair, and how the repair may be hastened or delayed by changing the various parameters. Further, a mathematical model is presented which predicts the heat straightening affect with reasonable accuracy. However, additional research is needed to fully develop the practical potential of the method. This needed research includes.

1. A thorough evaluation of the interaction between the thermal stress effect and buckling. The plastic deformation induced by heat straightening causes large residual stresses, which may reduce the buckling strength of a column. Further, study is needed to determine the maximum applied loads which can be safely supported while a structural member is being heated to a given temperature and geometry.

2. The mathematical model provides an accurate indication of the local and global effects of heat straightening but it is presently applicable only to rectangular plates. The model should be extended to include structural shapes and more complex structural geometries.

3. The use of the mathematical model is somewhat impractical for actual damage repair, because it requires a great deal of computer time. The analytical method should be simplified for practical applications. One method of simplification would be the development of dimensionless design nomographs similar to curves shown in Chapter 5. These nomographs would cover a wide range of load conditions, geometries, temperatures and material properties, and could be used in the design and selection of an appropriate heating program. Other simplified methods of analysis could also be employed.

4. Experiments are needed on structural shapes and more complex geometries to check the accuracy and validity of the mathematical model under these conditions.

5. Further studies are needed into the effect of elevated temperatures on material properties. Present

limitations on temperatures are probably conservative for most structural steels, but damage repair could be accomplished much more rapidly if higher temperatures could be used. Further, a better understanding of the effects on material properties would permit the possible extension of this method to other metals such as aluminum.

References

1. Newmark, N. M. and Rosenblueth, E., Fundamentals of Earthquake Engineering, Prentice-Hall, Englewood Cliffs, New Jersey, 1971.

2. Uniform Building Code, 1982 Edition, International Conference of Building Officials, Whittier, California, 1982.

3. Tentative Provisions for the Development of Seismic Regulations for Buildings. Report ATC 03-06, Applied Technology Council, Palo Alto, California 1978.

4. Krawinkler, H., Bertero, V. V., and Popov, E. P., Inelastic Behavior of Steel Beam-To-Column Subassemblages, EERC Report 71-7, University of California, Berkeley, California 1971.

5. Bertero, V. V., Krawinkler, H., and Popov, E. P., Further Studies on Seismic Behavior of Steel Beam-Column Subassemblages, EERC Report 73-27, University of California, Berkeley, California 1973.

6. Popov, E. P., Bertero, V. V., and Chandramouli, S. Hysteretic Behavior of Steel Columns, EERC Report 75-11, University of California, Berkeley, California 1975.

7. Carpenter, L. D., and Lu, Le-Wu, Reversed and Repeated Load Tests of Full-Scale Steel Frames, Bulletin 24, American Iron and Steel Institute, April 1973.

8. Gugerli, H., and Goel, S. C., Inelastic Cyclic Behavior of Steel Bracing Members, UMEE 82R1, The University of Michigan, Ann Arbor, Michigan 1982.

9. Jain, A. K., Goel, S. C., and Hanson, R. D., Hysteresis Behavior of Bracing Members and Seismic Response of Braced Frames with Different Proportions, Report UMEE 78R3, University of Michigan, Ann Arbor, Michigan 1978.

10. Wakabayashi, M., "Behavior of Braces and Braced Frames Under Earthquake Loading", International Journal of Structures, Vol. 2, No. 2., Wem Chand, Roorkee, India 1982.

11. Roeder, C. W., and Popov, E. P., "Eccentrically Braced Steel Frames for Earthquakes," ASCE, Journal of Structural Division, Vol. 100, No. ST3, March 1978.

12. Malley, J. O., and Popov, E. P., "Shear Links in Eccentrically Braced Frames," ASCE, Journal of Structural Division, Vol. 110, No. ST9, September 1984.

13. Allred, L. H., "Pressure Injection of Epoxy Adhesive Solves Problem of Floor Cracking, Food Processing, July 1974.

14. Phase II Test Results, Proceedings of Sixth Joint Technical Coordinating Committee US-Japan Cooperative Research Program Utilizing Large Scale Testing Facilities, Maui, Hawaii, June 1985.

15. Shanafelt, G. O., and Horn, W. B., "Guidelines for Evaluation and Repair of Damaged Steel Bridges," NCHRP Report 271, National Research Council, Washington, D.C., June 1984.

16. Holt, R. E., "Flame Straightening Basics," Welding Engineer Journal, 1965.

17. "How Fire Destroyed and Fire Repair Air Force Hangars," Engineering News Record, June 18 1959.

18. Stout, R. D., and Doty, W. D., Weldability of Steels, Welding Research Council, 1971.

19. Boley, B. A., and Weiner, J. H., Theory of Thermal Stresses, John Wiley and Sons, New York, 1960.

20. Carslaw, H. S., and Jeager, J. C., Conduction of Heat in Solids, Second Edition, Oxford University Press, Fair Lawn, New Jersey, 1959.

21. Mishler, H. W., and Lewis, B. N., "Evaluation of Repair Techniques for Damaged Steel Bridge Members," Final Report NCHRP Project 12-17, (Unpublished), National Research Council, May 1981.

22. McGannon, H. E., Editor, The Making, Shaping and Treating of Steel, Eighth Edition, US Steel Corporation, Pittsburgh, Pennsylvania, 1964.

23. Uddin, T., and Culver, C. G., "Effects of Elevated Temperature on Structural Members," Journal of Structural Division, ASCE, Vol. 101, No. ST7, July 1975.

24. Smith, W. F., Structure and Properties of Engineering Alloys, McGraw Hill, New York, 1981.

25. Harrison, H. L., "Straightening Structural Members in Place," Welding Journal, Vol. 31, May 1952.

26. Harrison, H. L., and Mills, B. D., "Effects of Light Peening on the Yielding of Steel," Welding Journal, Vol. 30, May 1951.

27. Rothman, R. L., and Monroe, R. E., "Effects of Temperature and Strain Upon Ship Steels," Ship Structures Committee Report SSC-235, 1970.

28. Pattee, H. E. Evans, R. M., and Monroe, R. E., "Effect of Flame Straightening on Material Properties of Weldments," Ship Structures Committee Report SSC-207, 1970.

29. Pattee, H. E., Evans, R.M., and Monroe,R. E., "Flame Straightening its Effect on Base Metal Properties," Ship Structures Committee Report SSC-198, August 1969.

30. Moberg, K. L., "Damage Assessment and Contraction Straightening of Steel Structures," Masters Thesis in Civil Engineering, University of Washington, 1979.

31. Graham, R., "Investigation of Flame Straightening Methods for Steel Structures," Boeing Company Manufacturing Report MDR 2-32075, October 1975.

32. Holt, R. E., "Primary Concepts in Flame Bending," Welding Engineer, Vol. 50., No. 9, September 1965.

33. Goodier, J. N., "Thermal Stress," ASME, Journal of Applied Mechanics, March 1937.

34. Brockenbraugh, R. L., "Theoretical Stresses and Strains from Heat Curving," ASCE, Journal of Structural Division, Vol. 96, No. ST7, July 1970.

35. Brockenbraugh, R. L., and Ives, K. D., "Experimental Stresses and Strains from Heat Curving," ASCE, Journal of Structural Engineering, Vol. 96, No. ST7, July 1970.

36. Nichols, J. T., and Weerth, D. E., "Investigation of Triangular Heats Applied to Mild Steel Plates," AISC, Engineering Journal, Vol. 9, October 1972.

37. Baldwin, J. W., and Guell, D. C., Final Report to NCHRP Projects 12-1 and 12-6, National Research Council, 1971.

38. Weerth, D. E., "Theoretical and Experimental Analysis of Heat Curved Mild Steel," Masters Thesis in Civil Engineering, University of Washington, 1971.

39. Ehredt, M. J., "Experimental Analysis of Plastic Strains Due to Heat curving," Masters Thesis in Civil Engineering, University of Washington, 1982.

40. Manual of Steel Construction, Eighth Edition, AISC, Chicago, Illinois, 1980.

41. Clark, Shelley R., "An Experimental Analysis of Heat Curving on Steel Plates and Columns," Masters Thesis in Civil Engineering, University of Washington, 1984.

42. Bruning, James L., and Kintz, B. L. Computational Handbook of Statistics, Scott Foresman and Co., Glenview, Illinois, 1968.

43. Plastic Design in Steel: A Guide and Commentary, Second Edition, ASCE Manual 41, New York, New York, 1971.

44. Dusenberre, G. M., Heat-Transfer Calculations by Finite Difference, International Textbook Co., Scranton, PA. 1961.

45. Zienkiewicz, O. C., The Finite Element Method, 3rd Edition, McGraw Hill, New York, New York, 1977.

46. Malvern, L. E., Introduction to Mechanics of a Continuous Meduium, Prentice Hall, Englewood Cliffs, New Jersey, 1969.

47. Bathe, K. J., Finite Element Procedures in Engineering Analysis, Prentice Hall, Englewood Cliffs, New Jersey, 1982.

48. Schneider, S. P., "A Thermo-Plastic Finite Element Analysis to Predict the Behavior of Flame Cambered Beams," Masters Thesis in Civil Engineering, University of Washington, 1984.

49. Blich, F., Buckling Strength of Metal Structures, McGraw Hill, New York, 1952.

APPENDIX A

HEAT FLOW COMPUTER PROGRAM

```
1 ! PROGRAM "H T B E A M"
2 !
3 !   PROGRAM "HTBEAM" WAS WRITTEN TO CALCULATE THE TEMPERATURE DISTRIBUTION OF
4 !   A PLATE USING A TWO-DIMENSIONAL FINITE DIFFERENCE METHOD.  THIS PROGRAM
5 !   WAS WRITTEN IN BASIC TO EXECUTE ON THE "HP9816" SERIES 200 PC.
6 !
7 !   PROGRAMMED BY :   STEPHEN P. SCHNEIDER
8 !   DATE          :   10/30/83
9 !
10!
11! CONTROL PARAMETERS:
12!
13!   ITPEL. . . . . X LOCATION OF THE HEATED ELEMENT
14!   ITPEND . . . . X LOCATION OF ELEMENT IN BOTTOM ROW WHICH IS LAST BE HEATED
15!   JTPEL. . . . . Y LOCATION OF THE HEATED ELEMENT
16!   NELTP. . . . . NUMBER OF ELEMENTS THAT HAVE BEEN HEATED
17!   NROWTP . . . . NUMBER OF ROWS IN THE VEE-HEAT THAT HAVE BEEN HEATED
18!   NPROB. . . . . PROBLEM NUMBER CURRENTLY IN PROGRESS
19!   NTMTP. . . . . NUMBER OF TIME STEPS FOR THE HEATING
20!
21! MATERIAL PROPERTIES:
22!
23!   CPDV . . . . . PRODUCT OF (DENSITY)*(SPECIFIC HEAT)*(ELEMENT VOLUME)
24!   DEN. . . . . . DENSITY OF THE MATERIAL IN lb/cu ft
25!   SH . . . . . . SPECIFIC HEAT OF THE MATERIAL IN Bt/(lb)*(Degree F)
26!
27! DISCRETIZATION:
28!
29!   ANGLE. . . . . ANGLE OF THE VEE-SHAPED HEATED AREA
30!
31!   DX . . . . . . DIMENSION OF ELEMENT IN X-DIRECTION
32!   DY . . . . . . DIMENSION OF ELEMENT IN Y-DIRECTION
33!   Z. . . . . . . DIMENSION OF ELEMENT IN Z-DIRECTION
34!
35!   NCOL . . . . . NUMBER OF COLUMNS FOR THE DISCRETIZATION IN THE X-DIRECTION
36!   NCOL1. . . . . NUMBER OF COLUMNS PLUS ONE FOR THE DISCRETIZATION
37!   NCOL2. . . . . NUMBER OF COLUMNS PLUS TWO FOR THE DISCRETIZATION
38!
39!   NROW . . . . . NUMBER OF ROWS FOR THE DISCRETIZATION IN THE Y-DIRECTION
40!   NROW1. . . . . NUMBER OF ROWS PLUS ONE FOR THE DISCRETIZATION
41!   NROW2. . . . . NUMBER OF ROWS PLUS TWO FOR THE DISCRETIZATION
42!
43!   NROWV. . . . . NUMBER OF ROWS TO BE HEATED IN THE VEE-SHAPED PATTERN
44!
45! TEMPERATURE VARIABLES:
46!
47!   TPCON(*) . . . COEFFICIENT OF CONDUCTION HEAT TRANSFER FOR EACH ELEMENT
48!
49!   TPEL1. . . . . PREVIOUS TEMPERATURE OF HEATED ELEMENT WHEN OUTPUT OF
50!                  TEMPERATURE DISTRIBUTION WAS LAST TAKEN
51!
52!   TPEL2. . . . . CURRENT TEMPERATURE OF THE HEATED ELEMENT
53!
54!   TPEXP. . . . . EXPONENTIAL FOR HEAT FLUX CONSTANT b
55!
56!   TPFACT . . . . FACTOR FOR THE HEAT FLUX CONSTANT a
57!
58!   TPFLAG . . . . FLAG TO INDICATE WHEN TEMP DISTRIBUTION MUST BE STORED
59!                  0 = DO NOT OUTPUT ELEMENT TEMPERATURES
60!                  1 = OUTPUT TEMPERATURE DISTRIBUTIONS
61!                  2 = OUTPUT FINAL TEMPERATURE DISTRIBUTION AND STOP
62!
63!   TPIN(*). . . . INPUT HEAT FLUX FOR EACH ELEMENT
64!
65!   TPINC. . . . . TEMPERATURE INCREMENT OF HEATED ELEMENT AT WHICH THE
66!                  TEMPERATURE DISTRIBUTION MUST BE STORED
67!
68!   TPLIM. . . . . TEMPERATURE LIMIT FOR ANY HEATED ELEMENT
69!
70!   TPRM . . . . . INITIAL AMBIENT (ROOM) TEMPERATURE
71!
72!   TPWEB1(*). . . TEMPERATURE OF ELEMENTS FOR CURRENT TIME STEP
73!
74!   TPWEB2(*). . . TEMPERATURE OF ELEMENTS FOR THE NEXT TIME STEP
75!
76! TIME VARIABLES:
77!
78!   TMINC1 . . . . TIME ELAPSED SINCE LAST TEMPERATURE OUTPUT
79!
80!   TMLIM. . . . . TIME LIMIT FOR ENDING THE TEMPERATURE CALCULATIONS
81!
82!   TMLIM1 . . . . TIME ELAPSED SINCE BEGINING OF TEMPERATURE CALCULATIONS
83!
84!   TMPO . . . . . TIME INCREMENT FOR WHICH "TMINC1" MUST EXCEED FOR
85!                  STORING TEMPERATURE DISTRIBUTIONS
86!
87! FILES:
88!
89!   HTDATA$. . . . STORAGE OF PARAMETERS FOR DISCRETIZATION OF SYSTEM
90!
91!   HTDATA$a . . . STORAGE FOR TEMPERATURES AT SPECIFIC THERMOCOUPLE LOCATIONS
92!
93!   HTDATA$b . . . STORAGE FOR ALL ELEMENT TEMPERATURE DATA
94!
95!   @PATH. . . . . INPUT/OUTPUT PATH ASSIGNED TO FILE HTDATA$a
96!
97!   @PATH1 . . . . INPUT/OUTPUT PATH ASSIGNED TO FILE HTDATA$b
```

```
1         OPTION BASE 1
2         COM /Dims/ Dx,Dy,Z,Cpdv,Angle,@Path,@Path1,Tpfact,Tpexp
3         COM /Temp/ Tpweb1(42,22),Tpweb2(42,22),Tpcon(42,22),Tpin(42,22)
4         COM /Temp2/ Tpel1,Tpel2,Tpinc,Tplim,Tpflag,Tprm
5         COM /Time/ Tminc,Tminc1,Tmlim,Tmlim1,Tmpo
6         COM /Disc/ Nrow,Nrow1,Nrow2,Ncol,Ncol1,Ncol2
7         COM /Data/ Nprob,Nrowv,Neltp,Nrowtp,Itpel,Jtpel,Itpend
8              !
9              ! N U M B E R  O F  P R O B L E M S
10             !
11        DATA 1,3
12             !
13             ! D A T A  S E T  F O R  P R O B L E M  1
14             !
15        DATA 5.9,.375
16        DATA 20,12,7,45.0
17        DATA 0.5,30.0,600.0
18        DATA 77.0,1000.0,100.0,1250.0,0.8
19        DATA 489.0,0.1275
20             !
21             ! D A T A  S E T  F O R  P R O B L E M  2
22             !
23        DATA 5.9,.375
24        DATA 20,12,7,82.0
25        DATA 0.5,30.0,600.0
26        DATA 77.0,1000.0,100.0,1250.0,0.8
27        DATA 489.0,0.1275
28             !
29             ! D A T A  S E T  F O R  P R O B L E M  3
30             !
31        DATA 5.9,.375
32        DATA 20,15,9,45.0
33        DATA .5,5.0,600.0
34        DATA 77.0,725.0,100.0,1200.0,0.8
35        DATA 489.0,0.1275
36             !
37             ! D O  H E A T  T R A N S F E R  F O R  E A C H  C A S E
38             !
39        READ Np,Np1
40             !
41        Nprob=Np-1
42        Nprob=Nprob+1
43             !
44             ! R E A D  I N  D A T A  F R O M  A B O V E
45             !
46        READ Y,Z
47        READ Ncol,Nrow,Nrowv,Angle
48        READ Tminc,Tmpo,Tmlim
49        READ Tprm,Tplim,Tpinc,Tpfact,Tpexp
50        READ Den,Sh
51             !
52             ! DISPLAY WHICH PROBLEM IS IN PROGRESS
53             !
54        OUTPUT 1;"     P R O B L E M  N U M B E R  :";Nprob-Np+1;"  I S  I N
 P R O G R E S S"
55             !
56             ! KEEP ALL FILES ON TAPE IN PORT 0 UNLESS FULL
57             !
58        MASS STORAGE IS ":HP82901,700,0"
59        F1$="HTDATA"&VAL$(Nprob)
60        ON ERROR GOTO 65
61        CREATE BDAT F1$,1,88
62        CREATE BDAT F1$&"a",50*1,8*12
63        CREATE BDAT F1$&"b",50*Ncol,8*Nrow
64        GOTO 72
65        OFF ERROR
66        ON ERROR GOTO 69
67        PURGE F1$
68        PURGE F1$&"a"
69        OFF ERROR
70        MASS STORAGE IS ":HP82901,700,1"
71        GOTO 61
72        OFF ERROR
73        ASSIGN @Path TO F1$&"a"
74        ASSIGN @Path1 TO F1$&"b"
75             !
76        CALL Htbeam(Y,Den,Sh)
77        IF Nprob<Np1 THEN 42
78             !
79        OUTPUT 1 USING "/////////"
80        OUTPUT 1;"P R O G R A M  I S  F I N I S H E D  W I T H  I T ' S  C O
M P L E T E  R U N"
81        MASS STORAGE IS ":HP82901,700,0"
82        STOP
83        END
84     SUB Htbeam(Y,Den,Sh)
85        COM /Dims/ Dx,Dy,Z,Cpdv,Angle,@Path,@Path1,Tpfact,Tpexp
86        COM /Temp/ Tpweb1(*),Tpweb2(*),Tpcon(*),Tpin(*)
87        COM /Temp2/ Tpel1,Tpel2,Tpinc,Tplim,Tpflag,Tprm
88        COM /Time/ Tminc,Tminc1,Tmlim,Tmlim1,Tmpo
89        COM /Disc/ Nrow,Nrow1,Nrow2,Ncol,Ncol1,Ncol2
90        COM /Data/ Nprob,Nrowv,Neltp,Nrowtp,Itpel,Jtpel,Itpend
91             !
92             ! SUBROUTINE HTBEAM:
93             !             SUBROUTINE WILL CONTROL ALL SUBROUTINE ITERATIONS FO
R THE GIVEN PARAMETERS
94             !
95             ! INPUT VARIABLES:
96             !
97             !       ANGLE . . . ANGLE OF VEE-SHAPED HEAT
98             !       DEN . . . . DENSITY OF MATERIAL
99             !       DX. . . . . DIMENSION OF ELEMENT IN X-DIRECTION
100            !       NCOL. . . . NUMBER OF COLUMNS FOR THE DISCRETIZATION
101            !       NROW. . . . NUMBER OF ROWS FOR THE DISCETIZATION
102            !       NROWV . . . NUMBER OF ROWS TO BE HEATED IN THE VEE-HEAT
103            !       TMLIM . . . TIME LIMIT FOR THE TEMPERATURE CALCULATIONS
104            !       TMPO. . . . TIME INCREMENT TO OUTPUT THE ELEMENT TEMPERAT
URE DISTRIBUTIONS
105            !       TPEXP . . . EXPONENTIAL COMPONENT OF HEAT FLUX PARAMETER
106            !       TPFACT. . . CONSTANT SCALING FACTOR FOR HEAT FLUX PARAMET
ER
107            !       TPLIM . . . TEMPERATURE LIMIT FOR HEATED ELEMENT
108            !       TPRM. . . . AMBIENT TEMPERATURE OF ALL ELEMENTS
109            !       Y . . . . . DEPTH OF SECTION
110            !
111            ! OUTPUT:
112            !
113            !       HTDATA# . . PARAMETERS FOR DISCRETIZING THE SYSTEM
114            !       HTDATA#a. . TEMPERATURE DISTRIBUTIONS AT USER SPECIFIED L
OCATIONS IN THE PROBLEM
115            !       HTDATA#b. . TEMPEATURE DISTRIBUTION FOR ALL ELEMENTS IN T
HE SYSTEM
116            !
117            ! INITIALIZE COUNTING PARAMETER
118            !
```

```
119        Ntmtp=0.
120             !
121             ! OBTAIN THE DATA TO DISCRETIZE THE SYSTEM
122             !
123        CALL Temp_read(Y,Den,Sh)
124             !
125             ! B E G I N   T E M P E R A T U R E   C A L C U L A T I O N S
126             !
127        Tpflag=0
128        IF Itpel<>1 AND Jtpel<>1 THEN CALL Temp_add
129             !
130             ! INCREMENT COUNTERS FOR THIS STEP
131             !
132        Tmlim1=Tmlim1+Tminc
133        Tminc1=Tminc1+Tminc
134             !
135        CALL Temp_con
136        CALL Temp_web(2,2,0.,1.0)
137        CALL Temp_web(Nrow1,Nrow1,1.0,0.)
138        CALL Temp_web(3,Nrow,1.0,1.0)
139        CALL Temp_chng
140             !
141             ! OUTPUT DATA IF REQUIRED
142             !
143        IF Tpflag>=1 THEN CALL Temp_prin(Ntmtp)
144        IF Tpflag>=2 THEN 149
145             !
146             ! INCREMENT FOR ANOTHER LOAD STEP
147             !
148        GOTO 127
149        SUBEND
150    SUB Temp_read(Y,Den,Sh)
151        COM /Dims/ Dx,Dy,Z,Cpdv,Angle,@Path,@Path1,Tpfact,Tpexp
152        COM /Temp/ Tpweb1(*),Tpweb2(*),Tpcon(*),Tpin(*)
153        COM /Temp2/ Tpel1,Tpel2,Tpinc,Tplim,Tpflag,Tprm
154        COM /Time/ Tminc,Tminc1,Tmlim,Tmlim1,Tmpo
155        COM /Disc/ Nrow,Nrow1,Nrow2,Ncol,Ncol1,Ncol2
156        COM /Data/ Nprob,Nrowv,Neltp,Nrowtp,Itpel,Jtpel,Itpend
157             !
158             ! SUBROUTINE HTBEAM:
159             !          DISCRETIZE THE SYSTEM INTO ROWS AND COLUMNS
160             !
161             ! D I S C R E T I Z E   I N T O   E L E M E N T S
162             !
163        Dy=Y/Nrow
164        DEG
165        Dx=Dy*TAN(Angle/2)
166        X=Dx*Ncol
167        Nrow1=Nrow+1
168        Nrow2=Nrow+2
169        Ncol1=Ncol+1
170        Ncol2=Ncol+2
171             !
172             ! M A T E R I A L   P R O P E R T I E S
173             !
174        Cp=Den*Sh/1728.0
175        Cpdv=Dx*Dy*Z*Cp*3600.0/Tminc
176             !
177             ! I N I T I A L I Z E   P A R A M E T E R S
178             !
179        Itpel=2
180        Jtpel=Nrowv+1
181        Nrowtp=1
182        Neltp=0
183        Tminc1=0.
184        Tmlim1=0.
185        Tpel1=Tprm
186             !
187        Nrowv1=Nrowv-(2*(INT(Nrowv/2)))
188        IF Nrowv1=0 THEN Itpend=2
189        IF Nrowv1=1 THEN Itpend=Nrowv+1
190             !
191        FOR I=1 TO Ncol2
192        FOR J=1 TO Nrow2
193        R=(((I-Itpel)*Dx)^2+((J-Jtpel)*Dy)^2)^.5
194        Tpin(I,J)=Tpfact*EXP((-1)*Tpexp*R)*Dx*Dy
195        Tpweb1(I,J)=Tprm
196        NEXT J
197        NEXT I
198        SUBEND
199    SUB Temp_add
200        COM /Dims/ Dx,Dy,Z,Cpdv,Angle,@Path,@Path1,Tpfact,Tpexp
201        COM /Temp/ Tpweb1(*),Tpweb2(*),Tpcon(*),Tpin(*)
202        COM /Temp2/ Tpel1,Tpel2,Tpinc,Tplim,Tpflag,Tprm
203        COM /Time/ Tminc,Tminc1,Tmlim,Tmlim1,Tmpo
204        COM /Disc/ Nrow,Nrow1,Nrow2,Ncol,Ncol1,Ncol2
205        COM /Data/ Nprob,Nrowv,Neltp,Nrowtp,Itpel,Jtpel,Itpend
206             !
207             ! SUBROUTINE TEMP_READ:
208             !          WILL CHECK THE HEATED ELEMENT FOR EXCEEDING THE TEMP
ERATURE LIMIT
209             !          CHANGES THE HEATED ELEMENT AS REQUIRED AND WHILE HEA
T IS BEING INPUT
210             !          SUBROUTINE WILL GOVERN THE OUTPUT OF TEMPERATURE DIS
TRIBUTIONS
211             !
212             ! T E S T   F O R   O U T P U T   O F   T E M P E R A T U R E S
213             !
214        Tpel2=Tpweb1(Itpel,Jtpel)
215        IF (Tpel2-Tpel1)>=Tpinc THEN Tpflag=1
216        IF Tpflag=1 THEN Tpel1=Tpel1+Tpinc
217        IF Tpel2<Tplim THEN SUBEXIT
218             !
219             ! H E A T E D   E L E M E N T   E X C E E D E D "T P L I M"
220             !
221           IF Itpel=Itpend AND Jtpel=2 THEN
222              Itpel=1
223              Jtpel=1
224             !
225             ! S E T   H E A T   I N P U T   T O   Z E R O
226             !
227              FOR I=1 TO Ncol2
228              FOR J=1 TO Nrow2
229              Tpin(I,J)=0.
230              NEXT J
231              NEXT I
232              Tpflag=1
233              SUBEXIT
234           ELSE
235             !
236             ! F I N D   A N O T H E R   E L E M E N T   T O   H E A T
237             !
238              Neltp=Neltp+1
239              Tpflag=1
240           END IF
```

```
241       Itpel=Itpel+Nrowtp
242       IF Itpel=1 THEN Itpel=2
243       K=0
244       FOR L=1 TO Nrowv
245       K=K+L
246       IF K=Neltp THEN Jtpel=Jtpel-1
247       IF K=Neltp THEN Nrowtp=(-1)*Nrowtp
248       NEXT L
249       Tpel1=Tpweb1(Itpel,Jtpel)
250          !
251          ! C H A N G E  H E A T  I N P U T  P A T T E R N
252          !
253       FOR I=1 TO Ncol2
254       FOR J=2 TO Nrow1
255       Rx=((I-Itpel)*Dx)^2
256       Ry=((J-Jtpel)*Dy)^2
257       R=(Rx+Ry)^.5
258       Tpin(I,J)=Tpfact*EXP((-1)*Tpexp*R)*Dx*Dy
259       NEXT J
260       NEXT I
261       GOTO 214
262       SUBEND
263    SUB Temp_con
264       COM /Dims/ Dx,Dy,Z,Cpdv,Angle,@Path,@Path1,Tpfact,Tpexp
265       COM /Temp/ Tpweb1(*),Tpweb2(*),Tpcon(*),Tpin(*)
266       COM /Temp2/ Tpel1,Tpel2,Tpinc,Tplim,Tpflag,Tprm
267       COM /Time/ Tminc,Tminc1,Tmlim,Tmlim1,Tmpo
268       COM /Disc/ Nrow,Nrow1,Nrow2,Ncol,Ncol1,Ncol2
269       COM /Data/ Nprob,Nrowv,Neltp,Nrowtp,Itpel,Jtpel,Itpend
270          !
271          ! SUBROUTINE TEMP_CON:
272          !          WILL ASSIGN THE THERMAL CONDUCTION PARAMETERS TO EAC
H ELEMENT
273          !
274          ! INPUT VARIABLES
275          !
276          !      TPWEB1(*) . CURENT TEMPERATURE OF THE ELEMENTS
277          !
278          ! OUTPUT VARIABLES:
279          !
280          !      TPCON(*). . THERMAL CONDUCTIVITY FOR EACH ELEMENT.
281          !
282       FOR I=1 TO Ncol2
283       FOR J=1 TO Nrow2
284       Tpcon(I,J)=(29.018-(.0074*Tpweb1(I,J)))/12.0
285       NEXT J
286       NEXT I
287       SUBEND
288    SUB Temp_web(Iy,Jy,Cn3,Cn4)
289       COM /Dims/ Dx,Dy,Z,Cpdv,Angle,@Path,@Path1,Tpfact,Tpexp
290       COM /Temp/ Tpweb1(*),Tpweb2(*),Tpcon(*),Tpin(*)
291       COM /Temp2/ Tpel1,Tpel2,Tpinc,Tplim,Tpflag,Tprm
292       COM /Time/ Tminc,Tminc1,Tmlim,Tmlim1,Tmpo
293       COM /Disc/ Nrow,Nrow1,Nrow2,Ncol,Ncol1,Ncol2
294       COM /Data/ Nprob,Nrowv,Neltp,Nrowtp,Itpel,Jtpel,Itpend
295          !
296          ! SUBROUTINE TEMP_WEB:
297          !          PERFORM THE FORWARD DIFFERENCE EQUATIONS FOR THE SOL
UTION
298          !
299          ! UPDATED VARIABLES:
300          !
301          !       TPWEB(*) . NEW TEMPERATURE OF THE ELEMENTS
302          !
303       Hw=0.
304       FOR I=2 TO Ncol1
305       FOR J=Iy TO Jy
306       Ip=I-1
307       Im=I+1
308       Jp=J-1
309       Jm=J+1
310       C1=.5*(Tpcon(Ip,J)+Tpcon(I,J))*Z*Dy/Dx
311       C2=.5*(Tpcon(Im,J)+Tpcon(I,J))*Z*Dy/Dx
312       C3=Cn3*.5*(Tpcon(I,Jp)+Tpcon(I,J))*Z*Dx/Dy
313       C4=Cn4*.5*(Tpcon(I,Jm)+Tpcon(I,J))*Z*Dx/Dy
314       IF Itpel<>1 AND Jtpel<>1 THEN 319
315       H12=.58*ABS(Tpweb1(I,J)*12.0/Dy)^.25
316       H3=(1.0-Cn3)*ABS(Tpweb1(I,J)*12.0/Z)^.25
317       H4=(1.0-Cn4)*ABS(Tpweb1(I,J)*12.0/Z)^.25
318       Hw=((H12*Dx*Dy)+((H3+H4)*Z*Dx))/144.0
319       Tpw1=(C1*Tpweb1(Ip,J))+(C2*Tpweb1(Im,J))
320       Tpw2=(C3*Tpweb1(I,Jp))+(C4*Tpweb1(I,Jm))
321       Tpw3=(Cpdv-(C1+C2+C3+C4+Hw))*Tpweb1(I,J)
322       Tpweb2(I,J)=((Tpw1+Tpw2+Tpw3)+(Hw*Tprm)+Tpin(I,J))/Cpdv
323       NEXT J
324       NEXT I
325       SUBEND
326    SUB Temp_chng
327       COM /Dims/ Dx,Dy,Z,Cpdv,Angle,@Path,@Path1,Tpfact,Tpexp
328       COM /Temp/ Tpweb1(*),Tpweb2(*),Tpcon(*),Tpin(*)
329       COM /Temp2/ Tpel1,Tpel2,Tpinc,Tplim,Tpflag,Tprm
330       COM /Time/ Tminc,Tminc1,Tmlim,Tmlim1,Tmpo
331       COM /Disc/ Nrow,Nrow1,Nrow2,Ncol,Ncol1,Ncol2
332       COM /Data/ Nprob,Nrowv,Neltp,Nrowtp,Itpel,Jtpel,Itpend
333          !
334          ! SUBROUTINE TEMP_CHNG:
335          !          WILL CHANGE THE TEMPERATURE OF THE ELEMENTS FROM TPW
EB2(*) TO TPWEB1(*)
336          !          ALSO WILL GOVERN WHEN TEMPERATURES WILL BE STORED
337          !
338       FOR J=2 TO Nrow1
339       Tpweb1(1,J)=Tpweb2(2,J)
340       Tpweb1(Ncol2,J)=2*Tpweb2(Ncol1,J)-Tpweb2(Ncol,J)
341       NEXT J
342       Tpmax=Tprm
343       FOR I=2 TO Ncol1
344       FOR J=2 TO Nrow1
345       Tpweb1(I,J)=Tpweb2(I,J)
346       IF Tpweb1(I,J)>Tpmax THEN Tpmax=Tpweb1(I,J)
347       NEXT J
348       NEXT I
349       IF Itpel<>1 AND Jtpel<>1 THEN SUBEXIT
350          !
351          ! C O N D I T I O N  F O R  O U T P U T I N G  T E M P E R A T U
 R E S
352          !
353       IF Tminc1>Tmpo THEN Tpflag=1
354          !
355          ! C O N D I T I O N S  F O R  E N D I N G  P R O G R A M
356          !
357       IF Tpmax<200. THEN Tpflag=2
358       IF Tmlim1>=Tmlim THEN Tpflag=2
359       SUBEND
360    SUB Temp_prin(Ntmtp)
```

```
361     COM /Dims/ Dx,Dy,Z,Cpdv,Angle,@Path,@Path1,Tpfact,Tpexp
362     COM /Temp/ Tpweb1(*),Tpweb2(*),Tpcon(*),Tpin(*)
363     COM /Temp2/ Tpel1,Tpel2,Tpinc,Tplim,Tpflag,Tprm
364     COM /Time/ Tminc,Tminc1,Tmlim,Tmlim1,Tmpo
365     COM /Disc/ Nrow,Nrow1,Nrow2,Ncol,Ncol1,Ncol2
366     COM /Data/ Nprob,Nrowv,Neltp,Nrowtp,Itpel,Jtpel,Itpend
367     ALLOCATE REAL T1(0:11),T(1:Ncol,1:Nrow)
368         !
369         ! SUBROUTINE TEMP_PRIN:
370         !           OUTPUT THE TEMPERATURE DISTRIBUTIONS FOR THE SYSTEM
371         !
372     Tminc1=0.
373     Ntmtp=Ntmtp+1
374     T1(0)=Tmlim1                      !   45 DEGREES 60 DEGREES
375     IF Nprob=3 THEN 388
376     T1(1)=Tpweb2(5,7)                 !    ( 5 , 7 ) ( 2 , 8 )
377     T1(2)=Tpweb2(9,7)                 !    ( 9 , 7 ) ( 5 , 8 )
378     T1(3)=Tpweb2(13,7)                !   ( 13 , 7 ) ( 4 , 6 )
379     T1(4)=Tpweb2(17,7)                !   ( 17 , 7 ) ( 7 , 6 )
380     T1(5)=Tpweb2(7,5)                 !    ( 7 , 5 ) ( 13 , 6 )
381     T1(6)=Tpweb2(11,5)                !   ( 11 , 5 ) ( 17 , 6 )
382     T1(7)=Tpweb2(15,5)                !   ( 15 , 5 ) ( 4 , 4 )
383     T1(8)=Tpweb2(19,5)                !   ( 19 , 5 ) ( 9 , 4 )
384     T1(9)=Tpweb2(9,3)                 !    ( 9 , 3 ) ( 13 , 4 )
385     T1(10)=Tpweb2(13,3)               !   ( 13 , 3 ) ( 17 , 4 )
386     T1(11)=Tpweb2(17,3)               !   ( 17 , 3 ) ( 18 , 4 )
387     GOTO 399
388     T1(1)=Tpweb2(2,8)
389     T1(2)=Tpweb2(5,8)
390     T1(3)=Tpweb2(4,6)
391     T1(4)=Tpweb2(7,6)
392     T1(5)=Tpweb2(13,6)
393     T1(6)=Tpweb2(17,6)
394     T1(7)=Tpweb2(4,4)
395     T1(8)=Tpweb2(9,4)
396     T1(9)=Tpweb2(13,4)
397     T1(10)=Tpweb2(17,4)
398     T1(11)=Tpweb2(18,4)
399     OUTPUT @Path;T1(*)
400     FOR I=2 TO Ncol1
401     FOR J=2 TO Nrow1
402     T(I-1,J-1)=Tpweb2(I,J)
403     NEXT J
404     NEXT I
405     OUTPUT @Path1;T(*)
406     DEALLOCATE T1(*),T(*)
407     IF Tpflag<>2 THEN SUBEXIT
408     ASSIGN @Path TO *
409     ASSIGN @Path1 TO *
410     ASSIGN @Path TO "NTDATA"&VAL$(Nprob)
411     Y=Nrow*Dy
412     OUTPUT @Path;Y,Z,Ncol,Nrow,Nrowv,Angle,Tpfact,Tpexp,Tplim,Ntmtp,Tprm
413     ASSIGN @Path TO *
414     SUBEND
```

APPENDIX B

FINITE ELEMENT COMPUTER PROGRAM

```
1 ! PROGRAM "F I N I T E"
2 !
3 !  PROGRAM "FINITE" WAS WRITTEN TO CALCULATE THE PLASTIC STRESSES AND STRAIN
4 !  OF A THERMALLY LOADED SYSTEM.  THE TEMPERATURE DISTRIBUTION MUST ALREADY
5 !  EXIST.  THE PROGRAM WAS WRITTEN IN BASIC TO EXECUTE ON THE "HP 9816"
6 !  SERIES 200 PERSONAL COMPUTER.
7 !
8 !  PROGRAMMED BY :  STEPHEN P. SCHNEIDER
9 !  DATE          :  5/30/84
10!
11!
12! CONTROL PARAMETERS:
13!
14!  IFLAG. . . . . INDICATES WHEN PROGRAM IS IN ITERATION SUBROUTINE
15!  ISTR . . . . . COUNTER FOR THE ITERATION BETWEEN LOAD STEPS
16!  KTYPE. . . . . STIFFNESS TYPE
17!  NTMSTR . . . . NUMBER OF LOAD STEPS REQUIRED BY THE PROBLEM
18!  NSTR . . . . . NUMBER OF STEPS COMPLETED BY PROGRAM
19!  STYPE. . . . . SOLUTION TYPE
20!  PRINT. . . . . PRINTOUT TYPE
21!
22! MATERIAL PROPERTIES:
23!
24!  RATIO. . . . . RATIO OF THE PLASTIC TANGENT MODULUS TO THE ELASTIC MODULUS
25!  PRO. . . . . . POISSON'S RATIO FOR AN ELASTIC ELEMENT
26!  PR1. . . . . . POISSON'S RATIO FOR A PLASTIC ELEMENT
27!  YM . . . . . . YOUNG'S MODULUS OF AN ELEMENT AT AMBIENT (ROOM) TEMPERATURE
28!  YS . . . . . . YIELD STRESS OF AN ELEMENT AT AMBIENT (ROOM) TEMPERATURE
29!
30! LOADING PARAMETERS:
31!
32!  MSCL . . . . . APPLIED MOMENT IN LB-INCHES (COMPRESSION ON BOTTOM (+)ve)
33!  PSCL . . . . . APPLIED AXIAL LOAD IN LBS   (TENSION (+)ve)
34!  VSCL . . . . . APPLIED SHEAR LOAD IN LBS   (COUNTER-CLOCKWISE SHEAR (+)ve)
35!
36! DISCRETIZATION:
37!
38!  DX . . . . . . DIMENSION OF ELEMENT IN X-DIRECTION
39!  DY . . . . . . DIMENSION OF ELEMENT IN Y-DIRECTION
40!  DZ . . . . . . DIMENSION OF ELEMENT IN Z-DIRECTION
41!
42!  NB . . . . . . MAXIMUM BAND WIDTH
43!  NE . . . . . . TOTAL NUMBER OF ELEMENTS
44!  NEQ. . . . . . TOTAL NUMBER OF EQUATIONS
45!  NN . . . . . . TOTAL NUMBER OF NODES
46!
47!  NX . . . . . . NUMBER OF ELEMENTS IN X-DIRECTION
48!  NY . . . . . . NUMBER OF ELEMENTS IN Y-DIRECTION
49!
50! PERMANENT ARRAYS:
51!
52!  BB(*). . . . . TRANSFORMATION MATRIX FOR EACH SAMPLING POINT
53!
54!  D(*) . . . . . STRESS-STRAIN RELATION MATRIX
55!                 0 FOR THE ELASTIC CASE
56!                 1 FOR THE PLASTIC CASE
57!
58!  DT(*). . . . . TEMPERATURE INCREMENT FROM THE PREVIOUS LOAD STEP
59!                 TO THE CURRENT STEP FOR EACH ELEMENT
60!
61!  FE(*). . . . . TOTAL FORCE VECTOR USED FOR ENERGY CALCULATIONS
62!
63!  FT(*). . . . . TOTAL FORCE VECTOR USED TO SOLVE THE SIMULTANEOUS EQUATIONS
64!
65!  FTH(*) . . . . TOTAL THERMAL LOAD VECTOR FOR EACH LOAD STEP
66!
67!  HH(*). . . . . SHAPE FUNCTION FOR EACH SAMPLING POINT
68!
69!  IDE(*) . . . . ELEMENT IDENTIFICATION ARRAY ;
70!                 MAPPING ELEMENTS TO EACH OF ITS FOUR NODES
71!
72!  IDN(*) . . . . NODAL IDENTIFICATION ARRAY ;
73!                 MAPPING THE NODES TO THE CORRESPONDING DOFS;
74!                 Y-DOF IS ASSUMED TO BE 1 HIGHER THAN THE X-DOF
75!
76!  JYIELD(*). . . YIELD SURFACE RADIUS OF THE PREVIOUS LOAD STEP
77!
78!  LM(*). . . . . LOCATION MATRIX ;
79!                 MAPPING ELEMENT DOFS TO GLOBAL DEGREES OF FREEDOM
80!
81!  TEMP(*). . . . CURRENT TEMPERATURE OF EACH ELEMENT
82!
83!  PLAST(*) . . . ELASTIC/PLASTIC CONDITION OF ELEMENT
84!
85!  UT(*). . . . . TOTAL DISPLACEMENT ARRAY FOR EACH DEGREE OF FREEDOM
86!
87!  XY(*). . . . . X & Y GLOBAL LOCATION FOR EACH NODE
88!
89! TEMPORARY ARRAYS:
90!
91!  F2(*). . . . . STORES THE INTERNAL FORCE VECTOR FOR SUBROUTINE "STRESSK"
92!
93!  KG(*). . . . . GLOBAL STIFFNESS ARRAY
94!
95!  STR(*) . . . . STRESS & STRAIN ARRAY FROM PREVIOUS CALCULATIONS
96!
97!  T(*) . . . . . ARRAY FOR OBTAINING TEMPERATURE DATA
98 !
99 !  U2(*). . . . . THE INCREMENTAL DISPLACEMENTS THROUGH SUBROUTINE "STRESSK"
100!
101!FILES:
102!
103!  HTDATA$. . . . STORAGE FOR DISCRETIZATION PARAMETERS FOR SYSTEM
104!
105!  HTDATA$b . . . STORAGE FOR ALL ELEMENT TEMPERATURE DATA
106!
107!  KG . . . . . . STORAGE FOR PREVIOUS GLOBAL STIFFNESS
108!
109!  STRESS . . . . STORAGE FOR PREVIOUS STRESS & STRAINS
110!
111!  @TEMP1 . . . . I/O PATH TO RECOVER TEMPERATURE DATA FROM FILE "HTDATA$b"
```

```
1     COM Dx,Dy,Dz,Nx,Ny,Nn,Nb,Ne,Neq
2     COM /Bk1/ Bb(0:4,1:3,1:8),Hh(0:4,1:4),D(0:1,1:3,1:3),Wt(0:4)
3     COM /Bk2/ Ktype,Stype,Iflag,Istr,Enrgy1,Enrgy2
4     COM /Bk3/ Ys,Ym,Ratio,Pr0,Pr1
5     COM /Bk4/ Nstr,Pscl,Vscl,Mscl
6     PRINTER IS 701
7     PRINT CHR$(27)&"&k2S"
8         !
9         ! READ IN:   SOLUTION TYPE  (STYPE)
10        !            STIFFNESS TYPE (KTYPE)
11        !            PRINTOUT TYPE  (PRINT)
12        !
13        !  STYPE=  1 ADD CORRECTION OF LOADS ON NEXT STEP
14        !          2 ITERATE UNTIL CORRECTION BECOMES NEGLIGABLE
15        !
16        !  KTYPE=  0 CONSTANT STIFFNESS THROUGHOUT SOLUTION
17        !          1 CHANGE STIFFNESS AT EVERY LOADSTEP
18        !          2 CHANGE STIFFNESS AT EVERY ITERATION STEP
19        !
20        !  PRINT=  0 DO NOT PRINT OUTPUT FOR EVERY LOADSTEP
21        !          1 PRINT OUTPUT FOR EVERY LOAD STEP
22        !
23    DATA 2,0,0
24    READ Stype,Ktype,Print
25        !
26        ! SPECIFY MATERIAL PROPERTIES (USUALLY THE SAME FOR EACH CASE)
27        !
28    DATA 30000000.0,0.01,36000.0,0.3,0.5
29    READ Ym,Ratio,Ys,Pr0,Pr1
30        !
31        ! CALL SUBROUTINE TO OBTAIN DISCRETIZATION OF DATA
32        !
33    CALL Data1(Tprm,Ntmstr,@Temp1)
34        !
35        ! ALLOCATE STORAGE ACCORDING TO PARAMETERS
36        !
37    ALLOCATE INTEGER Ide(1:4,1:Ne),Idn(1:2,1:Nn),Lm(1:8,1:Ne),Plast(1:2,
1:Ne)
38    ALLOCATE REAL Xy(1:2,1:Nn),Jyield(1:Ne),Temp(1:Ne),Dt(1:Ne)
39    DIM K1(0:1,1:8,1:8)
40        !
41        ! GENERATE DATA INTO DISCTETE ELEMENTS
42        !
43    CALL Data2(Xy(*),Ide(*),Idn(*),Lm(*))
44    CALL Data3(Print)
45        !
46        ! DIMENSION FORCE, DISPLACEMENT AND STRESS-STRAIN ARRAYS
47        !
48    ALLOCATE REAL F1(0:Neq),Ft(0:Neq),Fth(0:Neq),Fe(0:Neq),Ut(0:Neq),Str
(1:Ne,1:6)
49        !
50        ! INITIALIZE & STORE STRESSES
51        !
52    ON ERROR GOTO 54
53    PURGE "STRESS:HP82901,700,0"
54    OFF ERROR
55    CREATE BDAT "STRESS:HP82901,700,0",Ne,48
56        !
57    FOR I=1 TO Ne
58    FOR J=1 TO 6
59    Str(I,J)=0.
60    NEXT J
61    NEXT I
62        !
63    ASSIGN @P TO *
64    ASSIGN @P TO "STRESS:HP82901,700,0"
65    OUTPUT @P;Str(*)
66    ASSIGN @P TO *
67    DEALLOCATE Str(*)
68        !
69        ! INITIALIZE VARIABLES
70        !
71    FOR I=0 TO Neq
72    Fth(I)=0
73    Ft(I)=0
74    Ut(I)=0
75    NEXT I
76        !
77    FOR I=1 TO Ne
78    Temp(I)=Tprm
79    Jyield(I)=(Ys*Ys)/3
80    FOR J=1 TO 2
81    Plast(J,I)=0
82    NEXT J
83    NEXT I
84        !
85        ! INITIALIZE PARAMETERS FOR FIRST ITERATION
86        !
87    Nstr=1
88    Istr=1
89    Iflag=0
90    Enrgy1=0
91    Enrgy2=0
92        !
93    CALL Dmatrix
94    CALL Bmatrix(Xy(*),Ide(*))
95    CALL Kmatrix(K1(*))
96    Kchng=0
97        !
98        ! EXCHANGE PERMANANT LOAD VECTOR TO TOTAL LOAD VECTOR
99        !
100   CALL Data4(Temp(*),Dt(*),@Temp1)
101   CALL Thermf(Fth(*),Temp(*),Dt(*),Ide(*),Idn(*),Plast(*))
102   CALL Fmatrix(F1(*),Idn(*))
103       !
104       ! ADJUST YIELD VALUE FOR THE NEW TEMPERATURE
105       !
106   ALLOCATE REAL Str(1:Ne,1:6),Fp(0:Neq)
107   ASSIGN @P TO *
108   ASSIGN @P TO "STRESS:HP82901,700,0"
109   ENTER @P;Str(*)
110   ASSIGN @P TO *
111       !
112   FOR Ielm=1 TO Ne
113   T1=Temp(Ielm)
114   T0=T1-Dt(Ielm)
115   CALL Yield(T0,R0)
116   CALL Yield(T1,R1)
117   R2=(R1*R1)/(R0*R0)
118   Jyield(Ielm)=R2*Jyield(Ielm)
119       !
120       ! CORRECT THE YIELD STRESS FOR THE PLASTIC ELEMENTS
```

```
121          !
122     IF Plast(2,Ielm)=0 THEN 144
123     FOR I=1 TO 3
124     S(I)=(1-SQR(R2))*Str(Ielm,I)
125     Str(Ielm,I)=SQR(R2)*Str(Ielm,I)
126     NEXT I
127          !
128          ! FIND EQUIVALENT FORCES ON THE ELEMENTS
129          !
130     FOR I=1 TO 8
131     P(I)=0.
132     FOR J=1 TO 3
133     P(I)=P(I)+Bb(0,J,I)*S(J)*Wt(0)
134     NEXT J
135     NEXT I
136          !
137          ! LOAD ONTO CORRECTION FORCE VECTOR
138          !
139     FOR I=1 TO 4
140     Node=Ide(I,Ielm)
141     Fp(Idn(1,Node))=Fp(Idn(1,Node))+P(2*I-1)
142     Fp(Idn(2,Node))=Fp(Idn(2,Node))+P(2*I)
143     NEXT I
144     NEXT Ielm
145          !
146          ! RE-STORE THE STRESSES REDUCED FOR THIS STEP
147          !
148     ASSIGN @P TO *
149     ASSIGN @P TO "STRESS:HP82901,700,0"
150     OUTPUT @P;Str(*)
151     ASSIGN @P TO *
152          !
153          ! FIND TOTAL LOAD VECTOR
154          !
155     FOR I=1 TO Neq
156     Ft(I)=Fl(I)+Fp(I)-Ft(I)-Fth(I)
157     Fe(I)=Ft(I)+Fth(I)
158     NEXT I
159     DEALLOCATE Str(*),Fp(*)
160          !
161          ! ASSEMBLE AND INVERT THE STIFFNESS MATRIX
162          !
163     ALLOCATE REAL Kg(1:Neq,1:Nb)
164     IF Kchng=0 THEN CALL Assembk(Kg(*),Kl(*),Temp(*),Lm(*),Plast(*))
165     CALL Invert(Kg(*),Ft(*),Kchng)
166     DEALLOCATE Kg(*)
167          !
168          ! CALCULATE THE STRESSES AND STRAINS FOR THIS LOADSTEP
169          !
170     CALL Stressk(Ft(*),Fe(*),Ut(*),Xy(*),Temp(*),Dt(*),Jyield(*),Ide(*),
Idn(*),Lm(*),Plast(*))
171          !
172          ! ITERATE THE SOLUTION IF REQUIRED
173          !
174     IF Stype=2 THEN CALL Iterate(Fl(*),Ft(*),Fe(*),Ut(*),Kl(*),Xy(*),Tem
p(*),Dt(*),Jyield(*),Ide(*),Idn(*),Lm(*),Plast(*))
175     IF Print=1 THEN CALL Dataout(Ut(*),Idn(*),Plast(*))
176     OUTPUT 1;"COMPLETED ";Nstr;" OF ";Ntmstr+1;" LOAD STEPS"
177     OUTPUT 1;" "
178     Kchng=1
179     IF Ktype>0 THEN Kchng=0
180     IF Nstr=0 THEN 195
181     Nstr=Nstr+1
182     IF Nstr<=Ntmstr THEN 100
183          !
184          ! SET TEMPERATURE VALUES BACK TO ROOM (AMBIENT) TEMPERATURE
185          !
186     FOR I=1 TO Ne
187     Dt(I)=Tprm-Temp(I)
188     Temp(I)=Tprm
189     NEXT I
190     Mscl=0
191     Pscl=0
192     Vscl=0
193     Nstr=0
194     GOTO 101
195     IF Print<>1 THEN CALL Dataout(Ut(*),Idn(*),Plast(*))
196     STOP
197     END
198   SUB Iterate(Fl(*),Ft(*),Fe(*),Ut(*),Kl(*),Xy(*),Temp(*),Dt(*),Jyield(*),
INTEGER Ide(*),Idn(*),Lm(*),Plast(*))
199     COM Dx,Dy,Dz,Nx,Ny,Nn,Nb,Ne,Neq
200     COM /Bk1/ Bb(*),Hh(*),D(*),Wt(*)
201     COM /Bk2/ Ktype,Stype,Iflag,Istr,Enrgy1,Enrgy2
202     COM /Bk3/ Ys,Ym,Ratio,Pr0,Pr1
203     COM /Bk4/ Nstr,Ps,Vs,Ms
204          !
205          ! SUBROUTINE ITERATE :
206          !          ITERATES THE OUT-OF-BALANCE LOAD VECTOR UNTIL WITHI
N THE TOLERABLE LIMIT
207          !          THE FIRST IS FOR THE INCREMENTAL ENERGY TO BE LESS
THAN THE INITIAL FOR THIS STEP (ENRGY1)
208          !          THE SECOND IS FOR THE INCREMENTAL ENERGY TO BE LESS
 THAN THE RUNNING TOTAL (ENRGY2)
209          !
210          ! UPDATED VARIABLE:
211          !
212          !       IFLAG . . . USED TO INDICATE THAT THE PROGRAM IS IN THE
 ITERATION ROUTINE
213          !       ISTR. . . . NUMBER OF ITERATIONS FOR THIS LOAD STEP
214          !
215          ! INDICATE THAT THE PROGRAM IS IN ITERATION SUBROUTINE
216          !
217     Iflag=1
218          !
219          ! CHECK ENERGY CRITERION FOR CONVERGENCE
220          !
222     IF ABS(Fe(0))<=ABS(.001*Enrgy1) THEN Etype=1
223     IF ABS(Fe(0))<=ABS(.001*Enrgy1) THEN 251
224     IF ABS(Fe(0))<=ABS(.000000001*Enrgy2) THEN Etype=2
225     IF ABS(Fe(0))<=ABS(.000000001*Enrgy2) THEN 251
226     Fe1=Fe(0)/Enrgy1
227     Fe2=Fe(0)/Enrgy2
228     DISP "INCREMENTAL ENERGY :";DROUND(Fe1,5);" ; TOTAL ENERGY :";DROUND
(Fe2,5);" FOR ITERATION : ";Istr
229          !
230          ! FIND NEW CORRECTION FORCE VECTOR
231          !
232     FOR I=1 TO Neq
233     Ft(I)=Fl(I)-Ft(I)
234     Fe(I)=Ft(I)
235     NEXT I
236          !
237          ! ASSEMBLE & INVERT NEW STIFFNESS MATRIX IF NECESSARY
```

```
239        Istr=Istr+1
240        Kchng=1
241        IF Ktype>1 THEN Kchng=0
242        ALLOCATE REAL Kg(1:Neq,1:Nb)
243        IF Kchng=0 THEN CALL Assembk(Kg(*),Kl(*),Temp(*),Lm(*),Plast(*))
244        CALL Invert(Kg(*),Ft(*),Kchng)
245        DEALLOCATE Kg(*)
246             !
247             ! FIND STRESSES FOR UPDATED STIFFNESS
248             !
249        CALL Stressk(Ft(*),Fe(*),Ut(*),Xy(*),Temp(*),Dt(*),Jyield(*),Ide(*),
Idn(*),Lm(*),Plast(*))
250        GOTO 222
251        OUTPUT 1;" NO. OF ITERATIONS FOR LOAD STEP :";Istr;" : CONVERGED BY
ENERGY CHECK ";Etype
252        Istr=1
253        Iflag=0
254        SUBEND
255     SUB Data1(Tprm,Ntmstr,@Temp1)
256        COM Dx,Dy,Dz,Nx,Ny,Nn,Nb,Ne,Neq
257        COM /Bk4/ Nstr,Pscl,Vscl,Mscl
258             !
259             ! SUBROUTINE DATA1 :
260             !              WILL OBTAIN PARAMETERS FROM FILE "HTDATA*b" PREVIOU
SLY GENERATATED
261             !              FOR DISCRETIZATION OF SYSTEM INTO ELEMENTS
262             !
263             ! OUTPUT VARIABLES:
264             !
265             !         DX. . . . . ELEMENT DIMENSION IN THE X-DIRECTION
266             !         DY. . . . . ELEMENT DIMENSION IN THE Y-DIRECTION
267             !         DZ. . . . . ELEMENT DIMENSION IN THE Z-DIRECTION
268             !
269             !         NX. . . . . NUMBER OF ELEMENTS IN THE X-DIRECTION
270             !         NY. . . . . NUMBER OF ELEMENTS IN THE Y-DIRECTION
271             !
272             !         NE. . . . . TOTAL NUMBER OF ELEMENTS OF THE SYSTEM
273             !         NN. . . . . TOTAL NUMBER OF NODES FOR THE SYSTEM
274             !         NB. . . . . TOTAL BANDWIDTH OF THE SYSTEM
275             !
276             !         PSCL. . . . AXIAL LOAD OF PROBLEM
277             !         MSCL. . . . APPLIED MOMENT OF PROBLEM
278             !         VSCL. . . . SHEAR LOAD FOR PROBLEM
279             !
280             !         TPRM. . . . AMBIENT TEMPERATURE OF THE SYSTEM
281             !         NTMSTR. . . NUMBER OF THERMAL APLICATION LOAD STEPS
282             !
283             !         @TEMP1. . . I/O PATH FOR ELEMENT TEMPERATURE PROFILES
284             !
285             ! OBTAIN SYSTEM DISCRETIZATION FROM FILE HTDATA*
286             !
287        ASSIGN @Temp1 TO *
288        INPUT "INPUT ""HTDATA"" FILENUMBER FOR TEMPERATURE CALCULATIONS",F1$
289        MASS STORAGE IS ":HPB2901,700,0"
290        F1$="HTDATA"&F1$
291        ASSIGN @Temp1 TO F1$
292        ENTER @Temp1;Y,Z,Nx,Ny,Nyv,Ang,Tpf,Tpe,Tpl,Ntmstr,Tprm
293        Nx=Nx/2
294        Ny=Ny/2
295        ASSIGN @Temp1 TO *
296        F1$=F1$&"b"
297        ASSIGN @Temp1 TO F1$
```

```
299             ! DISCRETIZE INTO FINITE ELEMENTS
300             !
301        Dy=Y/Ny
302        Dz=Z
303        DEG
304        Dx=Dy*TAN(Ang/2)
305        Ne=Nx*Ny
306        Nn=(Nx+1)*(Ny+1)
307        Nb=(Ny+3)*2
308             !
309             ! INPUT THE LOAD OF THE SYSTEM
310             !
311        INPUT "INPUT THE AXIAL LOAD IN lbs.",Pscl
312        INPUT "INPUT THE SHEAR LOAD IN lbs.",Vscl
313        INPUT "INPUT THE APLIED MOMENT IN  lb-ins.",Mscl
314             !
315             ! DISPLAY THE VARIABLE JUST INPUT
316             !
317        OUTPUT 1 USING "///////"
318        OUTPUT 1 USING "25X,18A,SDDDDDD.DDD";"AXIAL LOAD IS :",Pscl
319        OUTPUT 1 USING "25X,18A,SDDDDDD.DDD";"SHEAR LOAD IS :",Vscl
320        OUTPUT 1 USING "25X,18A,SDDDDDD.DDD";"APPLIED MOMENT IS :",Mscl
321        SUBEND
322     SUB Data2(Xy(*),INTEGER Ide(*),Idn(*),Lm(*))
323        COM Dx,Dy,Dz,Nx,Ny,Nn,Nb,Ne,Neq
324             !
325             ! SUBROUTINE DATA2 :
326             !              WILL GENERATE MAPPING ARRAYS OF THE NODES AND ELEME
NTS OF DISCRETIZATION
327             !
328             ! OUTPUT VARIABLES:
329             !
330             !         IDE(*). . . ARRAY FOR MAPPING ELEMENTS TO ITS FOUR CORR
ESPONDING NODE
331             !         IDN(*). . . ARRAY FOR MAPPING NODES TO CORRESPONDING DE
GREES OF FREEDOM
332             !         LM(*) . . . LOCATION MATRIX ARRAY FOR MAPPING LOCAL DEG
REES OF FREEDOM TO GLOBAL
333             !         XY(*) . . . COORDINATE LOCATION OF THE NODES IN THE X A
ND Y DIRECTION
334             !
335             ! DISCRETIZE INTO X & Y COORDINATES
336             !
337        Nn1=0
338        FOR I=0 TO Nx
339        FOR J=0 TO Ny
340        Nn1=Nn1+1
341        Xy(1,Nn1)=I*Dx
342        Xy(2,Nn1)=J*Dy
343        NEXT J
344        NEXT I
345             !
346             ! OBTAIN THE BOUNDARY CONDITIONS FOR THE BEAM
347             !
348        CALL Disp(Idn(*))
349             !
350             ! CREATE A NODE-TO-ELEMENT AND GLOBAL DOF LOCATION MAP
351             !
352        Ne1=0
353        FOR I=1 TO Nx
354        FOR J=1 TO Ny
```

```
357        N(2)=N(1)+Ny+1
358        N(3)=N(2)+1
359        N(4)=N(1)+1
360        FOR L=1 TO 4
361        Ide(L,Ne1)=N(L)
362        L11=2*L-1
363        L12=L11+1
364        Lm(L11,Ne1)=Idn(1,N(L))
365        Lm(L12,Ne1)=Idn(2,N(L))
366        NEXT L
367        NEXT J
368        NEXT I
369        SUBEND
370     SUB Disp(INTEGER Idn(*))
371        COM Dx,Dy,Dz,Nx,Ny,Nn,Nb,Ne,Neq
372           !
373           ! SUBROUTINE DISP :
374           !            WILL GENERATE MAPPING MATRIX IDN(*) FROM THE DISPLA
CEMENT BOUNDARY CONDITIONS OF SYSTEM
375           !
376           ! OUTPUT VARIABLES:
377           !
378           !       IDN(*). . . IDENTIFICATION MATRIX FOR THE NODES
379           !
380        FOR J=1 TO Nn
381        FOR I=1 TO 2
382        Idn(I,J)=0
383        NEXT I
384        NEXT J
385           !
386           ! APPLY THE BOUNDARY CONDITIONS:
387           !
388           !         IDN(*)= 0 IF FREE IN SPECIFIED DIRECTION
389           !                 1 IF RESTRAINED IN SPECIFIED DIRECTION
390           !
391        FOR J=1 TO Ny+1
392        Idn(1,J)=1
393        NEXT J
394        Idn(2,INT((Ny+2)/2))=1
395           !
396           ! ASSIGN EQUATION NUMBER TO EACH NODE
397           !
398        Neq=0
399        FOR J=1 TO Nn
400        FOR I=1 TO 2
401        IF Idn(I,J)=1 THEN 405
402        Neq=Neq+1
403        Idn(I,J)=Neq
404        GOTO 406
405        Idn(I,J)=0
406        NEXT I
407        NEXT J
408        SUBEND
409     SUB Data3(Print)
410        COM Dx,Dy,Dz,Nx,Ny,Nn,Nb,Ne,Neq
411        COM /Bk2/ Ktype,Stype,Iflag,Istr,Enrgy1,Enrgy2
412        COM /Bk4/ Nstr,Ps,Vs,Ms
413           !
414           ! SUBROUTINE DATA3 :
415           !            WILL ECHO THE DATA FOR THIS PROBLEM
416           !
417           !
418           ! FORMAT STATEMENTS FOR THE OUTPUT
419           !
420        IMAGE ///,20X,46A,//
421        IMAGE #,37X,24A,DDD
422        IMAGE 5X,48A
423        IMAGE 69X,48A
424        IMAGE /,37X,26A,DDD
425        IMAGE /,37X,35A,DDD
426        IMAGE /,37X,35A,DD.DDD
427        IMAGE /,37X,35A,SDDDDDDD.DD,7A
428           !
429           !
430           !
431        PRINT USING 420;"I N P U T   P A R A M E T E R S :           "
432        PRINT USING 421;"SOLUTION TYPE (STYPE) :";Stype
433        PRINT USING 422;"(STYPE)=  1 ADD CORRECTION OF LOADS ON NEXT STEP"
434        PRINT USING 423;"          2 ITERATE CORRECTION UNTIL TOLERABLE  "
435        PRINT
436        PRINT USING 421;"STIFFNESS TYPE (KTYPE):";Ktype
437        PRINT USING 422;"(KTYPE)=  0 USE CONSTANT STIFFNESS FOR SOLUTION "
438        PRINT USING 423;"          1 CHANGE STIFFNESS EVERY LOADSTEP     "
439        PRINT USING 423;"          2 CHANGE STIFFNESS EVERY ITERATION    "
440        PRINT
441        PRINT USING 421;"PRINTOUT TYPE (PRINT): ";Print
442        PRINT USING 422;"(PRINT)=  0 DO NOT PRINT OUTPUT FOR EACH STEP   "
443        PRINT USING 423;"          1 PRINT OUTPUT FOR EACH STEP          "
444        PRINT USING 420;"E L E M E N T   D I S C R E T I Z A T I O N :"
445        PRINT USING 424;"NUMBER OF ELEMENTS IS :   ";Ne
446        PRINT USING 424;"NUMBER OF NODES IS :      ";Nn
447        PRINT USING 424;"BAND WIDTH IS :           ";Nb
448        PRINT USING 424;"NUMBER OF EQUATIONS IS :  ";Neq
449        PRINT
450        PRINT USING 425;"NO OF ELEMENTS IN X-DIRECTION IS : ";Nx
451        PRINT USING 425;"NO OF ELEMENTS IN Y-DIRECTION IS : ";Ny
452        PRINT
453        PRINT USING 426;"DIM OF ELEMENT IN X-DIRECTION IS : ";Dx
454        PRINT USING 426;"DIM OF ELEMENT IN Y-DIRECTION IS : ";Dy
455        PRINT USING 426;"DIM OF ELEMENT IN Z-DIRECTION IS : ";Dz
456        PRINT USING 420;"A P P L I E D   L O A D I N G S :"
457        PRINT USING 427;"APPLIED AXIAL LOAD IS : ";Ps;" lbs."
458        PRINT USING 427;"APPLIED SHEAR LOAD IS : ";Vs;" lbs."
459        PRINT USING 427;"APPLIED END MOMENT IS : ";Ms;" lb-ins"
460        SUBEND
461     SUB Data4(T1(*),Dt(*),@Temp1)
462        COM Dx,Dy,Dz,Nx,Ny,Nn,Nb,Ne,Neq
463        COM /Bk4/ Nstr,Pscl,Vscl,Mscl
464           !
465           ! SUBROUTINE DATA4 :
466           !            WILL OBTAIN THE TEMPERATURE PROFILE FOR EACH LOAD S
TEP
467           !
468           ! INPUT VARIABLES:
469           !
470           !       T1(*) . . . ELEMENT TEMPERATURES FROM PREVIOS LOAD STEP
471           !       @TEMP1. . . I/O PATH FOR TEMPERATURE DISTRIBUTION
472           !
473           ! UPDATED VARIABLE:
474           !
475           !       DT(*) . . . TEMPERATURE CHANGE FROM PREVIOUS TO CURRENT
ELEMENT TEMPS
476           !       T1(*) . . . CURRENT ELEMENT TEMPERATURES
477           !
478        Nx1=Nx*2
```

```
481        ENTER @Templ;T2(*)
482        FOR I=1 TO Nx
483        FOR J=1 TO Ny
484        I1=I*2
485        J1=J*2
486        T3(I,J)=.25*(T2(I1-1,J1-1)+T2(I1-1,J1)+T2(I1,J1-1)+T2(I1,J1))
487        NEXT J
488        NEXT I
489        I1=0
490        FOR I=1 TO Nx
491        FOR J=1 TO Ny
492        I1=I1+1
493        T4(I1)=T3(I,J)
494        NEXT J
495        NEXT I
496        FOR I=1 TO Ne
497        Dt(I)=T4(I)-T1(I)
498        T1(I)=T4(I)
499        NEXT I
500        DEALLOCATE T2(*),T3(*),T4(*)
501        GOTO 519
502        ALLOCATE REAL T(1:Ne)
503        ENTER @Templ;T(*)
504        Dt_max=0
505        FOR I=1 TO Ne
506        Dt(I)=T(I)-T1(I)
507        IF Dt(I)>Dt_max THEN Dt_max=Dt(I)
508        NEXT I
509        IF Dt_max<50 THEN
510        Nstr=Nstr+1
511        GOTO 503
512        END IF
513        IF Dt_max>50 THEN
514        FOR I=1 TO Ne
515        T1(I)=T(I)
516        NEXT I
517        END IF
518        DEALLOCATE T(*)
519        SUBEND
520     SUB Young(T,P,E)
521        COM /Bk2/ Ktype,Stype,Iflag,Istr,Enrgy1,Enrgy2
522        COM /Bk3/ Ys,Ym,Ratio,Pr0,Pr1
523            !
524            ! SUBROUTINE YOUNG :
525            !          CALCULATES YOUNGS MODULUS FOR ELEMENTS WITH GIVEN T
EMPERATURES
526            !
527            ! INPUT VARIABLES:
528            !
529            !      P . . . . . INDICATES WHETHER ELEMENT IS ELASTIC OFR PL
ASTIC
530            !      T . . . . . CURRENT TEMPERATURE OF THE ELEMENT
531            !
532            !
533            ! OUTPUT VARIABLE:
534            !
535            !      E . . . . . TEMPERATURE DEPENDENT YOUNGS MODULUS FOR EL
EMENT IN LBS/SQ. IN.
536            !
537            ! FIND THE APPROPRIATE RATIO FOR ELASTIC MODULUS
538            !
539        IF P=0 THEN R=1
```



```
541            !
542            ! COMPUTE YOUNGS MODULUS FOR ELEMENT
543            !
544        IF T<=100. THEN E=R*Ym
545        IF T>=100. AND T<=700. THEN E=R*Ym*(1.0185-.000185*T)
546        IF T>=700. THEN E=R*Ym*(500000.+1333.*T-1.111*T^2)*10^(-6)
547        SUBEND
548     SUB Yield(T,R)
549            !
550            ! SUBROUTINE YIELD :
551            !          CALCULATES THE YIELD RATIO FOR THE CURRENT ELEMENT
TEMPERATURE
552            !
553            ! INPUT VARIABLE:
554            !
555            !      T . . . . . CURRENT ELEMENT TEMPERATURE
556            !
557            ! OUTPUT VARIABLE:
558            !
559            !      R . . . . . RATIO OF THE CURRENT TEMPERATURE YIELD STRE
SS TO REFERENCE TEMP YIELD STRESS
560            !
561            ! COMPUTE THE REDUCTION RATIO FOR TEMP YIELD AND REFERENCE TEMP
562            !
563        IF T<=100. THEN R=1
564        IF T>100. AND T<=800. THEN R=(1.0-(T-100)/5833)
565        IF T>=800. THEN R=(-720000.0+4200.0*T-2.75*T^2)*10^(-6)
566        SUBEND
567     SUB Alpha(T1,T0,A)
568            !
569            ! SUBROUTINE ALPHA :
570            !          FINDS THE AVERAGE VALUE OF THE COEFFICEINT OF THERM
AL EXPANSION
571            !
572            ! INPUT VARIABLES:
573            !
574            !      T0. . . . . PREVIOUS ELEMENT TEMPERATURE
575            !      T1. . . . . CURRENT ELEMENT TEMPERATURE
576            !
577            ! OUTPUT VARIABLE:
578            !
579            !      A . . . . . AVERAGE VALUE OF THERMAL EXPANSION IN IN/IN
/DEGREES F
580            !
581            !
582            ! COMPUTE THE COEFFICIENT OF THERMAL EXPANSION
583            !
584        IF T0<=200. THEN A0=.0000065
585        IF T0>=200. THEN A0=.0000061+.000000002*T
586        IF T1<=200. THEN A1=.0000065
587        IF T1>=200. THEN A1=.0000061+.000000002*T
588        A=.5*(A1+A0)
589        SUBEND
590     SUB Fmatrix(F1(*),INTEGER Idn(*))
591        COM Dx,Dy,Dz,Nx,Ny,Nn,Nb,Ne,Neq
592        COM /Bk4/ Nstr,Ps,Vs,Ms
593            !
594            ! SUBROUTINE FMATRIX :
595            !          DISCRETIZES THE THREE INPUT LOADS TO THE NODES ON T
HE EDGE OF THE BEAM
596            !
597            ! INPUT VARIABLES:
598            !
```

```
660        FOR I=0 TO 2*Ny
661        Y=I/Ny
662        Ld(I)=M*(Y-1)+P
663        NEXT I
664        Ld(2*Ny+1)=0.
665        Ld(0)=Ld(0)/2.
666        Ld(2*Ny)=Ld(2*Ny)/2.
667            !
668            ! ADD THE FORCES TO THE GLOBAL FORCE VECTOR
669            !
670        FOR J=0 TO Ny
671        Ii=Ii+1
672        Jj=2*J
673        F1=Ny1*(Dy/3)*(Ld(Jj-1)+Ld(Jj)+Ld(Jj+1))
674        IF Idn(1,Ii)=0 THEN 676
675        Fl(Idn(1,Ii))=Fl(Idn(1,Ii))+F1
676        NEXT J
677            !
678            ! APPLY MOMENT AND AXIAL LOADS TO THE L.H.S. OF BEAM
679            !
680        IF Ii<(Ny+1)*Nx THEN 685
681        Ii=0
682        Ny1=-1
683        Ms1=(Ms-Vs*Nx*Dx)
684        GOTO 657
685        DEALLOCATE Ld(*)
686        SUBEND
687    SUB Thermf(Fl(*),Temp(*),Dt(*),INTEGER Ide(*),Idn(*),Plast(*))
688        COM Dx,Dy,Dz,Nx,Ny,Nn,Nb,Ne,Neq
689        COM /Bk1/ Bb(*),Hh(*),D(*),Wt(*)
690        COM /Bk2/ Ktype,Stype,Iflag,Istr,Enrgy1,Enrgy2
691        COM /Bk3/ Ys,Ym,Ratio,Pr0,Pr1
692        COM /Bk4/ Nstr,Pscl,Vscl,Mscl
693            !
694            ! SUBROUTINE THERMF :
695            !              APPLIES THE CHANGE IN TEMPERATURE TO THE SYSTEM AS
INITIAL STRESSES
696            !
697            ! INPUT VARIABLES:
698            !
699            !       BB(*) . . . STRAIN DISPLACEMENT TRANSFORMATION MATRIX
700            !       DT(*) . . . CHANGE IN TEMPERATURE FOR EACH ELEMENT
701            !       TEMP(*) . . CURRENT TEMPERATURE FOR EACH ELEMENT
702            !       WT(*) . . . WEIGHTED RESIDUALS
703            !
704            ! OUTPUT VARIABLES:
705            !
706            !       Fl(*) . . . APPLIED THERMAL LOAD FOR THE CHANGE IN TEMP
ERATURE
707            !
708            ! INITIALIZE THE THERMAL FORCE VECTOR TO ZERO
709            !
710        FOR I=0 TO Neq
711        Fl(I)=0
712        NEXT I
713            !
714            ! FIND THE STRESSES AND STRAINS DUE TO THERMAL LOADINGS
715            !
716        FOR Ielm=1 TO Ne
717            !
718            ! SET MATERIAL PROPERTIES FOR EACH ELEMENT
719            !
720        P1=Plast(2,Ielm)
```

```
599            !       PS . . . . . AXIAL LOAD : ASSUMED CONSTANT STRESS AT LE
FT END
600            !       MS . . . . . MOMENT     : ASSUMED LINEAR STRESS AT LEFT
 END
601            !       VS . . . . . SHEAR LOAD : ASSUMED PARABOLIC STRESS AT L
EFT AND RIGHT EDGE
602            !
603            ! OUTPUT VARIABLE:
604            !
605            !       FL(*). . . . TOTAL EXTERNALLY APPLIED LOAD VECTOR
606            !
607            ! INTIALIZE LOAD TO ZERO
608            !
609        FOR I=0 TO Neq
610        Fl(I)=0
611        NEXT I
612            !
613        ALLOCATE REAL Ld(-1:2*Ny+1)
614            !
615        IF Vs=0. AND Ms=0. AND Ps=0. THEN 685
616        IF Vs=0. THEN 650
617            !
618            ! APPLY THE SHEAR LOAD TO THE R.H.S. OF BEAM
619            !
620        V=6*Vs/(Ny*Dy)
621        Ld(-1)=0
622        FOR I=0 TO 2*Ny
623        Y=.5*I/Ny
624        Ld(I)=V*(Y-Y^2)
625        NEXT I
626        Ld(2*Ny+1)=0.
627        Ii=(Ny+1)*Nx
628        Ny1=1
629            !
630            ! ADD THE FORCES TO THE GLOBAL FORCE VECTOR
631            !
632        FOR J=0 TO Ny
633        Ii=Ii+1
634        Jj=2*J
635        F1=Ny1*(Dy/3)*(Ld(Jj-1)+Ld(Jj)+Ld(Jj+1))
636        IF Idn(2,Ii)=0 THEN 638
637        Fl(Idn(2,Ii))=Fl(Idn(2,Ii))+F1
638        NEXT J
639            !
640            ! APPLY THE SHEAR LOAD TO THE L.H.S. OF BEAM
641            !
642        IF Ii<(Ny+1)*Nx THEN 650
643        Ii=0
644        Ny1=-1
645        GOTO 632
646            !
647            ! IF MSCALE AND PSCALE ARE ZERO THEN ADD THE MOMENT
648            ! DUE TO THE SHEAR FORCE TO THE L.H.S. OF THE BEAM
649            !
650        IF Ms=0. AND Ps=0. THEN 681
651            !
652            ! APPLY THE MOMENT AND AXIAL LOADS TO THE R.H.S. OF BEAM
653            !
654        Ny1=1
655        Ii=(Ny+1)*Nx
656        Ms1=Ms
657        M=6*Ms1/(Ny*Dy)^2
658        P=Ps/Ny*Dy
```

```
721         T1=Temp(Ielm)
722         T0=T1-Dt(Ielm)
723         CALL Young(T1,P1,E1)
724         CALL Alpha(T1,T0,A1)
725             !
726             ! STRESSES WILL BE OPPOSITE OF THE STRAINS
727             !
728         Ep(1)=(-1)*A1*Dt(Ielm)
729         Ep(2)=Ep(1)
730         Ep(3)=0.
731         FOR I=1 TO 3
732         S(I)=0.
733         FOR J=1 TO 3
734         S(I)=S(I)+E1*D(P1,I,J)*Ep(J)
735         NEXT J
736         NEXT I
737         FOR I=1 TO 8
738         P(I)=0.
739         FOR J=1 TO 3
740         P(I)=P(I)+Bb(0,J,I)*S(J)*Wt(0)
741         NEXT J
742         NEXT I
743             !
744             ! LOAD INTO TOTAL FORCE VECTOR
745             !
746         FOR I=1 TO 4
747         Node=Ide(I,Ielm)
748         F1(Idn(1,Node))=F1(Idn(1,Node))+P(2*I-1)
749         F1(Idn(2,Node))=F1(Idn(2,Node))+P(2*I)
750         NEXT I
751             !
752         NEXT Ielm
753         SUBEND
754     SUB Bmatrix(Xy(*),INTEGER Ide(*))
755         COM Dx,Dy,Dz,Nx,Ny,Nn,Nb,Ne,Neq
756         COM /Bk1/ Bb(*),Hh(*),D(*),Wt(*)
757             !
758             ! SUBROUTINE BMATRIX:
759             !           USES GAUSSIAN INTEGRATION TO FIND THE INTERPOLATION
 AND STRAIN-DISPLACEMENT FUNCTIONS
760             !
761             ! INPUT VARIABLE:
762             !
763             !       WT(*). . . . WEIGHTING VALUE FOR SAMPLING POINTS
764             !
765             ! OUTPUT VARIABLE:
766             !
767             !       BB(*). . . . STRAIN-DISPLACEMENT TRANSFORMATION MATRIX
768             !       HH(*). . . . INTERPOLATION (SHAPE) FUNCTION
769             !       WT(*). . . . WEIGHTING RESIDUALS FOR THE SAMPLING POINT
S
770             !
771             !
772             ! INPUT DATA FOR INTEGRATION POINTS
773             !
774         DATA 0,0,-1,-1,1,-1,1,1,-1,1
775         FOR I=0 TO 4
776         READ R(I),S(I)
777         IF I=0 THEN 780
778         R(I)=R(I)/SQR(3)
779         S(I)=S(I)/SQR(3)
780         NEXT I
781             !
782             ! ASSIGN VALUE FOR EACH SAMPLING POINT
783             !
784         FOR J=1 TO 4
785         FOR I=1 TO 2
786         X1(I,J)=Xy(I,Ide(J,1))
787         NEXT I
788         NEXT J
789         FOR Intg=0 TO 4
790         Rp=(1+R(Intg))
791         Rm=(1-R(Intg))
792         Sp=(1+S(Intg))
793         Sm=(1-S(Intg))
794             !
795             ! CONSTRUCT THE SHAPE FUNCTIONS
796             !       1.) W.R.T. R
797             !       2.) W.R.T. S
798             !       3.) TOTAL INTERPOLATION FUNCTION
799             !
800         H1(1,1)=(-1)*.25*Sm
801         H1(1,2)=.25*Sm
802         H1(1,3)=.25*Sp
803         H1(1,4)=(-1)*.25*Sp
804         H1(2,1)=(-1)*.25*Rm
805         H1(2,2)=(-1)*.25*Rp
806         H1(2,3)=.25*Rp
807         H1(2,4)=.25*Rm
808         H1(3,1)=.25*Rm*Sm
809         H1(3,2)=.25*Rp*Sm
810         H1(3,3)=.25*Rp*Sp
811         H1(3,4)=.25*Rm*Sp
812             !
813             ! EVALUATE JACOBIAN MATRIX
814             !
815         FOR I=1 TO 2
816         FOR J=1 TO 2
817         Xj(I,J)=0.
818         FOR K=1 TO 4
819         Xj(I,J)=Xj(I,J)+H1(I,K)*X1(J,K)
820         NEXT K
821         NEXT J
822         NEXT I
823             !
824             ! EVALUATE THE DETERMINATE
825             !
826         Det=Xj(1,1)*Xj(2,2)-Xj(2,1)*Xj(1,2)
827             !
828             ! FIND THE INVERSE OF THE JACOBIAN MATRIX
829             !
830         Xji(1,1)=Xj(2,2)/Det
831         Xji(1,2)=(-1)*Xj(1,2)/Det
832         Xji(2,1)=(-1)*Xj(2,1)/Det
833         Xji(2,2)=Xj(1,1)/Det
834             !
835             ! FIND THE TRANSFORMATION MATRIX AND STORE IN MATRIX BB
836             !
837         FOR K=1 TO 4
838         K1=2*K-1
839         K2=2*K
840         B1(1,K1)=0.
```

```
841        B1(2,K1)=0.
842        B1(1,K2)=0.
843        B1(2,K2)=0.
844        FOR L=1 TO 2
845        B1(1,K1)=B1(1,K1)+Xji(1,L)*Hi(L,K)
846        B1(2,K2)=B1(2,K2)+Xji(2,L)*Hi(L,K)
847        NEXT L
848        B1(3,K2)=B1(1,K1)
849        B1(3,K1)=B1(2,K2)
850        NEXT K
851        IF Intg=0 THEN Det=Det*4
852        Wt(Intg)=Det*Dz
853        FOR I=1 TO 3
854        FOR J=1 TO 8
855        Bb(Intg,I,J)=B1(I,J)
856        NEXT J
857        NEXT I
858        FOR I=1 TO 4
859        Hb(Intg,I)=Hi(3,I)
860        NEXT I
861        NEXT Intg
862        SUBEND
863     SUB Dmatrix
864        COM Dx,Dy,Dz,Nx,Ny,Nn,Nb,Ne,Neq
865        COM /Bk1/ Bb(*),Hh(*),D(*),Wt(*)
866        COM /Bk2/ Ktype,Stype,Iflag,Istr,Enrgy1,Enrgy2
867        COM /Bk3/ Ys,Ym,Ratio,Pr0,Pr1
868            !
869            ! SUBROUTINE DMATRIX :
870            !          COMPUTES THE CONSTITUTIVE MATRIX FOR TWO DIFFERENT
POISSON RATIOS
871            !          THIS ASSUMES THAT YOUNG'S MODULUS HAS BEEN FACTORED
 OUT
872            !
873            ! INPUT VARIABLES:
874            !
875            !       PR0 . . . . ELASTIC ELEMENT POISSON RATIO
876            !       PR1 . . . . PLASTIC ELEMENT POISSON RATIO
877            !
878            ! OUTPUT VARIABLSE:
879            !
880            !       D(0,*). . . ELASTIC STRESS-STRAIN MATRIX
881            !       D(1,*). . . PLASTIC STRESS-STRAIN MATRIX
882            !
883        FOR I=0 TO 1
884        IF I=0 THEN Pr=Pr0
885        IF I=1 THEN Pr=Pr1
886        E=1
887        D1=E/(1-Pr*Pr)
888        D2=D1*Pr
889        D3=(D1-D2)/2
890            !
891            ! ASSEMBLE ELEMENT STRESS-STRAIN MATRIX
892            !
893        D(I,1,1)=D1
894        D(I,2,2)=D1
895        D(I,3,3)=D3
896        D(I,1,2)=D2
897        D(I,2,1)=D2
898        D(I,1,3)=0.
899        D(I,2,3)=0.
900        D(I,3,1)=0.
901        D(I,3,2)=0.
902        NEXT I
903        SUBEND
904     SUB Kmatrix(K1(*))
905        COM Dx,Dy,Dz,Nx,Ny,Nn,Nb,Ne,Neq
906        COM /Bk1/ Bb(*),Hh(*),D(*),Wt(*)
907            !
908            ! SUBROUTINE KMATRIX:
909            !          COMPUTES ELEMENT STIFFNESS MATRIX ACCORDING TO THE
DIMENSIONS OF THE FIRST ELEMENT ONLY
910            !
911            ! INPUT VARIABLES:
912            !
913            !       BB(*). . . . STRAIN-DISPLACEMENT TRANSFORMATION MATRIX
914            !       D(*) . . . . CONSTITUTIVE MATRIX
915            !       WT(*). . . . WEIGHTING VALUE FOR SAMPLING POINTS
916            !
917            ! OUTPUT VARIABLES:
918            !
919            !       KL(0,*). . . ELASTIC ELEMENT STIFFNESS MATRIX
920            !       KL(1,*). . . PLASTIC ELEMENT STIFFNESS MATRIX
921            !
922            !
923        FOR Num=0 TO 1
924        FOR I=1 TO 8
925        FOR J=1 TO 8
926        K1(Num,I,J)=0.
927        NEXT J
928        NEXT I
929        FOR Intg=1 TO 4
930        FOR J=1 TO 8
931        FOR K=1 TO 3
932        Db(K)=0.
933        FOR L=1 TO 3
934        Db(K)=Db(K)+D(Num,K,L)*Bb(Intg,L,J)
935        NEXT L
936        NEXT K
937        FOR I=1 TO 8
938        Ke=0.
939        FOR L=1 TO 3
940        Ke=Ke+Bb(Intg,L,I)*Db(L)
941        NEXT L
942        K1(Num,I,J)=K1(Num,I,J)+Ke*Wt(Intg)
943        NEXT I
944        NEXT J
945        NEXT Intg
946        NEXT Num
947        SUBEND
948     SUB Assembk(Kg(*),K1(*),Temp(*),INTEGER Lm(*),Plast(*))
949        COM Dx,Dy,Dz,Nx,Ny,Nn,Nb,Ne,Neq
950            !
951            ! SUBROUTINE ASSEMBK:
952            !          ASSEMBLES THE STIFFNESS MATRIX KNOWING THE STIFFNES
SES OF THE ELEMENTS
953            !
954            ! INPUT VARIABLES:
955            !
956            !       KL(*). . . . ELEMENT STIFFNESS MATRIX
957            !       TEMP(*). . . TEMPERATURE PROFILE OF SYSTEM
958            !       PLAST(*) . . ELASTIC/PLASTIC CONDITION OF ELEMENT
959            !
960            ! OUTPUT VARIABLE:
```

```
961         !
962         !       KG(*). . . . TOTAL ASSEMBLED GLOBAL STIFFNESS MATRIX
963         !
964         !
965         ! INITIALIZE VALUES TO ZERO
966         !
967      FOR I=1 TO Neq
968      FOR J=1 TO Nb
969      Kg(I,J)=0.
970      NEXT J
971      NEXT I
972         !
973      FOR Ielm=1 TO Ne
974         !
975      P1=Plast(2,Ielm)
976      T1=Temp(Ielm)
977      CALL Young(T1,P1,E1)
978         !
979         ! A S S E M B L E   G L O B A L   S T I F F N E S S   M A T R I
X
980         !
981      FOR I=1 TO 8
982      Ii=Lm(I,Ielm)
983      IF Ii=0 THEN 991
984      FOR J=1 TO 8
985      Jj=Lm(J,Ielm)
986      IF Jj=0 THEN 990
987      Ji=Jj-Ii
988      IF Ji<0 THEN 990
989      Kg(Ii,Ji+1)=Kg(Ii,Ji+1)+E1*K1(P1,I,J)
990      NEXT J
991      NEXT I
992      NEXT Ielm
993      SUBEND
994   SUB Invert(Kg(*),F(*),Kchng)
995      COM Dx,Dy,Dz,Nx,Ny,Nn,Nb,Ne,Neq
996         !
997         ! SUBROUTINE INVERT:
998         !           REDUCES THE STIFFNESS MATRIX AS NEEDED AND THE INCR
EMENTAL LOAD VECTOR EVERY TIME
999         !
1000        ! INPUT VARIABLE:
1001        !
1002        !       KCHNG. . . . PARAMETER TO INDICATE IF NEW STIFFNESS HAS
 BEEN SUPPLIED
1003        !       KG(*). . . . TOTAL ASSEMBLED GLOBAL STIFFNESS MATRIX
1004        !       F(*) . . . . TOTAL INCREMENTAL LOAD VECTOR
1005        !
1006        ! UPDATED VARIABLE:
1007        !
1008        !       F(*) . . . . LOCAL NODAL DISPLACEMENT VECTOR
1009        !
1010     IF Kchng=1 THEN 1045
1011        !
1012        ! R E D U C E   T H E   S T I F F N E S S   M A T R I X
1013        !
1014     FOR N=1 TO Neq-1
1015     N1=N-1
1016     Nb1=Nb
1017     IF Neq-N1<Nb1 THEN Nb1=Neq-N1
1018     Piv=Kg(N,1)
1019     FOR L=2 TO Nb1
1020     C=Kg(N,L)/Piv
1021     I=N1+L
1022     J=0
1023     FOR K=L TO Nb1
1024     J=J+1
1025     Kg1=Kg(N,K)
1026     Kg(I,J)=Kg(I,J)-C*Kg(N,K)
1027     Kg1=Kg(I,J)
1028     NEXT K
1029     Kg(N,L)=C
1030     Kg1=Kg(N,L)
1031     NEXT L
1032     NEXT N
1033     ON ERROR GOTO 1035
1034     PURGE "KG:HP82901,700,1"
1035     OFF ERROR
1036     CREATE BDAT "KG:HP82901,700,1",Neq*2,(Nb/2)*8
1037     ASSIGN @P TO *
1038     ASSIGN @P TO "KG:HP82901,700,1"
1039     OUTPUT @P;Kg(*)
1040     ASSIGN @P TO *
1041     GOTO 1049
1042        !
1043        ! R E D U C E   T H E   F O R C E   V E C T O R
1044        !
1045     ASSIGN @P TO *
1046     ASSIGN @P TO "KG:HP82901,700,1"
1047     ENTER @P;Kg(*)
1048     ASSIGN @P TO *
1049     FOR N=1 TO Neq-1
1050     N1=N-1
1051     Nb1=Nb
1052     IF Neq-N1<Nb1 THEN Nb1=Neq-N1
1053     C=F(N)
1054     F(N)=C/Kg(N,1)
1055     FOR L=2 TO Nb1
1056     I=N1+L
1057     F(I)=F(I)-C*Kg(N,L)
1058     NEXT L
1059     NEXT N
1060        !
1061        ! B A C K   S U B S T I T U T E
1062        !
1063     F(Neq)=F(Neq)/Kg(Neq,1)
1064     FOR N=1 TO Neq-1
1065     N1=Neq-N
1066     N2=N1-1
1067     Nb1=Nb
1068     IF Neq-N2<Nb1 THEN Nb1=Neq-N2
1069     FOR K=2 TO Nb1
1070     L=N2+K
1071     F(N1)=F(N1)-F(L)*Kg(N1,K)
1072     NEXT K
1073     NEXT N
1074     SUBEND
1075  SUB Stressk(F1(*),F3(*),Ut(*),Xy(*),Temp(*),Dt(*),Jyield(*),INTEGER Ide(*
),Idn(*),Lm(*),Plast(*))
1076     COM Dx,Dy,Dz,Nx,Ny,Nn,Nb,Ne,Neq
1077     COM /Bk1/ Bb(*),Hh(*),D(*),Wt(*)
1078     COM /Bk2/ Ktype,Stype,Iflag,Istr,Enrgy1,Enrgy2
1079     COM /Bk3/ Ys,Ym,Ratio,Pr0,Pr1
1080     COM /Bk4/ Nstr,Pscl,Vscl,Mscl
```

```
1133        U11(I*2-1)=0.
1134        U11(I*2)=0.
1135        X1(1,I)=Xy(1,L1(I))
1136        X1(2,I)=Xy(2,L1(I))
1137        NEXT I
1138          !
1139          ! INTEGRATE DISPLACEMENTS OVER EACH SAMPLING POINT
1140          !
1141        FOR I=1 TO 4
1142        FOR J=1 TO 4
1143        U11(2*J-1)=U11(2*J-1)+Hh(I,J)*U1(2*J-1)
1144        U11(2*J)=U11(2*J)+Hh(I,J)*U1(2*J)
1145        NEXT J
1146        NEXT I
1147          !
1148          ! SET THE NEGLIGABLE DISPLACEMENTS TO ZERO
1149          ! AND ADD ONTO THE TOTAL DISPLACEMENT VECTOR
1150          !
1151        FOR I=1 TO 8
1152        IF ABS(U11(I))<10^(-10) THEN U11(I)=0.
1153        U2(Lm(I,Ielm))=U11(I)
1154        NEXT I
1155          !
1156          ! OBTAIN INITIAL STRAINS IF FIRST ITERATION OF LOADSTEP
1157          !
1158        Ep1(1)=0.
1159        IF Iflag=0 THEN Ep1(1)=-A1*Dt(Ielm)
1160        Ep1(2)=Ep1(1)
1161        Ep1(3)=0.
1162          !
1163          ! FIND INCREMENTAL STRAINS FOR ITERATION STEP
1164          !
1165        FOR I=1 TO 3
1166        FOR J=1 TO 8
1167        Ep1(I)=Ep1(I)+Bb(0,I,J)*U1(J)
1168        NEXT J
1169        NEXT I
1170          !
1171          ! FIND THE INCREMENTAL STRESSES FOR ITERATION STEP
1172          !
1173        FOR I=1 TO 3
1174        S1(I)=0.
1175        FOR J=1 TO 3
1176        S1(I)=S1(I)+E1*D(P1,I,J)*Ep1(J)
1177        NEXT J
1178        NEXT I
1179          !
1180          ! RECOVER THE PREVIOUS STRESSES & STRAINS
1181          !
1182        FOR I=1 TO 3
1183        S0(I)=Str(Ielm,I)
1184        Ep0(I)=Str(Ielm,I+3)
1185        NEXT I
1186          !
1187          ! CHECK THE YIELDING CRITERION
1188          !
1189        CALL Plastic(Jyield(*),S0(*),S1(*),Ep1(*),T1,Ielm,Plast(*))
1190          !
1191          ! STORE THE FINAL STRESSES & STRAINS FROM SUBROUTINE "PLASTIC"
1192          !
1193        FOR I=1 TO 3
1194        Str(Ielm,I)=S0(I)+S1(I)
1195        Str(Ielm,I+3)=Ep0(I)+Ep1(I)
```

```
1081          !
1082          ! SUBROUTINE STRESSK:
1083          !           FINDS INCREMENTAL DISPLACEMENTS, STRAINS AND STRESS
ES OF THE SYSTEM.
1084          !           CALCULATES THE EQUIVALENT NODAL LOADS FROM CORRECTE
D STRESSES
1085          !
1086          ! INPUT VARIABLES:
1087          !
1088          !        EP0(*) . . . STRAIN FROM ALL PREVIOUS CALCULATION
1089          !        EP1(*) . . . INCREMENTAL STRAIN CALCULATED FOR THIS ITE
RATION
1090          !        F1(*). . . . INCREMENTAL LOCAL NODAL DISPLACEMENT VECTO
R
1091          !        F2(*). . . . INITIALIZED TO FIND THE EQUIVALENT INTERNA
L FORCES
1092          !        F3(*). . . . INCREMENTAL LOAD VECTOR FOR THIS ITERATION
 USED TO CALCULATE ENERGY FOR THIS STEP
1093          !        S0(*). . . . STRESS FROM ALL PREVIOUS CALCULATION
1094          !        S1(*). . . . INCREMENTAL STRESS CALCULATED FOR THIS ITE
RATION
1095          !        U2(*). . . . INITIALIZED TO STORE GLOBAL NODAL DISPLACE
MENTS
1096          !        UT(*). . . . TOTAL GLOBAL DISPLACEMENT VECTOR FROM ALL
PREVIOUS ITERATION STEPS
1097          !
1098          ! UPDATED VARIABLES:
1099          !
1100          !        ENRGY1 . . . INCREMENTAL ENERGY OF THIS TIME STEP
1101          !        ENRGY2 . . . TOTAL ENERGY OF THE SYSTEM
1102          !        F1(*). . . . TOTAL EQUIVALENT FORCE FOR SYSTEM
1103          !        F3(0). . . . ENERGY OF THE SYSTEM FOR THIS ITERATION ST
EP
1104          !        STR(*) . . . TOTAL STRESS AND STRAIN ARRAY FOR ALL PREV
IOUS AND CURRENT ANALYSIS
1105          !        UT(*). . . . TOTAL DISPLACEMENT VECTOR FROM ALL PREVIOU
S AND CURRENT ANALYSIS
1106          !
1107          ! DIMENSION ELEMENT STRESS & STRAIN MATRICES
1108          !
1109        ALLOCATE REAL Str(1:Ne,1:6),F2(0:Neq),U2(0:Neq)
1110        ALLOCATE REAL S0(1:3),S1(1:3),Ep0(1:3),Ep1(1:3),P(1:8)
1111          !
1112          ! OBTAIN PREVIOUS STRESSES & DISPLACEMENTS
1113          !
1114        ASSIGN @P TO *
1115        ASSIGN @P TO "STRESS:HP82901,700,0"
1116        ENTER @P;Str(*)
1117        ASSIGN @P TO *
1118          !
1119          !C H E C K   S T R E S S E S   O V E R   E A C H   E L E M
1120          !
1121        FOR Ielm=1 TO Ne
1122          !
1123        P1=Plast(2,Ielm)
1124        T1=Temp(Ielm)
1125        T0=T1-Dt(Ielm)
1126        CALL Young(T1,P1,E1)
1127        CALL Alpha(T1,T0,A1)
1128          !
1129        FOR I=1 TO 4
1130        L1(I)=Ide(I,Ielm)
1131        U1(I*2-1)=F1(Idn(I,L1(I)))
```

```
1196      NEXT I
1197          !
1198          ! CORRECT THE STRESSES TO EQUIVALENT NODAL LOADS
1199          !
1200      FOR I=1 TO 8
1201      P(I)=0
1202      FOR J=1 TO 3
1203      P(I)=P(I)+Bb(0,J,I)*Str(Iela,J)*Wt(0)
1204      NEXT J
1205      NEXT I
1206          !
1207          ! ADD ONTO THE CORRECTION FORCE VECTOR
1208          !
1209      FOR I=1 TO 4
1210      Node=Ide(I,Iela)
1211      F2(Idn(1,Node))=F2(Idn(1,Node))+P(2*I-1)
1212      F2(Idn(2,Node))=F2(Idn(2,Node))+P(2*I)
1213      NEXT I
1214      NEXT Iela
1215          !
1216          ! ADD THE DISPLACMENTS FROM THIS STEP TO THE PREVIOUS STEP
1217          !
1218      F3(0)=0
1219      FOR I=1 TO Neq
1220      F3(0)=F3(0)+U2(I)*F3(I)
1221      F1(I)=F2(I)
1222      Ut(I)=Ut(I)+U2(I)
1223      NEXT I
1224          !
1225          ! RE-ADJUST THE ENERGY PARAMETERS
1226          !
1227      IF Istr=1 THEN Enrgy1=F3(0)
1228      Enrgy2=Enrgy2+F3(0)
1229          !
1230          ! STORE THE STRESSES & DISPLACEMENTS IN THE APPROPRIATE FILE
1231          !
1232      ASSIGN @P TO *
1233      ASSIGN @P TO "STRESS:HP82901,700,0"
1234      OUTPUT @P;Str(*)
1235      ASSIGN @P TO *
1236          !
1237          !
1238          !
1239      DEALLOCATE S0(*),S1(*),Ep0(*),Ep1(*),P(*)
1240      DEALLOCATE Str(*),F2(*),U2(*)
1241      SUBEND
1242  SUB Plastic(Jy(*),S0(*),S1(*),Ep1(*),T1,Iela,INTEGER Plast(*))
1243      COM Dx,Dy,Dz,Nx,Ny,Nn,Nb,Ne,Neq
1244      COM /Bk1/ Bb(*),Hh(*),D(*),Wt(*)
1245      COM /Bk2/ Ktype,Stype,Iflag,Istr,Enrgy1,Enrgy2
1246      COM /Bk3/ Ys,Ym,Ratio,Pr0,Pr1
1247      COM /Bk4/ Nstr,Pscl,Vscl,Mscl
1248          !
1249          ! SUBROUTINE PLAST :
1250          !           CORRECTS THE STRESSES AND ADJUSTS THE YIELD CONSTAN
T VALUE FOR YIELDED ELEMENTS
1251          !
1252          ! INPUT VARIABLES:
1253          !
1254          !       DELM(*). . . . ARRAY OF YIELDED ELEMENTS
1255          !       EP1(*) . . . . INCREMENTAL STRAIN FOR CURRENT LOAD STEP
1256          !       JYIELD(*). . . ARRAY OF PREVIOUS YIELD SURFACE RADIUS
1257          !       NYIELD . . . . NUMBER OF ELEMENTS YIELDED
1259          !       S1(*). . . . . TRIAL STRESS INCREMENT FOR PLASTIC CHECK
1260          !       T0 . . . . . . PREVIUOS ELEMENT TEMPERATURE
1261          !       T1 . . . . . . CURRENT ELEMENT TEMPERATURE
1262          !
1263          ! UPDATED VARIABLES:
1264          !
1265          !       S1(*). . . . . TRUE STRESS INCREMENT AT END OF STEP
1266          !       S2(*). . . . . ERROR ON THE STRESSES (FOR CORRECTION
1267          !                      OF THE FORCE TO BE ADDED ON NEXT STEP)
1268          !       YR . . . . . . YIELD FOR THE ELEMENT (WILL BE REPLACED
1269          !                      IN THE "JYIELD" ARRAY FOR NEXT STEP)
1270          !       PLAST(*) . . . CURRENT CONDITION OF EACH ELEMENT
1271          !                      PLAST(*)=0  ELASTIC ELEMENT
1272          !                               1  PLASTIC ELEMENT
1273          !
1274          !
1275      FOR I=1 TO 3
1276      S(I)=S0(I)+S1(I)
1277      NEXT I
1278          !
1279          ! OBTAIN REQUIRED DATA FOR YIELDING CONDITIONS
1280          !
1281      Yr=Jy(Iela)
1282      CALL Yield(T0,R0)
1283      CALL Yield(T1,R1)
1284          !
1285          ! EVALUATE THE SECOND INVARIANT OF THE STRESS TENSOR
1286          !
1287      Q(3)=(-1/3)*(S(1)+S(2))
1288      Q(1)=S(1)+Q(3)
1289      Q(2)=S(2)+Q(3)
1290      Q(4)=SQR(2)*S(3)
1291      J1=0.
1292      FOR I=1 TO 4
1293      J1=J1+Q(I)*Q(I)
1294      NEXT I
1295      J1=J1/2
1296          !
1297          !
1298          ! 4 COMBINATIONS OF ELEMENT STRESS:
1299          !
1300          !         1.) ELASTIC & REMAINING ELASTIC
1301          !         2.) ELASTIC & YIELDING
1302          !         3.) PLASTIC & STRAIN HARDENING
1303          !         4.) PLASTIC & UNLOADING AS AN ELASTIC ELEMENT
1304          !
1305          !
1306      IF J1<Yr AND Plast(2,Iela)=0 THEN SUBEXIT       !  CASE 1.)
1307      IF J1>=Yr AND Plast(2,Iela)=0 THEN 1313         !  CASE 2.)
1308      IF J1>=Yr AND Plast(2,Iela)=1 THEN 1384         !  CASE 3.)
1309      IF J1<Yr AND Plast(2,Iela)=1 THEN 1389          !  CASE 4.)
1310          !
1311          !C A S E  2 . )  E L E M E N T  I S  Y I E L D I N G
1312          !
1313      Plast(1,Iela)=1
1314      Plast(2,Iela)=1
1315      P1=1
1316          !
1317          ! FIND THE PREVIOUS SECOND INVARIANT
1318          !
1319      Q(3)=(-1/3)*(S0(1)+S0(2))
1320      Q(1)=S0(1)+Q(3)
```

```
1321        Q(2)=S0(2)+Q(3)
1322        Q(4)=SQR(2)*S0(3)
1323        J0=0.
1324        FOR I=1 TO 4
1325        J0=J0+Q(I)*Q(I)
1326        NEXT I
1327        J0=J0/2
1328            !
1329            ! FIND THE SCALING RATIO
1330            !
1331        Ru=(SQR(J1)-SQR(Yr))/(SQR(J1)-SQR(J0))
1332        Rl=(SQR(Yr)-SQR(J0))/(SQR(J1)-SQR(J0))
1333            !
1334            ! SCALE THE STRAINS BY THIS AMOUNT
1335            !
1336        FOR I=1 TO 3
1337        Dep(I)=Ru*Ep1(I)
1338        NEXT I
1339            !
1340            ! FIND THE NEW ELASTIC MODULUS
1341            !
1342        CALL Young(T1,P1,E1)
1343            !
1344            ! FIND NEW STRESSES FOR THE NEW STRAIN INCREMENT
1345            !
1346        FOR I=1 TO 3
1347        Q(I)=0
1348        FOR J=1 TO 3
1349        Q(I)=Q(I)+E1*D(P1,I,J)*Dep(J)
1350        NEXT J
1351        NEXT I
1352            !
1353            ! FIND TRUE STRESS AT END OF STEP
1354            !
1355        FOR I=1 TO 3
1356        S1(I)=S1(I)*Rl+Q(I)
1357        NEXT I
1358            !
1359            ! FIND NEW VALUE OF STRESS
1360            !
1361        FOR I=1 TO 3
1362        S(I)=S0(I)+S1(I)
1363        NEXT I
1364            !
1365            ! FIND THE NEW YIELD RADIUS FOR THIS ELEMENT
1366            !
1367        Q(3)=(-1/3)*(S(1)+S(2))
1368        Q(1)=S(1)+Q(3)
1369        Q(2)=S(2)+Q(3)
1370        Q(4)=SQR(2)*S(3)
1371        J1=0.
1372        FOR I=1 TO 4
1373        J1=J1+Q(I)*Q(I)
1374        NEXT I
1375        J1=J1/2
1376            !
1377            ! MUST SCALE THE NEW YIELD RADIUS
1378            !
1379        Jy(Ielm)=J1
1380        SUBEXIT
1381            !
1382            !C A S E   3 . )   E L E M E N T   I S   P L A S T I C
1383            !
1384        Jy(Ielm)=J1
1385        SUBEXIT
1386            !
1387            !C A S E   4 . )   E L E M E N T   I S   U N L O A D I N G
1388            !
1389        Plast(2,Ielm)=0
1390        P1=0
1391            !
1392            ! FIND NEW ELASTIC MODULUS
1393            !
1394        CALL Young(T1,P1,E1)
1395            !
1396            ! FIND THE STRESS INCREMENT IF THE ELEMENT WAS ELASTIC
1397            !
1398        FOR I=1 TO 3
1399        S1(I)=0.
1400        FOR J=1 TO 3
1401        S1(I)=S1(I)+E1*D(P1,I,J)*Ep1(J)
1402        NEXT J
1403        NEXT I
1404        SUBEND
1405    SUB Dataout(Ut(*),INTEGER Idn(*),Plast(*))
1406        COM Dx,Dy,Dz,Nx,Ny,Nn,Nb,Ne,Neq
1407            !
1408            ! SUBROUTINE DATAOUT :
1409            !           PRINT THE OUTPUT OF STRESS,STRAIN AND DISPLACEMENT
1410            !
1411        ALLOCATE REAL Str(1:Ne,1:6),S0(1:3),Ep0(1:3)
1412            !
1413            ! RECOVER STRESSES & DISPLACEMENTS FROM FILE
1414            !
1415        ASSIGN @P TO *
1416        ASSIGN @P TO "STRESS:HP82901,700,0"
1417        ENTER @P;Str(*)
1418        ASSIGN @P TO *
1419            !
1420            ! FORMAT OUTPUT FOR ELEMENT & NODAL DATA
1421            !
1422        IMAGE 45X,36A,DD
1423        IMAGE 38X,50A,DD
1424        IMAGE 4A,1X,3A,3X,8A,7X,8A,6X,9A,7X,8A,7X,8A,6X,9A
1425        IMAGE #,SD.DDDDESZZ,4X
1426        IMAGE #,5A,3X,12A,3X,12A
1427        IMAGE #,SD.DDDDDESZZ,3X,SD.DDDDDESZZ
1428            !
1429            !
1430            !
1431        Pag=1
1432        PRINT CHR$(12)
1433        PRINT USING "//"
1434        PRINT USING 1422;"E L E M E N T   D A T A  :  P A G E ";Pag
1435        PRINT
1436        PRINT USING "#,16X"
1437        PRINT USING 1424;"ELEM","E/P","X-STRESS","Y-STRESS","XY-STRESS","X-S
TRAIN","Y-STRAIN","XY-STRAIN"
1438        PRINT
1439        FOR Ielm=1 TO Ne
1440            !
```

```
1441        ! OBTAIN STRESSES AND STRAINS FROM STRESS ARRAY
1442        !
1443     FOR I=1 TO 3
1444     S0(I)=Str(Ielm,I)
1445     Ep0(I)=Str(Ielm,I+3)
1446     NEXT I
1447        !
1448        ! PRINT THE STRESS TO THE APPROPRIATE FORMAT
1449        !
1450     PRINT USING "#,15X"
1451     PRINT USING "#,1X,DDD,2X";Ielm
1452     IF Plast(1,Ielm)=0 THEN PRINT USING "#,1A";" "
1453     IF Plast(1,Ielm)=1 THEN PRINT USING "#,1A";"*"
1454     IF Plast(2,Ielm)=0 THEN PRINT USING "#,1A,2X";" "
1455     IF Plast(2,Ielm)=1 THEN PRINT USING "#,1A,2X";"*"
1456     FOR I=1 TO 3
1457     PRINT USING 1425;S0(I)
1458     NEXT I
1459     FOR I=1 TO 3
1460     PRINT USING 1425;Ep0(I)
1461     NEXT I
1462     PRINT
1463        !
1464        ! FORMAT OUTPUT FOR EACH PAGE
1465        !
1466     FOR I=55 TO 355 STEP 55
1467     IF Ielm=I THEN
1468     Pag=Pag+1
1469     PRINT CHR$(12)
1470     PRINT USING "//"
1471     PRINT USING 1422;"E L E M E N T   D A T A : P A G E ";Pag
1472     PRINT
1473     PRINT USING "#,16X"
1474     PRINT USING 1424;"ELEM","E/P","X-STRESS","Y-STRESS","XY-STRESS","X-S
TRAIN","Y-STRAIN","XY-STRAIN"
1475     PRINT
1476     END IF
1477     NEXT I
1478     NEXT Ielm
1479        !
1480        ! FIND THE NUMBER OF PAGES REQUIRED FOR DISPLACEMENT OUTPUT
1481        !
1482     IF Nn<=600 THEN Page=4
1483     IF Nn<=450 THEN Page=3
1484     IF Nn<=300 THEN Page=2
1485     IF Nn<=150 THEN Page=1
1486        !
1487        ! PRINTOUT OUTPUT FOR EACH PAGE
1488        !
1489     FOR P=1 TO Page
1490     PRINT CHR$(12)
1491     PRINT USING "//"
1492     PRINT USING 1423;"N O D A L   D I S P L A C E M E N T S : P A G E
";P
1493     PRINT
1494        !
1495        ! FIND THE NUMBER OF COLUMNS FOR THIS PAGE
1496        !
1497     Pag=(P-1)*150
1498     IF Nn>Pag AND Nn<=(Pag+50) THEN Ncol=1
1499     IF Nn>(Pag+50) AND Nn<=(Pag+100) THEN Ncol=2
1500     IF Nn>(Pag+100) THEN Ncol=3
1501        !
1502        ! PRINT HEADING FOR EACH COLUMN
1503        !
1504     PRINT USING "#,6X"
1505     FOR I=1 TO Ncol
1506     PRINT USING 1426;"NODE "," X-DIRECTION"," Y-DIRECTION"
1507     PRINT USING "#,7X"
1508     NEXT I
1509     PRINT
1510     PRINT USING "#,6X"
1511     FOR I=1 TO Ncol
1512     PRINT USING 1426;" NO. ","DISPLACEMENT","DISPLACEMENT"
1513     PRINT USING "#,7X"
1514     NEXT I
1515     PRINT
1516     PRINT
1517     FOR I=Pag+1 TO Pag+50
1518     P1=I
1519     P2=P1+50
1520     IF Ncol>1 AND P2>Nn THEN Ncol=1
1521     P3=P2+50
1522     IF Ncol>2 AND P3>Nn THEN Ncol=2
1523     IF P1>Nn THEN 1547
1524     PRINT USING "#,6X"
1525     PRINT USING "#,1X,DDD,4X";P1
1526     Ix=Idn(1,P1)
1527     Iy=Idn(2,P1)
1528     PRINT USING 1427;Ut(Ix),Ut(Iy)
1529     IF P1=Nn THEN 1545
1530     IF Ncol>1 THEN
1531     PRINT USING "#,7X"
1532     PRINT USING "#,1X,DDD,4X";P2
1533     Ix=Idn(1,P2)
1534     Iy=Idn(2,P2)
1535     PRINT USING 1427;Ut(Ix),Ut(Iy)
1536     END IF
1537     IF P2=Nn THEN 1545
1538     IF Ncol>2 THEN
1539     PRINT USING "#,7X"
1540     PRINT USING "#,1X,DDD,4X";P3
1541     Ix=Idn(1,P3)
1542     Iy=Idn(2,P3)
1543     PRINT USING 1427;Ut(Ix),Ut(Iy)
1544     END IF
1545     PRINT
1546     NEXT I
1547     NEXT P
1548     DEALLOCATE Str(*),S0(*),Ep0(*)
1549     SUBEND
```